ISTANBUL TECHNICAL UNIVERSITY ★ GRADUATE SCHOOL OF SCIENCE ENGINEERING AND TECHNOLOGY

THE INVESTIGATION OF THE 25 PERCENT RULE IN CONCENTRICALLY BRACE FRAME DUAL SYSTEM WITH SPECIAL MOMENT FRAME

M.Sc. THESIS

Samet KILIÇ

Department of Civil Engineering

Structural Engineering Programme

MAY, 2015

ISTANBUL TECHNICAL UNIVERSITY ★ GRADUATE SCHOOL OF SCIENCE ENGINEERING AND TECHNOLOGY

THE INVESTIGATION OF THE 25 PERCENT RULE IN CONCENTRICALLY BRACE FRAME DUAL SYSTEM WITH SPECIAL MOMENT FRAME

M.Sc. THESIS

Samet KILIÇ
(501121088

Department of Civil Engineering

Structural Engineering Programme

Thesis Advisor: Assist. Prof. Dr. Cüneyt VATANSEVER

MAY, 2015

İSTANBUL TEKNİK ÜNİVERSİTESİ ★ FEN BİLİMLERİ ENSTİTÜSÜ

MERKEZİ ÇAPRAZLI VE MOMENT AKTARAN ÇERÇEVELİ KARMA SİSTEMLERDE %25 KURALININ İNCELENMESİ

YÜKSEK LİSANS TEZİ

Samet KILIÇ
(501121088)

İnşaat Mühendisliği Anabilim Dalı

Yapı Mühendisliği Programı

Tez Danışmanı: Yrd. Doç. Dr. Cüneyt VATANSEVER

MAYIS, 2015

Samet KILIÇ, a **M.Sc.** student of ITU **Graduate School of Science Engineering and Technology** student ID **501121088**, successfully defended the **thesis** entitled "**THE INVESTIGATION OF THE 25 PERCENT RULE IN CONCENTRICALLY BRACE FRAME DUAL SYSTEM WITH SPECIAL MOMENT FRAME**", which he prepared after fulfilling the requirements specified in the associated legislations, before the jury whose signatures are below.

Thesis Advisor : **Assist. Prof. Dr. Cüneyt VATANSEVER** ....
İstanbul Technical University

Jury Members : **Prof. Dr. Konuralp GİRGİN** ....
İstanbul Technical University

Assist. Prof. Dr. Edip SEÇKİN ....
İstanbul Kültür University

Date of Submission : 04 May 2015
Date of Defense : 28 May 2015

To my family,

FOREWORD

I would like to express my deep appreciation and thanks for my advisor Assistant Prof.Dr. Cüneyt VATANSEVER. This work is supported by ITU Institute of Science and Technology.
In addition, my dear friend and civil engineer Mehmet Sinan ÖZDEMİR and Sümeyra YOLDAŞ contributed me in this thesis phase. I owe them a sincere thanks.

May 2015

Samet KILIÇ
(Civil Engineer)

TABLE OF CONTENTS

Page

ABBREVIATIONS

AISC **:** American Institute of Steel Construction
ASCE **:** American Society of Civil Engineers
BF **:** Braced Frame
CP **:** Collapse Prevention
CQC **:** Complete Quadratic Combination
DBE **:** Design Based Earthquake
DCR **:** Demand to Capacity Ratio
EQ **:** Earthquake
EW **:** East-West
FEMA **:** Federal Emergency Management Agency
IBC **:** International Building Code
IO **:** Immediate Occupancy Limit State
IS **:** Indian Seismic Code
LS **:** Life Safety Limit State
MCE **:** Maximum Considered Earthquake
MF **:** Moment Frame
MRF **:** Moment Resisting Frame
ND **:** Nonlinear Dynamic
NS **:** North-South
NEHRP **:** National Earthquake Hazards Reduction Program
PEER **:** Pacific Earthquake Engineering Research Center
SEAOC **:** Structural Engineers Association of California
SMRF **:** Special Moment Resisting Frame
TS **:** Total Shear
UBC **:** Uniform Building Code

LIST OF TABLES

Page

LIST OF FIGURES

Page

THE INVESTIGATION OF THE 25 PERCENT RULE IN CONCENTRICALLY BRACE FRAME DUAL SYSTEM WITH SPECIAL MOMENT FRAME

SUMMARY

Lateral forces induced by either earthquake or wind mostly play primary role in design of a multi-storey building. To carry the earthquake force, so many seismic force resisting systems have been developed recently. One of the most effective systems to resist the lateral earthquake forces is the dual systems that include moment frames and shear walls or braced frames together. According to ASCE 7-05, for dual systems the moment frames should resist at least 25 percent of the seismic design force. This rule is defined as 25 percent rule. In this paper the correlation between the height (the number of the stories) of the buildings and 25 percent requirement is investigated. The moment frames in dual systems considered have been designed for 15, 25 and 40 percent of seismic demand for different buildings: 12-storey, 16-storey and 20-storey.

Using SAP 2000 software, linear static and push-over analysis are performed. The braced frames of the dual systems are designed with concentric braces. During linear static analysis procedure, three different models having different story numbers are modelled and each of them are separated into three. Actually, nine models are available. By extracting the moment frame from the whole model, they are designed according to 15, 25 and 40 percent of the lateral load which they are expected to resist. After finishing planar system analysis they are adapted into model again and checked in the whole system whether they are over-stressed or not. After satisfying all conditions their base force proportion to sum of base reaction is determined. In this way, all the profiles and brace dimensions are determined. To get better results the structures are analyzed in three dimension however, the 25 percent rule is checked only in the x direction. In the y-direction only braced frames resist earthquake, in the x-direction dual system (both moment frames and braced frames) resist earthquake force. In the frames which braces are already exist, columns that are not part of braced frames are leaning columns whose connections to beams and to base are pinned. In the axis having moment frames, all beam-to-column connections are rigid. They are designed intentionally in this way to understand the events after yielding of the braces.

By push-over analysis, the expected behaviour of the structures is tried to be found out. Then the systems have been examined with non-linear static analysis using SAP 2000 software. While applying non-linear analysis on the structures an approximate

method is used. The structures are pushed in x directions about 3 percent of their height rather than the target displacement demands determined by a method. After obtaining the pushover curves, the target displacements are calculated and the performance point is determined. All the checks especially base shear distribution are done with respect to this point. During analysis procedure, the secant stiffness is used for hinge unloading method instead of unload entire structure option due to convergence problem. The FEMA hinge properties are assigned to frames. They are checked by hand calculation whether they meet the requirements of ASCE 41-06 or not. For this reason a cantilever column and a moment frame are analyzed. When compared to results, an agreement is observed. The axial hinge is assigned to in the middle of the braces. The P-M3 hinge is assigned to columns bottom and top parts. Delibrately, the P-M2-M3 hinge are not used, because M2 moment values are negligible. However, when they are used, convergence problem in SAP 2000 is encountered during analysis. Moment (M3) hinge assigned to beams, but no hinge is assigned to the beams which they are released in both ends. The anticipated behaviour of the structures can be defined as: First, braces yield under tensile forces and buckle due to compressive forces in a ductile manner, then, the moment frames start to resist the forces dominantly.At this time, the need of additional strength achieved by ensuring that the moment frames are capable of providing at least 25% required lateral strength is investigated Also the relation between the story number and this rule is examined.

During Time-History Analysis procedure, three different earthquake ground motions to represent the design based earthquake are taken from PEER. In addition, the systems are checked for Maximum Considered Earthquake. All the earthquake data satisfies the ASCE7-05 conditions. They are chosen according to the seismic zone criteria. In the models, initially the ramp functions are defined. Then earthquakes are defined. All the earthqukes are scaled. For a better scientific approach, the verification with another software is obligation. For that reason, OpenSEES is used to verify the results. The half of the building is modeled in this software. This model is developed in such a way to represent the whole structure. Only x-direction elements are added to the models. The beams and braces in transverse direction are not included in the models. However, their loads and self-weights are added to system joints as point loads. In order to prove that the models in OpenSEES represent the real models, gravity and eigen model analysis are conducted. In the gravity analysis, the column axial forces are checked. In the eigen modal analysis, the first mode direction and the natural vibration periods of the structures are compared. According to comparison of the periods, the OpenSEES models are more rigid. Their natural vibration periods are lower than SAP 2000 models. However the values are found to be comparable. In addition to this, the push-over analysis is carried out to compare the nonlinear behaviour of the models each other . Then, non-linear dynamic analyses are done and their results are evaluated after completions of analyses.

For the assessment of seismic performance of each building, story drifts, displacements and base shear distribution are evaluated. In the SAP 2000 models, the stages of plastic hinges and their distribution are also checked. The results are found as expected. Plastic hinges occur in the brace members under axial compressive force. Plastic hinges can also be observed in the moment resisting frames. Compared to brace hinges, their stages are more closer to IO, LS. Consequently, all systems are performed well and there is no clear evidence to show that one model is exhibiting better performance than the other.

MERKEZİ ÇAPRAZLI VE MOMENT AKTARAN ÇERÇEVELİ KARMA SİSTEMLERDE %25 KURALININ İNCELENMESİ

ÖZET

Deprem ya da rüzgâr sebebiyle oluşan yanal kuvvetler çoğunlukla çok katlı binanın tasarımında temel bir rol oynamaktadır. Deprem kuvvetini karşılamak için, pek çok yanal yük taşıyıcı sistem son zamanlarda geliştirilmiştir. Yatay deprem kuvvetleri karşı en etkili sistemlerinden biri moment çerçeveleri ile birlikte perde duvarlar veya çaprazların beraber kullanıldığı karma sistemlerdir. ASCE 7-05 göre, karma sistemler için moment çerçeveleri sismik tasarım kuvvetinin en az yüzde 25'ini karşılayabiliyor olmalıdır. Bu kural yüzde 25 kuralı olarak tanımlanmaktadır. Bu tezde binaların yüksekliği (kat sayısı) ve yüzde 25 şartı arasındaki korelasyon incelenmiştir. Taşıyıcı sistemi moment çerçeveleri deprem talebinin yüzde 15, 25 ve 40'ını karşılayacak şekilde tasarlanmış karma sistemlerden oluşan 12 katlı, 16 katlı ve 20 katlı yapılar dizayn edilmiştir.

SAP 2000 yazılımı kullanılarak, lineer statik ve push-over analizi yapılmıştır. Karma sistemler, merkezi çaprazlı olarak tasarlanmıştır. Lineer statik analiz işlemi sırasında, farklı kat sayılarına sahip üç farklı model geliştirilmiştir ve bunların her biri de kendi aralarında üçe ayrılmıştır. Aslında, dokuz model mevcuttur. Bütün modellerden birer adet moment çerçevesi ayıklanıp, yüzde 15, 25 ve 40 yanal yüke karşı koyacak şekilde dizayn edilmiştir. Düzlemsel sistem analizi bitirildikten sonra tekrar modele bu çerçeveler monte edilip, sistem içerisinde yeterli olup olmadıkları kontrol edilmiştir. Daha sonra moment çerçevelerindeki kolonların tabanında oluşan kesme kuvveti belirlenmiş ve tüm taban kesme kuvvetine oranları belirlenmiştir. Bu şekilde, tüm profillerin ve çaprazların boyutları belirlenmiştir. Yapılar ancak üç boyutta analiz edilmiştir fakat daha uygun ve anlaşılır sonuçlar elde etmek için, yüzde 25 kuralı sadece x yönünde kontrol edilmiştir. Y yönünde sadece çaprazlar x yönünde ise deprem kuvvetlerine karşı moment çerçeveleri ve çaprazlar birlikte çalışmaktadır. Çaprazlı çerçevelerde bulunan tüm kolonların taban bağlantısı mafsallıdır. Bu şekilde o akslarda deprem yükleri sadece çerçevelerce taşınacaktır. Kolonlar pandül ayak şeklinde düşünülmüştür. Moment çerçevesi olarak tasarlanan akslarda ise tüm kolonların taban bağlantıları ankastredir. Bu şekilde tasarım, çaprazların akma noktasına ulaşmasından sonraki davranışı daha iyi gözlemleyebilmek için bilerek yapılmıştır.

Bir sonraki bölümde, statik itme analizi ile, yapıların beklenen davranışı gösterip göstermediğinin anlaşılmasına çalışılmıştır. Sistemlerin doğrusal olmayan statik analizi için, SAP 2000 yazılımı kullanılarak incelenme yapılmıştır. Yapılar üzerinde

doğrusal olmayan analiz uygulanırken yaklaşık bir yöntem kullanılmıştır. Yapıların tam hedef deplasman talepleri hesaplanmasının yerine, yapıların tamamı yüksekliğinin yüzde 3 ile x yönünde itilmiştir. İtme eğrileri elde edildikten sonra, hedef yer değiştirme talepleri hesaplanıp, itme eğrisinde bu performans noktası belirlenmiştir. Tüm kontroller özellikle taban kesme kuvveti dağıtımı bu noktaya göre yapılmıştır. Analiz işlemi sırasında, sekant rijitliği yöntemi plastik mafsallardan yük boşaltma yöntemi olarak seçilmiştir. Bu yöntemin seçilmesinin en büyük nedeni diğer yöntemlerin büyük denklemleri çözme yetersizliğidir. FEMA plastik mafsal özellikleri ilk olarak tüm elemanlara atanmıştır. Bu plastik mafsalların ASCE 41-06 gereksinimlerine uygun olup olmadığını elle hesaplama yapılarak kontrol edilmiştir. Bu nedenle, bir moment çerçeve analizi yapılmıştır. Sonuçların makul olduğu yapılan hesaplar neticesinde kabul edilmiştir. Eksenel plastik mafsallar çaprazların ortasında atanmştır. P-M3 plastik mafsalları ise kolonların alt ve üst kısımlarına atanmıştır. Bilinçli olarak, P-M2-M3, plastik mafsal kullanılmamıştır. M2 moment değerleri M3 değerlerine oranla çok daha küçük oldukları için göz ardı edilmiştir ve kullanıldıkları zaman, SAP 2000 analizlerinde denklem çözme sorunları ile karşı karşıya kalınmıştır. Moment dönme (M3) plastik mafsalları sadece rijit bağlı, mafsallı olmayan kirişlerin her iki ucuna atanmıştır. Yapıların beklenen davranışı şöyle tanımlanabilir: ilk olarak çaprazlar deprem kuvvetlerini almaya başlayacak, onlar çekme kuvvetleri altında akmaya basınç kuvvetleri altında burkulmaya başladıktan sonra ise moment çerçeveleri taban kesme kuvvetini almaya başlayacaktır. Bu sırada moment çerçevelerinin ekstra dayanım ihtiyacının yüzde 25 kuralının sağlanmasıyla yeterli olup olmadığı anlaşılmaya çalışılmıştır. Ayrıca kat sayısı ile bu kural arasında bir bağ var mıdır control edilmiştir.

Zaman-tanım alanında analizi için tasarım depremi olarak üç farklı deprem verisi PEER'den alınmıştır. Ayrıca yapılar yapıya etkime olasılığı en büyük deprem altında da kontrol edilmiştir. Tüm deprem verileri ASCE7-05 koşullarını sağlayacak şekilde seçilmiştir. Ayrıca, deprem bölgesi ve zemin özelliklerine de dikkat edilerek seçim yapılmıştır. Sırayla depremler modellerde tanımlanmıştır. Tüm depremler tanımlanmadan önce PEER'den alınan değere göre ölçeklenmiştir. Daha iyi bir bilimsel yaklaşım için, başka bir yazılım ile doğrulama gereklidir. Bu nedenle, OpenSees sonuçları doğrulamak için kullanılmştır. Yapılar bu yazılımda modellenmiştir. Bu model bütün yapıyı temsil edecek şekilde tasarlanmıştır. Sadece x-yönü elemanları modellerde mevcuttur. Diğer yön çapraz ve kirişleri göz ardı edilmiştir. Onların yerine yükleri ve öz ağırlıkları nokta yükler olarak sistemin düğüm noktalarına etkitilmişir. OpenSees modellerin gerçek modelleri temsil ettiğini kanıtlamak için, düşey yük ve modal analiz yapılmıştır. Düşey yük analizinde, kolon eksenel kuvvetleri kontrol edilmişir. Eigen modal analizde ise, ilk mod yönü ve yapıların doğal titreşim periyotları karşılaştırılmıştır. Periyot karşılaştırılmasına göre OpenSees modeller daha rijittir. Opensees modellerin doğal titreşim periyotları SAP 2000 değerlerine yakın değerlerdir. Buna ek olarak, yapıların doğrusal olmayan davranışları da benzerlik göstermiştir. En son olarak, yapıların doğrusal olmayan dinamik analizi yapılmıştır ve depremlerden oluşan sonuçlar da değerlendirilmiştir.

Her binanın deprem performansının değerlendirilmesi için , göreli kat ötelenmeleri , yer değiştirmeler ve taban kesme kuvveti dağılımları değerlendirilmiştir. SAP 2000 modellerinde, plastik mafsal oluşum ve dağılımları da bir kriter olarak kontrol edilmiştir. Sonuçlar beklenildiği gibi olmuştur. Plastik mafsallar eksenel basınç kuvveti altında çaprazlarda ortaya çıkmıştır. Plastik mafsallar moment çerçevelerinde de görülmüştür . Çaprazlı çerçevelerde oluşan plastik mafsallar ile karşılaştırıldığında, bunların aşamalarının LS , IO daha yakın olduğu görülmüştür. Sonuç olarak, tüm sistemlerin analizleri tamamlandığında, bir modelin diğerinden daha iyi performans sergilediğini göstermek için açık kanıt yoktur.

1. INTRODUCTION

In the steel buildings, moment frame system is suitable for its high ductility. In addition to this, it supplies high absorption of earthquake energy. However lateral displacements of this kind of buildings are the major problem. In other words, there is lack of stiffness. In order to solve this problem, one way is using dual systems (both special moment frame and braces). Dual system may combine the advantages of constituent elements. Ductile frames with braces can provide high amount of energy dissipation, especially for upper stories of structures. Also the storey drifts may be minimized during earthquake due to large stiffness of frames.

In this paper, the called 25 percent rule is searched. The necessity of this rule and the exact percent of demand are tried to be justified. For comparison, 9 models have been considered. Basically there are three types of systems: 15 percent of the base shear (12-16-20 storey), 25 percent of the base shear (12-16-20 storey), 40 percent of the base shear (12-16-20 storey). Initially, in the SAP 2000 software all brace, column and beam dimensions are determined. To satisfy the 15, 25 and 40 percent of base shear strength, planar systems for x direction are constituted, separately. The other direction is ignored due to the hardness to organize moment frames and brace at the same time in the disposition plan. After that, three dimension frames are tested to figure out the amount of base shear which moment frames carry exactly. Next for the time history analysis, the earthquake records from PEER are taken and transformed into the SAP 2000 data. Seven earthquake records are enough to carry out such analysis. Additionally, the moment-rotation graphs of steel beams and axial load and moment interaction diagrams of columns are drawn with section designer. In this process, the acceleration loads, material, geometry, end releases, and hinges assigned in SAP 2000. All the analysis is finished. For all models, the performance points are calculated by using capacity spectrum. Finally drifts, displacements and story shears are compared.

1.1 Purpose of Thesis

The main objective of this thesis is to examine the necessity of 25 percent rule in the dual system.

1.2 Literature Review

SEAOC is structural engineering organization to provide the public with structures of safe and dependable performance; to give the structural engineering profession the most current information and tools for structural analysis, design.The Blue Book is SEAOC's signature publication, maintained by the SEAOC Seismology Committee. The dual system is mentioned Blue Book firstly in the 1959. Dual system has good elastic response control for moderate shaking; good energy dissipation for strong shaking. Moreover, damage to primary lateral force-resisting system does not affect stability of the vertical system and backup system provided in the form of a moment frame. (SEAOC Blue Book: Seismic Design Requirements 2007 p:9) Secondly, dual system is referred in the UBC 1961. In addition 25 percent rule is said here too. In the 1985, 1988, 1997, the requirement of dual system have changed gradually and the definition of this concept became clearer. In the 2000, NEHRP clarifies that moment frame is redundant however it changed nowadays due the acception that the lateral force is disturbuted to the braces and moment frames according to their stiffness. In the current practise, ASCE 7-05 12.5.1 describes dual system design in this way: "For dual system, the moment frames shall be capable of resisting at least 25 percent of the design seismic forces. The total seismic force resistance is to be provided by the combination of the moment frames and the shear walls or braced frames in proportion to their rigidities."

Qiang Xie (2008) discussed this topic in his study, "Dual System Design of Steel Frames Incorporating Buckling-Restrained Braces" A 4-story and 12 stories dual system buildings are designed for a location in Japan. This thesis examines the structural behaviour from story drift from time history analyses (Qiang Xie 2008).

The article"Comparison of Dual System Moment Frame and Thin Steel Plate Shear Walls with Dual Sstem of Steel Moment Frame and Cross Bracing or Chevron with a Design Method Based on Performance Levels" belonging to Yousef Zandi (2013) compares dual systems including intermediate moment frames and thin steel moment frame and intermediate moment frame and convergent braces (Yousef Zandi 2013).

Nabin Raj and S.Elavenil (2012) wrote similar paper ”Analytical Study on Seismic Performance of Hybrid (Dual) Structural System Subjected to Earthquake”. In this paper, the seismic performance of reinforced concrete building with concentric steel brace is examined. A 6-story, 12-story and 18-story dual system was designed according to IS 1893 for seismic V (Nabin Raj and S.Elavenil 2012).

Lisa Jaylene Aukeman (2011) presents a paper ”ASCE 7-05 Design Rule for Relative Strength in a Tall Buckling-Restrained Braced Frame Dual System”. In this thesis three 20-story buckling-restrained braced frame dual systems, which have moment frames are designed for 15%, 25% and 40% of seismic demands, are examined. The nonlinear static and dynamic analyses are conducted according to ASCE 41-06.

1.3 Hypothesis

In this thesis, the definition of 25 percent rule will be discussed by comparing a few structures and different software in order to evaluate the necessity. Firstly, it is assumed that, all the building models resist different amount of base shear. They are modeled in SAP 2000 during linear static analysis procedure. In this part it is important to avoid over-design and supply 15%, 25% and 40% of base shear capacity of moment frames in models in order to get more accurate solutions. Most probably, even though the moment frame capacities supply 15%, 25% and 40% of base shear in the planar system analysis, they do not resist that much force in the three dimensional model. In the nonlinear static analysis, it is expected that the moment frames begin to resist higher forces after braces are yielded. In the initial steps, the braces should yield, then moment frame must be involved, however, the moment frame base shear ratio to total shear will be higher compare to linear static analysis. Finally to get different software result for better scientific approach to problem, all the models will be solved in OPENSEES with nonlinear dynamic analysis. Same behavior is expected in time history analysis. What we expect is this rule will be identified an arbitrary rule after completion of all these analysis.

2. MODELLING

2.1 Prototype Steel Building

In the modelling phase, the disposition plan is drawn firstly. According to the regulation “ASCE 7-05 – Minimum Design Loads for Buildings and other Steel Structures”, the dead and live loads are determined and converted into metric units. The seismic loads are calculated by using ASCE 7-05 again. All the load combinations are determined from same regulation. This building is designed as an office building. Its load-bearing system is dual system containing concentrically braced frame as indicated above. It has seven spans through x-direction and five spans through y-direction. The distance between two axes is six meters at both directions. The other specialties of the buildings are shown below successively with respect to number of storey. Additionally, it can be seen above: One cross section and plan.

2.2 Plan and Elevation of the Building

The disposition plan is shown in the figure 2.1 and a section from braced axis is shown in figure 2.2 below.

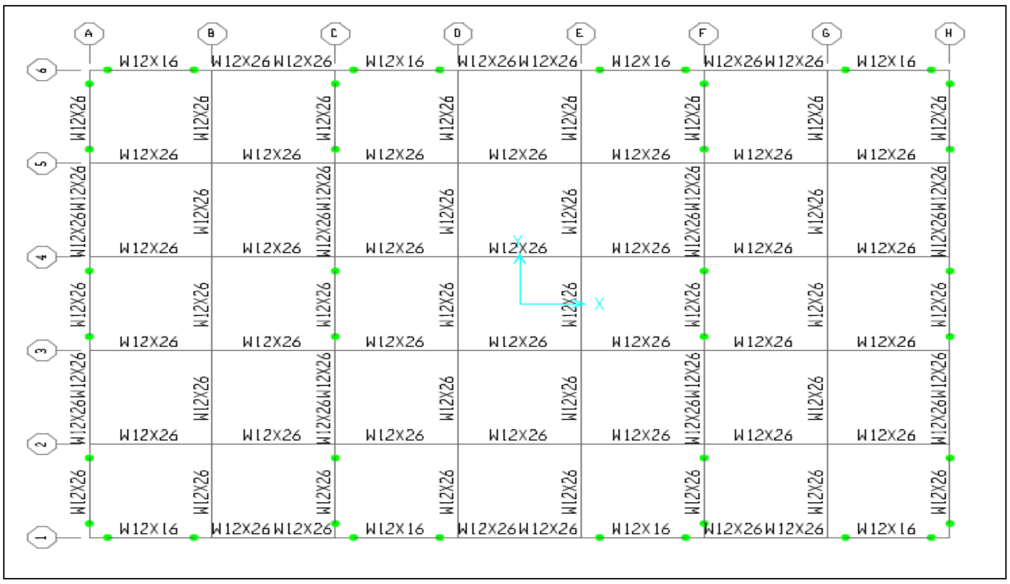

Figure 2.1 : Disposition plan.

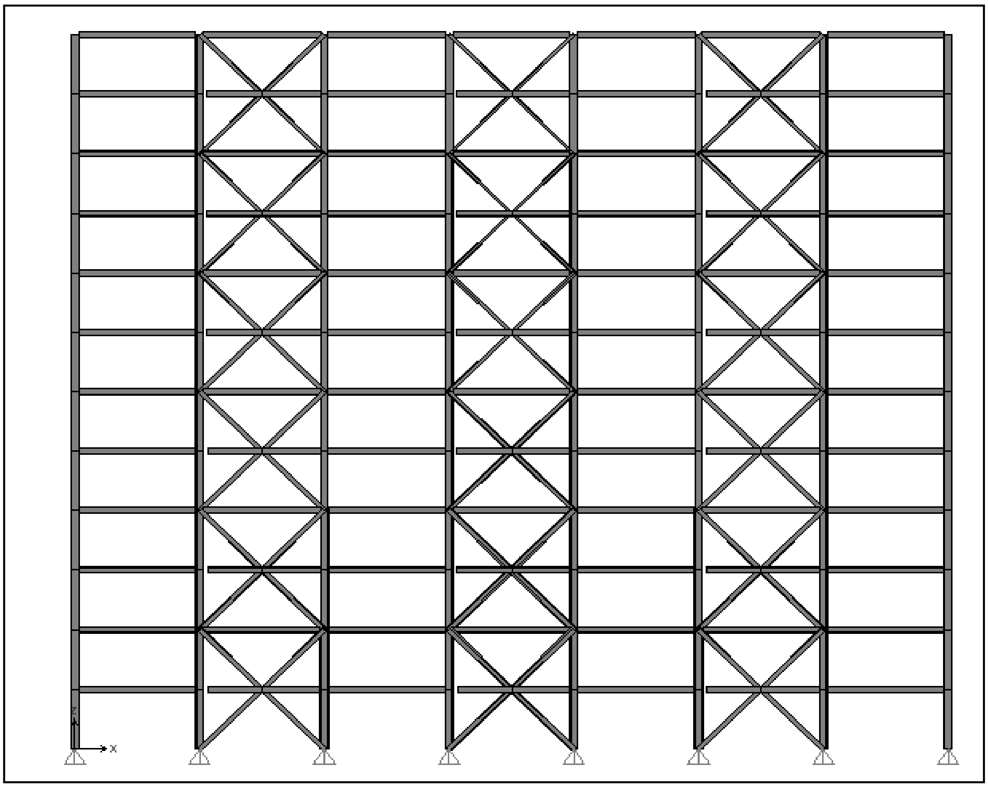

Figure 2.2 : Section.

2.3 Material Properties and Loads, Combinations, Spectrum

Material properties are determined as A992Fy50 as shown in the table 2.3. The loads are various for roof and the normal floor plan. The loads are indicated in table 2.1 in detailed way. The building information is illustrated in table 2.2.

Load combinations are determined from ASCE 7-05 as shown in table 2.4. Apart from basic combinations for ASD, ASCE 7-05 offers combinations with over-strength factor as shown in table 2.5. Some coefficients are introduced in table 2.6 like over-strength factor, redundancy factor and response modification coefficient. They are taken from related tables.

Table 2.1 : Loads.

Parameter	Description
Dead (normal floor)	3 kN/m^2
Live (normal floor)	2 kN/m^2
Dead (roof floor)	2 kN/m^2
Live (roof floor)	1,5 kN/m^2
Wall (normal floor)	4 kN/m

Table 2.2 : Building Information.

Parameter	Description
Structure Dual System	(SCBF+SMF)
Plan dimensions	42m*30m
Number of Stories	12-16-20
Storey Height	3m
Total Height	36-48-60m

Table 2.3 : Material Properties.

Parameter	Description
Steel	A576 grade50 (S350)
Young Modulus	200000 N/mm^2

Table 2.4 : Load Combinations-I.

Basic Combinations for Allowable Stress Design
1. D + F
2. D + F + H + L + T
3. D + F + H +(L or S or R)
4. D + F + H +0.75(L +T) +0.75(L_r or S or R)
5. $(1.0 + 0.14S_{DS})D + H + F + 0.7\ \rho\ Q_E$
6. $(1.0 + 0.105S_{DS})D + H + F + 0.525\ \rho\ Q_E + 0.75L + 0.75(L_r$ or S)
7. $(0.6 - 0.14S_{DS})D + 0.7\ \rho\ Q_E + H$

Table 2.5 : Table captions must be ended with a full stop.

Basic Combinations for ASD with Over-strength Factor (see Sections (see 2.4.1 and 2.2 for notation)
1. $(0.6 - 0.14S_{DS})D + 0.7\ \Omega_0\ Q_E + H + F$
2. $(1.0 + 0.105S_{DS})D + H + F + 0.525\ \Omega_0 Q_E + 0.75L + 0.75(L_r$ or S)
3. $(0.6 - 0.14S_{DS})D + 0.7\ \Omega_0\ Q_E + H$

These over-strength combinations are illustrated in ASCE 7-05 apart from basic load combinations. So that, they should be taken into consideration even the models contain basic combinations.

Table 2.6 : Dual System Parameters (ASCE7-05).

D.DUAL SYSTEMS WITH SPECIAL MOMENT FRAMES CAPABLE OF RESISTING AT LEAST 25% OF PRESCRIBED SEISMIC FORCES	ASCE 7 Section where Deatiling Requirements are Specified	Response Modification Coefficient, R	System Overstrength Factor, Ω_0^g	Deflection Amplification Factor, C_{db}
1.Steel EBF	14.1	8	2,5	4
2.Special steel CBF	14.1	7	2,5	5,5

The Design Response Spectrum is taken from ASCE 7-05 as indicated above in the figure 2.3. The site coefficients F_a and F_v are shown in table 2.7 and 2.8 respectively in table 2.7 and table 2.8.

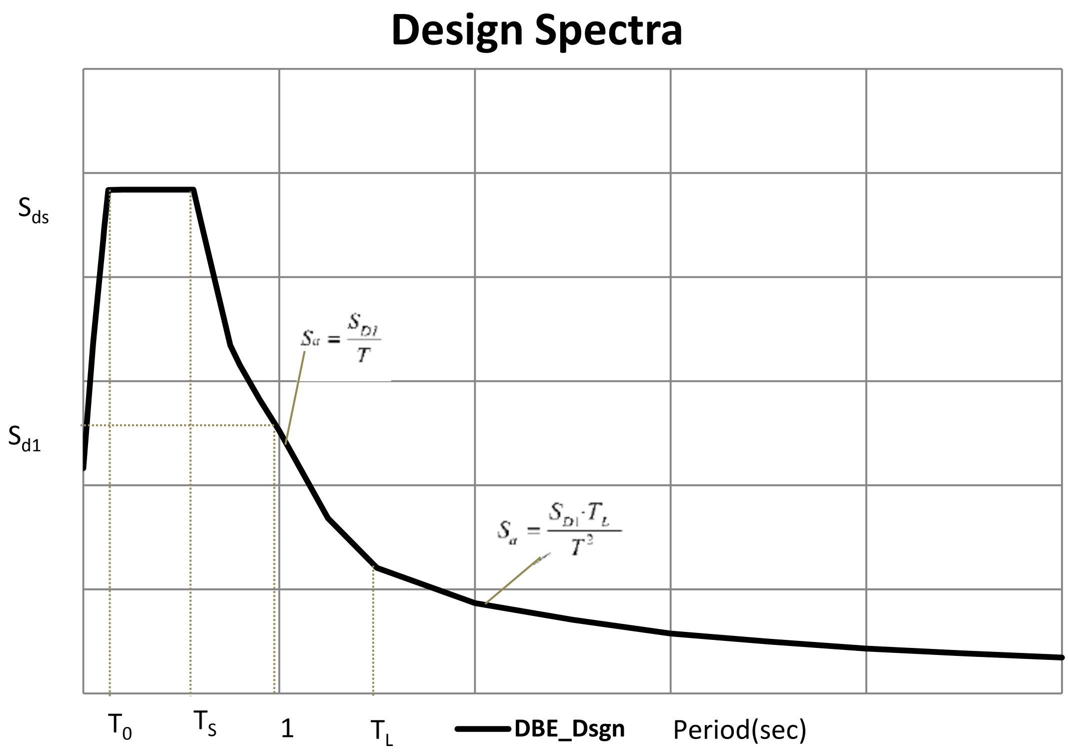

Figure 2.3 : Design Response Spectrum (ASCE 7-05, Figure 14.1-4).

Table 2.7 : Site coefficient, F_a (ASCE7-05).

Site Class	Mapped Maximum Considered Earthquake Spectral Response Acceleration Parameter at Short Period				
	$S_s \leq 0,25$	$S_s=0,5$	$S_s=0,75$	$S_s=1,0$	$S_s \geq 1,25$
A	0.8	0.8	0.8	0.8	0.8
B	1.0	1.0	1.0	1.0	1.0
C	1.2	1.2	1.1	1.0	1.0
D	1.6	1.4	1.2	1.1	1.0
E	2.5	1.7	1.2	0.9	0.9
F	See Section 11.4.7				

Table 2.8 : Site coefficient, F_v (ASCE7-05).

Site Class	Mapped Maximum Considered Earthquake Spectral Response Acceleration Parameter at 1-s Period				
	S_s≤0,1	S_s=0,2	S_s=0,3	S_s=0,4	S_s≥0,5
A	0.8	0.8	0.8	0.8	0.8
B	1.0	1.0	1.0	1.0	1.0
C	1.2	1.2	1.1	1.0	1.0
D	1.6	1.4	1.2	1.1	1.0
E	2.5	1.7	1.2	0.9	0.9
F	See Section 11.4.7				

Values of Approximate Period Parameters C_t and x are illustrated in table 2.9. Coefficinets For Upper Limit on Calculated Period are shown in table 2.10.

Table 2.9 : Values of Approximate Period Parameters C_t and x (ASCE7-05).

Structure Type	C_t	x
Moment-resisting frame systems in which the frames resist 100% of the required seismic force and are not enclosed or adjoined by components that are more rigid and will prevent the frames from deflecting where subjected to seismic forces:		
(0.0724)[a]	0.8	(0.0724)[a]
(0.0466)[a]	0.9	(0.0466)[a]
(0.0731)[a]	0.75	(0.0731)[a]
(0.0488)[a]	0.75	(0.0488)[a]

[a]Metric equivalents are shown in parantheses.

Table 2.10 : Coefficinet For Upper Limit on Calculated Period (ASCE7-05, 12.8-1).

Design Spectral Response Acceleration Parameter at 1 s, S_{d1}	Coefficient C_u
≥0.4	1.4
0.3	1.4
0.2	1.5
0.15	1.6
≤0.1	1.7

3. LINEAR STATIC ANALYSIS

3.1 12-Storey Building

S_s S_1 (mapped acceleration parameters) are taken from maps ASCE 7-05 figure 22-1 through 22-14 as shown in Table 3.1. According to geotechnical information, the site class is D. Note: These values are site specific and are based on MCE values for 2% in 50 year probability (≈2,500 year recurrence) Occupancy category are determined with respect to description of Hazard Represented by Building Collapse. It is chosen as "II" as indicated in Table 3.2.

$$S_{ms} = S_s \times F_a \tag{3.1}$$

$$S_{m1} = S_1 \times F_v \tag{3.2}$$

Table 3.1 : Mapped Acceleration Parameters (ASCE 7-05 figures 22-1).

Parameter		Period	
S_s=	1.5 g	T=	0.2 sec
S_1=	0.6 g	T=	1 sec

Table 3.2 : Occupancy Category (ASCE 7-05 table 1-1).

Occupancy Category	2

F_a and F_v the site coefficients are taken from ASCE 7-05 as shown in table 3.3. In addition the design spectral responses are calculated with respect to equation **(3.1)** and **(3.2)** as shown in table 3.4. Seismic Parameters are shown in table 3.5.

Table 3.3 : Site Coefficients (ASCE 7-05 11-4-1).

Parameter	Description
Fa=	1
Fv=	1.5

Table 3.4 : Design Spectral Response (ASCE 7-05 11-4-1).

Parameter	Value		Parameter	Value	
S_{ms}=	S_s*F_a	1.5	S_{ds}=	2/3*S_{ms}	1
S_{m1}=	S_1*F_v	0.9	S_{d1}=	2/3*S_{m1}	0.6

Table 3.5 : Seismic Ground Motion Parameters (ASCE 7-05 11-4-5).

		Period	
T_0=	$0.2*S_{d1}/S_{ds}$	0.12	Sec
T_s=	S_{d1}/S_{ds}	0.6	Sec

For the dual system with the special moment frame, the coefficients R, C_d and Ω are determined. "ρ" redundancy factor must be determined. It is for usage of more lateral-load resisting elements. The factor varies from 1.0 to 1.5. These parameters are taken from ASCE 7-05 12.3.4.2.

R=7, Ω=2,5, C_d=5, ρ=1,3

The approximate period is calculated as 0.72 sec. with the equation below

$$T_a = C_t \times H_n^{\ x} \tag{3.3}$$

h_n=	36
C_t=	0.0488
x=	0.75

(ASCE 7-05 eq. 12.8-7)

The approximate fundamental building period can be computed from the building height. But from the table, the metric equivalents are used. In addition to this, the upper limits are figured out with respect to equation **(3.3)**. However, while calculating the base shear, the periods from computer analysis are used.

Upper Limit

T<	C_u*T_a
T_{max}=	1.008
T_x=	1.680 sec
T_y=	1.326 sec

ASCE 7-05 eq. 12.8-2

T_{max}= 1.008

S_{DS}/(R/1)=1.0g/(7/1.0)=0.14286 (ASCE 7-05 eq. 12.8-3)

Cs need not exceed S_{DS}/(T*(R/1)) for T≤TL=(0.6g)/(0.53*(7/1.0)=0.084g

Seismic base shear per ASCE 7-05 12.8.1 V=Cs*W

Vertical distribution:

$$F_x = C_{vx} \times V \tag{3.4}$$

$$C_{vx} = \left(W_x \times h_x^k\right) / \left(\sum w_i h_i^k\right) \tag{3.5}$$

Where

F_x is horizontal force at each level X

W_x is the story weight

h_x is the story height

$V_x = \Sigma f_i$ is story shear sum of of levels above.

Example is based on rigid diaphragm. For this reason all the static forces are added to the system from centre of mass, however in this way the torsion would be neglected. To take torsion effects into consideration, after distribution of forces per stiffness and location, torsional moments to include both natural and accidental torsion must be calculated where:

Mt= %5

M_t= 0.05*42*F_x =2.1 F_x N-S

M_t= 0.05*30*F_x =1.5 F_x E-W

During analysis procedure, 3-D model assumed that resist 15% of base shear is made initially. 3-D model is used to determine force distribution to frames. Seismic weight is calculated by taking 100% of dead loads and wall loads plus 25% of roof and normal floor live loads into consideration. After that, the base shear calculated is distributed to stories. In order to test 25% rule, three different models are created. Then all of them are divided into two with respect to X and Y directions. The models in y direction are neglected. Both models are planar systems that consist only moment frames. Successively, the models adjusted to resist 15%, 25% and 40% of seismic design force. The members are determined. After that for linear static analysis, the equivalent seismic force is calculated with the equation **(3.4)** and distributed to story levels with respect to story feight and story weight as indicated in equation **(3.5)**. Here, in table 3.6, is the equivalent seismic force distribution of story levels:

Table 3.6 : Equivalent Static Force Distribution (12 storey).

Story	Wx	hx	hx^k	$Wx*hx^k$	C	Fx	Fy	Mx	My
1	7156	3	3.537443	25313.94	0.01105	74.43586	74.43586	156.3153	111.6538
2	7119	6	7.850077	55884.7	0.024395	164.3294	164.3294	345.0918	246.4941
3	7092	9	12.5135	88745.76	0.038739	260.9576	260.9576	548.0111	391.4365
4	6964	12	17.42041	121315.8	0.052956	356.73	356.73	749.133	535.095
5	6845	15	22.51671	154126.9	0.067279	453.2114	453.2114	951.7439	679.8171
6	6794	18	27.7692	188664	0.082355	554.7679	554.7679	1165.013	832.1519
7	6753	21	33.15524	223897.3	0.097735	658.372	658.372	1382.581	987.558
8	6627	24	38.65832	256188.7	0.11183	753.3249	753.3249	1581.982	1129.987
9	6600	27	44.2658	292154.3	0.12753	859.0821	859.0821	1804.072	1288.623
10	6550	30	49.96771	327288.5	0.142866	962.3946	962.3946	2021.029	1443.592
11	6496	33	55.75593	362190.5	0.158102	1065.024	1065.024	2236.551	1597.536
12	3166	36	61.62371	195100.7	0.085164	573.6952	573.6952	1204.76	860.5428
	78162			2290871					

Note that the Torsional moments for both directions are taken into account in order to ignore ±5% eccentricity. To calculate these moments the whole length of each dimension is multiplied with story seismic load and 0.05.

The seismic force is divided with the number of braces. Here, in table 3.6, are the forces for only one special moment frame system:

Table 3.7 : Equivalent Static Force Distribution for Single SMRF (12 storey).

FOR 15%, 25% 40% MODEL

	0.15	0.25	0.4
12	21.51357	35.85595	57.36952
11	39.93841	66.56401	106.5024
10	36.0898	60.14966	96.23946
9	32.21558	53.69263	85.90821
8	28.24968	47.08281	75.33249
7	24.68895	41.14825	65.8372
6	20.8038	34.673	55.47679
5	16.99543	28.32571	45.32114
4	13.37737	22.29562	35.673
3	9.785912	16.30985	26.09576
2	6.162354	10.27059	16.43294
1	2.791345	4.652241	7.443586

After applying those forces to the systems, the analysis results are exhibited below. There are results belonging to X direction. After the analysis the profiles are chosen as in table 3.8:

Table 3.8 : Column and Beam Sections (12 storey).

	15% model		25% model		40% model	
STOREY	Column	Beam	Column	Beam	Column	Beam
1	W14X211	W12X26	W14X283	W12X35	W14X342	W12X50
2	W14X211	W12X26	W14X283	W12X35	W14X342	W12X50
3	W14X159	W12X26	W14X176	W12X35	W14X193	W12X50
4	W14X159	W12X26	W14X176	W12X35	W14X193	W12X50
5	W14X109	W12X26	W14X120	W12X35	W14X120	W12X50
6	W14X109	W12X26	W14X120	W12X35	W14X120	W12X50
7	W14X74	W12X26	W14X82	W12X35	W14X90	W12X50
8	W14X74	W12X26	W14X82	W12X35	W14X90	W12X50
9	W14X48	W12X26	W14X48	W12X35	W14X61	W12X50
10	W14X48	W12X26	W14X48	W12X35	W14X61	W12X50
11	W14X30	W12X26	W14X30	W12X35	W14X38	W12X50
12	W14X30	W12X22	W14X30	W12X26	W14X38	W12X26

After the initial analysis the braces are chosen as in following table 3.9:

Table 3.9 : Brace (X-Y Directions) Sections (12 storey).

Storey	X	Y
12	180x180x10	180x180x10
11	180x180x10	180x180x10
10	200x200x16	200x200x16
9	200x200x16	200x200x16
8	200x200x20	200x200x20
7	200x200x20	200x200x20
6	220x220x20	220x220x20
5	220x220x20	220x220x20
4	250x250x20	250x250x20
3	250x250x20	250x250x20
2	250x250x20	250x250x20
1	250x250x20	250x250x20

3.1.1 %15 Model

2D model (15% X-direction planar system) with PMM ratio values and colors are indicated in figure 3.1.

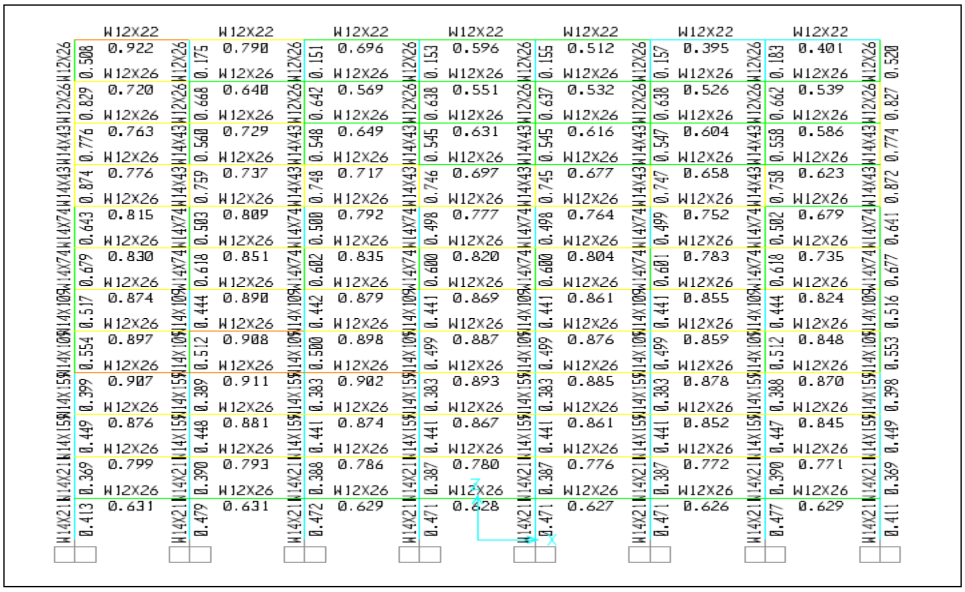

Figure 3.1 : PMM Ratios %15-MF-12 (SAP 2000).

After constituting the 3-D model with the frames of 2-d model, the actual base shear proportion of moment frames to whole system is calculated as %8. 3D model with PMM ratio colors is indicated in figure 3.2 below.

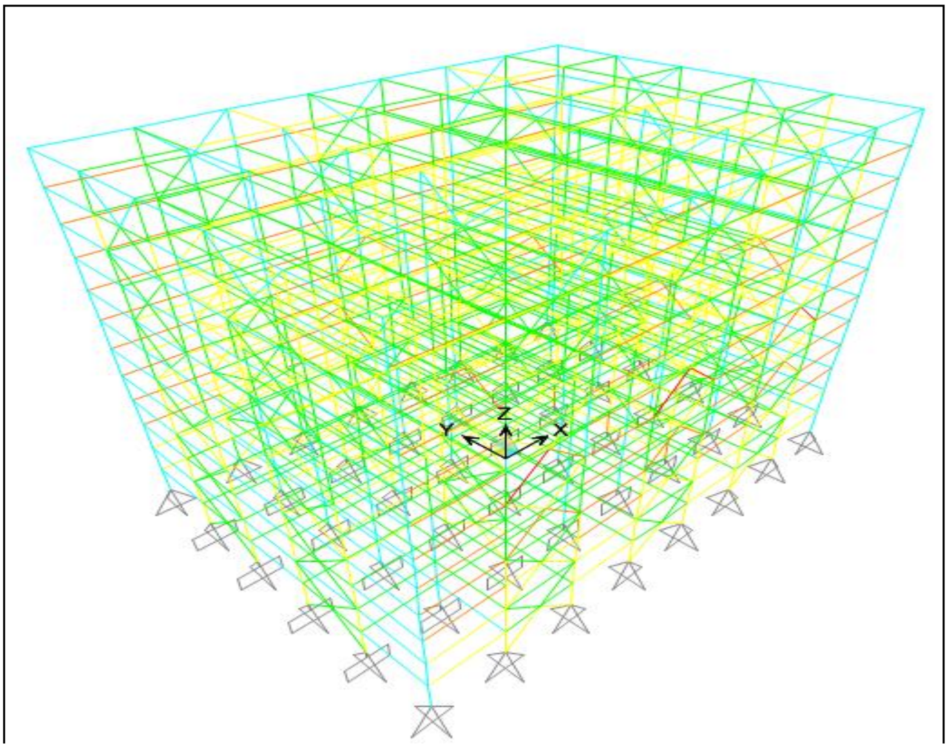

Figure 3.2 : PMM Ratios %15- 12 (SAP 2000).

To determine whether story drifts exceed the allowable limits four external points are chosen and their drifts are checked. In the chart, it can be easily seen that story drifts are smaller than 0.02 as shown in table 3.9.

Table 3.10 : Drift Check (12 storey-15% of base shear).

Joint	Output Case	Case Type	U1	
Text	Text	Text	m	
424	EQX	LinStatic	0.0912	0.016167
425	EQX	LinStatic	0.0815	0.018
426	EQX	LinStatic	0.0707	0.017167
427	EQX	LinStatic	0.0604	0.017
428	EQX	LinStatic	0.0502	0.016
429	EQX	LinStatic	0.0406	0.015
430	EQX	LinStatic	0.0316	0.013833
431	EQX	LinStatic	0.0233	0.011833
432	EQX	LinStatic	0.0162	0.010167
583	EQX	LinStatic	0.0101	0.007667
584	EQX	LinStatic	0.0055	0.006333
638	EQX	LinStatic	0.0017	0.002833

3.1.2 %25 Model

2D model (25% X-direction planar system) with PMM ratio values and colors are indicated in figure 3.3.

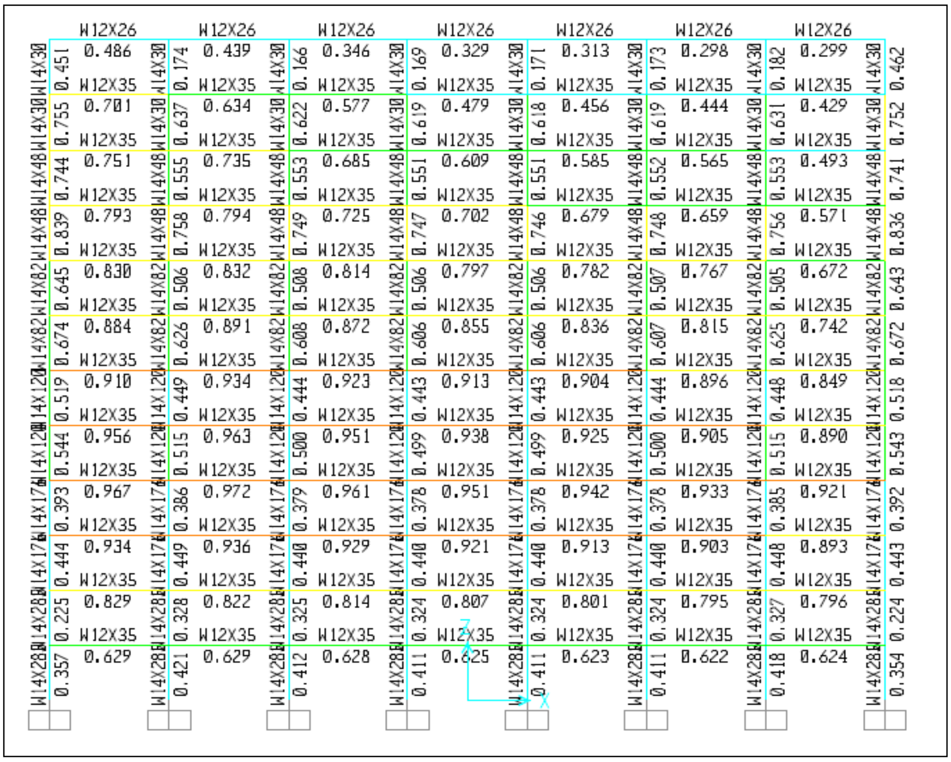

Figure 3.3 : PMM Ratios %25-MF-12 (SAP 2000).

After constituting the 3-D model with the frames of 2-d model, the actual base shear proportion of moment frames to whole system is calculated as %11. 3D model with PMM ratio colors is indicated in figure 3.4 below.

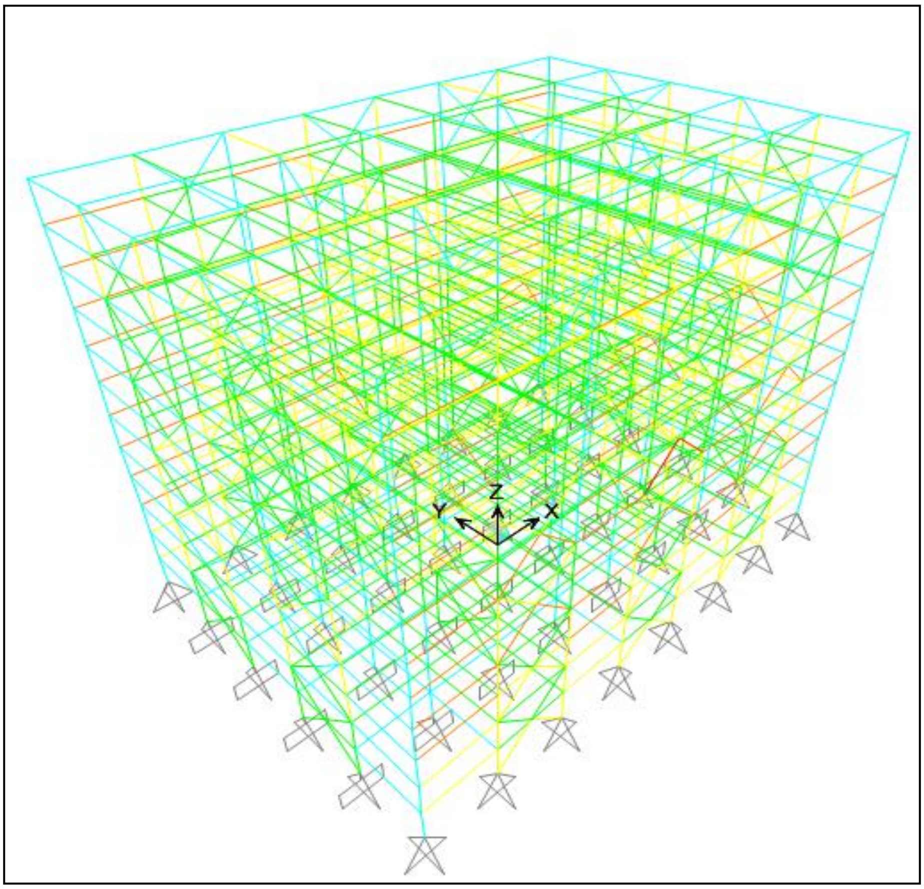

Figure 3.4 : PMM Ratios %25- 12 (SAP 2000).

The story drifts are smaller than 0.02 as shown in table 3.11.

Table 3.11 : Drift Check (12 storey-25% of base shear).

Joint	Output Case	Case Type	U1	
Text	Text	Text	m	
47	EQX	LinStatic	0.0881	0.0881
48	EQX	LinStatic	0.079	0.079
49	EQX	LinStatic	0.0685	0.0685
50	EQX	LinStatic	0.0586	0.0586
51	EQX	LinStatic	0.0487	0.0487
52	EQX	LinStatic	0.0394	0.0394
53	EQX	LinStatic	0.0307	0.0307
54	EQX	LinStatic	0.0227	0.0227
499	EQX	LinStatic	0.0158	0.0158
500	EQX	LinStatic	0.0098	0.0098
596	EQX	LinStatic	0.0054	0.0054
671	EQX	LinStatic	0.0017	0.0017

3.1.3 %40 Model

2D model (40% X-direction planar system) with PMM ratio values and colors are indicated in figure 3.5.

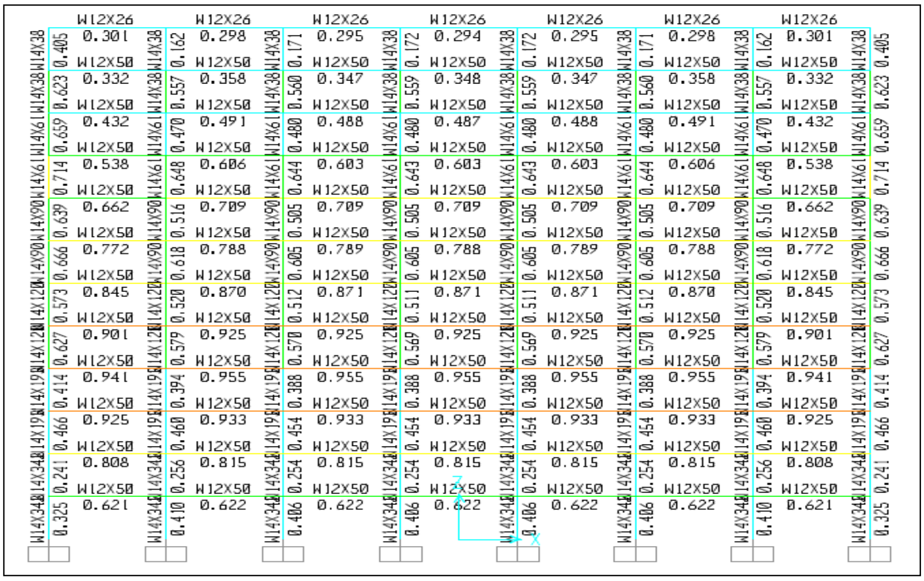

Figure 3.5 : PMM Ratios %40-MF-12 (SAP 2000).

After constituting the 3-D model with the frames of 2-d model, the actual base shear proportion of moment frames to whole system is calculated as %15. 3D model with PMM ratio colors is indicated in figure 3.6 below.

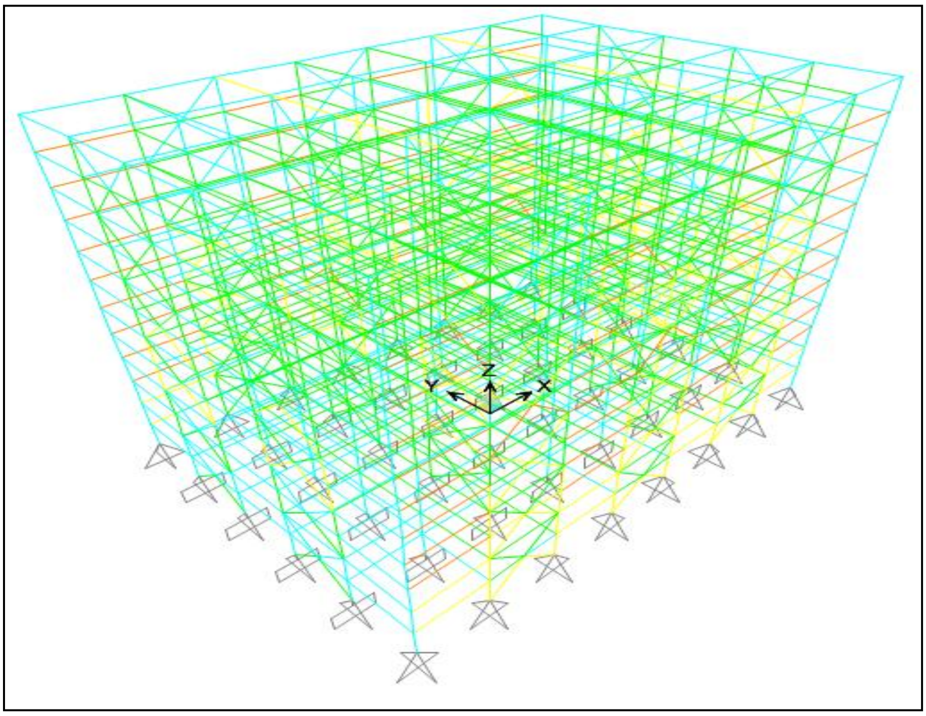

Figure 3.6 : PMM Ratios %40- 12 (SAP 2000).

After constituting the 3-D model with the frames of 2-d model, the actual base shear proportion of moment frames to whole system is calculated as %15. The story drifts are smaller than 0.02 as shown in table 3.11.

Table 3.12 : Drift Check (12 storey-40% of base shear).

Joint	Output Case	Case Type	U1	
Text	Text	Text	m	
47	EQX	LinStatic	0.0881	0.0881
48	EQX	LinStatic	0.079	0.079
49	EQX	LinStatic	0.0685	0.0685
50	EQX	LinStatic	0.0586	0.0586
51	EQX	LinStatic	0.0487	0.0487
52	EQX	LinStatic	0.0394	0.0394
53	EQX	LinStatic	0.0307	0.0307
54	EQX	LinStatic	0.0227	0.0227
499	EQX	LinStatic	0.0158	0.0158
500	EQX	LinStatic	0.0098	0.0098
596	EQX	LinStatic	0.0054	0.0054
671	EQX	LinStatic	0.0017	0.0017

3.2 16-Storey Building

S_s S_1 (mapped acceleration parameters) are taken from maps ASCE 7-05 figure 22-1 through 22-14 as shown in Table 3.13. According to geotechnical information, the site class is D. Note: These values are site specific and are based on MCE values for 2% in 50 year probability (≈2,500 year recurrence) Occupancy category are determined with respect to description of Hazard Represented by Building Collapse. It is chosen as “II” as indicated in Table 3.14.

$$S_{ms} = S_s \times F_a \tag{3.6}$$

$$S_{m1} = S_1 \times F_v \tag{3.7}$$

Table 3.13 : Mapped Acceleration Parameters (ASCE 7-05 figures 22-1).

Parameter	Period
S_s= 1.5 g	T= 0.2 sec
S_1= 0.6 g	T= 1 sec

Table 3.14 : Occupancy Category (ASCE 7-05 table 1-1).

Occupancy Category	2

F_a and F_v the site coefficients are taken from ASCE 7-05 as shown in table 3.15. In addition the design spectral responses are calculated with respect to equation **(3.6)** and **(3.7)** as shown in table 3.16. Seismic Parameters are shown in table 3.17.

Table 3.15 : Site Coefficients (ASCE 7-05 11-4-1).

Parameter	Description
Fa=	1
Fv=	1.5

Table 3.16 : Design Spectral Response (ASCE 7-05 11-4-1).

Parameter	Value		Parameter	Value	
S_{ms}=	S_s*F_a	1.5	S_{ds}=	2/3*S_{ms}	1
S_{m1}=	S_1*F_v	0.9	S_{d1}=	2/3*S_{m1}	0.6

Table 3.17 : Seismic Ground Motion Parameters (ASCE 7-05 11-4-5).

		Period	
T_0=	0.2*S_{d1}/S_{ds}	0.12	Sec
T_s=	S_{d1}/S_{ds}	0.6	Sec

For the dual system with the special moment frame, the coefficients R, C_d and Ω are determined. "ρ" redundancy factor must be determined. It is for usage of more lateral-load resisting elements. The factor varies from 1.0 to 1.5. These parameters are taken from ASCE 7-05 12.3.4.2.

R=7, Ω=2,5, C_d=5, ρ=1,3

The approximate period is calculated as 0.72 sec. with the equation below

$$T_a = C_t \times H_n^{\;x} \tag{3.8}$$

h_n=	48
C_t=	0.0488
x=	0.75

(ASCE 7-05 eq. 12.8-7)

The approximate fundamental building period can be computed from the building height. But from the table, the metric equivalents are used. In addition to this, the upper limits are figured out with respect to equation **(3.8)**. However, while calculating the base shear, the periods from computer analysis are used. Next the upper limits of periods are determined.

Upper Limit

T<	C_u*T_a
T_{max}=	1.246
T_x=	2.290 sec
T_y=	1.844 sec

ASCE 7-05 eq. 12.8-2

T_{max}= 1.246

S_{DS}/(R/1)=1.0g/(7/1.0)=0.14286 (ASCE 7-05 eq. 12.8-3)

Cs need not exceed S_{DS}/(T*(R/1)) for T≤TL=(0.6g)/(0.53*(7/1.0)=0.0686g

Seismic base shear per ASCE 7-05 12.8.1 V=Cs*W

Vertical distribution:

$$F_x = C_{vx} \times V \quad \textbf{(3.9)}$$

$$C_{vx} = \left(W_x \times h_x^k\right) / \left(\sum w_i h_i^k\right) \quad \textbf{(3.10)}$$

Where

F_x is horizontal force at each level X

W_x is the story weight

h_x is the story height

V_x= Σf_i is story shear sum of of levels above.

Exponent related to building period

k 1 for T≤ 0.5s

k 2 for T≥ 2.5s

Use linear interpolation between 0.5 and 2.5 for T=0.53s, k=1.15

Example is based on rigid diaphragm. For this reason all the static forces are added to the system from centre of mass, however in this way the torsion would be neglected. To take torsion effects into consideration, after distribution of forces per stiffness and location, torsional moments to include both natural and accidental torsion must be calculated where:

Mt= %5

M_t= 0.05*42*F_x =2.1 F_x N-S

M_t= 0.05*30*F_x =1.5 F_x E-W

During analysis procedure, 3-D model assumed that resist 15% of base shear is made initially. 3-D model is used to determine force distribution to frames. Seismic weight is calculated by taking 100% of dead loads and wall loads plus 25% of roof and normal floor live loads into consideration. After that, the base shear calculated is distributed to stories. In order to test 25% rule, three different models are created. Then all of them are divided into two with respect to X and Y directions. The models in y direction are neglected. Both models are planar systems that consist only moment frames. Successively, the models adjusted to resist 15%, 25% and 40% of seismic design force. The members are determined. After that for linear static analysis, the equivalent seismic force is calculated with the equation **(3.9)** and distributed to story levels with respect to story feight and story weight as indicated in equation **(3.10)**. Here, in table 3.18, is the equivalent seismic force distribution of story levels:

Table 3.18 : Equivalent Static Force Distribution (16 storey)

Storey	Wx	hx	hx^k	$Wx*hx^k$	C	Fx	Fy	Mx	My
1	7165	3	3.686222	26411.78	0.005392	39.72847	39.72847	83.4298	59.59271
2	7166	6	8.395656	60163.27	0.012283	90.4973	90.4973	190.0443	135.7459
3	7165	9	13.58823	97359.69	0.019878	146.448	146.448	307.5408	219.672
4	7166	12	19.12175	137026.5	0.027977	206.1146	206.1146	432.8406	309.1719
5	7165	15	24.92346	178576.6	0.03646	268.6141	268.6141	564.0896	402.9211
6	7054	18	30.94825	218309	0.044572	328.3793	328.3793	689.5965	492.5689
7	6952	21	37.16511	258371.8	0.052751	388.6417	388.6417	816.1475	582.9625
8	6880	24	43.55127	299632.8	0.061176	450.7062	450.7062	946.4829	676.0592
9	6818	27	50.08924	341508.5	0.069725	513.6954	513.6954	1078.76	770.5431
10	6766	30	56.76511	384072.7	0.078416	577.7204	577.7204	1213.213	866.5806
11	6725	33	63.56753	427491.6	0.08728	643.0308	643.0308	1350.365	964.5462
12	6662	36	70.48703	469584.6	0.095874	706.3469	706.3469	1483.329	1059.52
13	6610	39	77.51562	512378.2	0.104612	770.7169	770.7169	1618.505	1156.075
14	6564	42	84.64641	555619	0.11344	835.7595	835.7595	1755.095	1253.639
15	6696	45	91.87342	615184.4	0.125601	925.3574	925.3574	1943.251	1388.036
16	3188	48	99.19139	316222.1	0.064563	475.6598	475.6598	998.8857	713.4898
	106742			4897913					

Note that the Torsional moments for both directions are taken into account in order to ignore ±5% eccentricity. To calculate these moments the whole length of each dimension is multiplied with story seismic load and 0.05. The seismic force is divided with the number of braces. Here, in table 3.19, are the forces for only one special moment frame system:

Table 3.19 : Equivalent Static Force Distribution for Single SMRF (16 storey).

	0.15	0.25	0.4		0.15	0.25	0.4
16	17.83724	29.72874	47.56598	8	16.90148	28.16913	45.07062
15	34.7009	57.83484	92.53574	7	14.57406	24.29011	38.86417
14	31.34098	52.23497	83.57595	6	12.31422	20.52371	32.83793
13	28.90188	48.16981	77.07169	5	10.07303	16.78838	26.86141
12	26.48801	44.14668	70.63469	4	7.729297	12.88216	20.61146
11	24.11366	40.18943	64.30308	3	5.491799	9.152999	14.6448
10	21.66451	36.10752	57.77204	2	3.393649	5.656081	9.04973
9	19.26358	32.10596	51.36954	1	1.489818	2.48303	3.972847

After the analysis the profiles are chosen as in table 3.20:

Table 3.20 : Column and Beam Sections (16 storey).

	15% model		25% model		40% model	
STOREY	Column	Beam	Column	Beam	Column	Beam
1	W14X233	W12X35	W14X283	W12X40	W14X426	W12X53
2	W14X233	W12X35	W14X283	W12X40	W14X426	W12X53
3	W14X145	W12X35	W14X233	W12X40	W14X257	W12X53
4	W14X145	W12X35	W14X233	W12X40	W14X257	W12X53
5	W14X120	W12X35	W14X193	W12X40	W14X193	W12X53
6	W14X120	W12X35	W14X193	W12X40	W14X193	W12X53
7	W14X99	W12X35	W14X176	W12X40	W14X176	W12X53
8	W14X99	W12X35	W14X176	W12X40	W14X176	W12X53
9	W14X99	W12X35	W14X120	W12X40	W14X120	W12X53
10	W14X99	W12X35	W14X120	W12X40	W14X120	W12X53
11	W14X82	W12X35	W14X82	W12X40	W14X82	W12X53
12	W14X82	W12X35	W14X82	W12X40	W14X82	W12X53
13	W14X61	W12X35	W14X61	W12X40	W14X61	W12X53
14	W14X61	W12X35	W14X61	W12X40	W14X61	W12X53
15	W14X38	W12X35	W14X38	W12X40	W14X38	W12X53
16	W14X38	W12X16	W14X38	W12X16	W14X38	W12X26

After the initial analysis the braces are chosen as in following table 3.21:

Table 3.21 : Brace (X-Y Directions) Sections (16 storey)

Storey	X	Y	Storey	X	Y
16	100x100x10	100x100x10	8	200x200x14	200x200x14
15	100x100x10	100x100x10	7	200x200x14	200x200x14
14	120x120x12	120x120x12	6	200x200x16	200x200x16
13	120x120x12	120x120x12	5	200x200x16	200x200x16
12	150x150x10	150x150x10	4	200x200x20	200x200x20
11	150x150x10	150x150x10	3	200x200x20	200x200x20
10	180x180x12	180x180x12	2	220x220x20	220x220x20
9	180x180x12	180x180x12	1	220x220x20	220x220x20

3.2.1 %15 Model

2D model (15% X-direction planar system) with PMM ratio values and colors are indicated in figure 3.7.

Figure 3.7 : PMM Ratios %15-MF-16 (SAP 2000).

After constituting the 3-D model with the frames of 2-d model, the actual base shear proportion of moment frames to whole system is calculated as %5. 3D model with PMM ratio colors is indicated in figure 3.8 below.

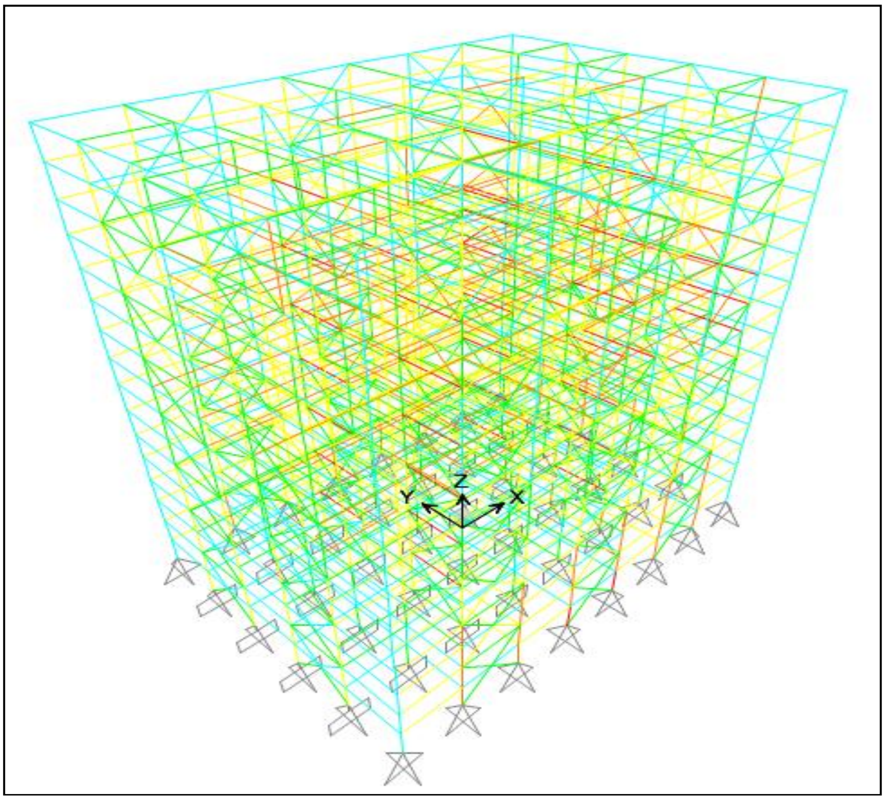

Figure 3.8 : PMM Ratios %15- 16 (SAP 2000).

The story drifts are smaller than 0.02 as shown in table 3.22.

Table 3.22 : Drift Check (16 storey-%15 of base shear).

Joint	Output Case	Case Type	U1	
Text	Text	Text	m	
424	EQX	LinStatic	0.1546	0.018833
425	EQX	LinStatic	0.1433	0.018833
426	EQX	LinStatic	0.132	0.019167
427	EQX	LinStatic	0.1205	0.018667
428	EQX	LinStatic	0.1093	0.018833
429	EQX	LinStatic	0.098	0.018833
430	EQX	LinStatic	0.0867	0.0195
431	EQX	LinStatic	0.075	0.02
432	EQX	LinStatic	0.063	0.019167
583	EQX	LinStatic	0.0515	0.018833
584	EQX	LinStatic	0.0402	0.017833
638	EQX	LinStatic	0.0295	0.014833
692	EQX	LinStatic	0.0206	0.013333
583	EQX	LinStatic	0.0126	0.0095
584	EQX	LinStatic	0.0069	0.008167
638	EQX	LinStatic	0.002	0.003333

3.2.2 %25 Model

2D model (25% X-direction planar system) with PMM ratio values and colors are indicated in figure 3.9.

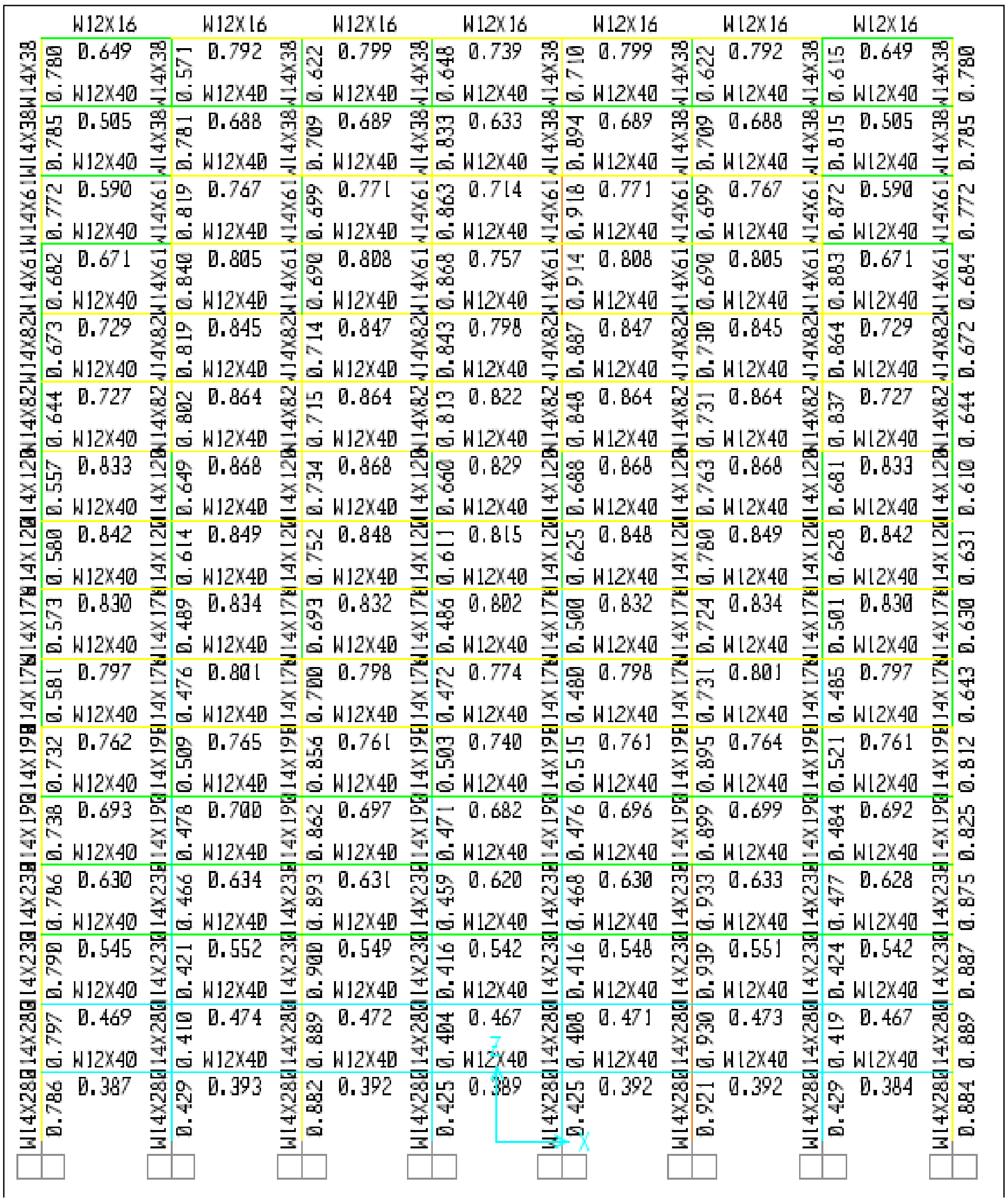

Figure 3.9 : PMM Ratios %25-MF-16 (SAP 2000).

After constituting the 3-D model with the frames of 2-d model, the actual base shear proportion of moment frames to whole system is calculated as %8. Even though, the whole members in two dimensional model are enough to carry loads, they must be checked in three dimensional model too. So that, they controlled in three model and 3D model with PMM ratio colors is indicated in figure 3.10 below.

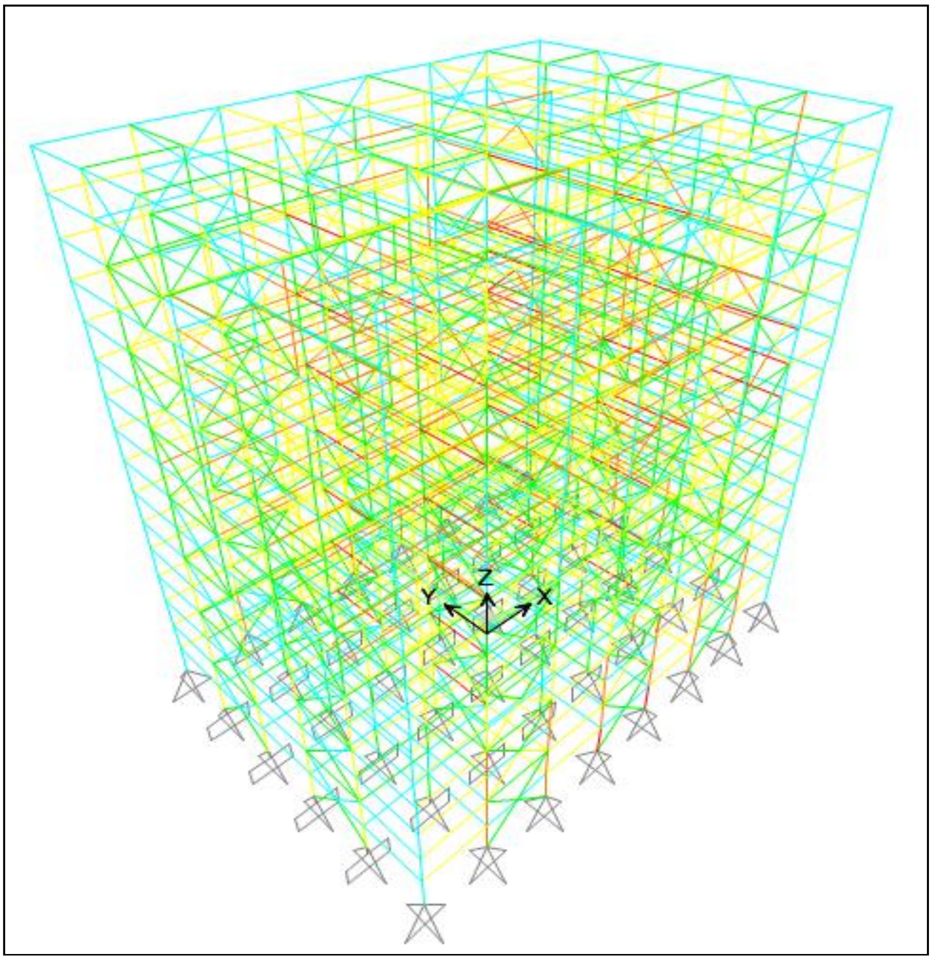

Figure 3.10 : PMM Ratios %25- 16 (SAP 2000).

The story drifts are smaller than 0.02 as shown in table 3.23.

Table 3.23 : Drift Check (16 storey-%25 of base shear).

Joint	Output Case	Case Type	U1	
Text	Text	Text	m	
424	EQX	LinStatic	0.1482	0.018333
425	EQX	LinStatic	0.1372	0.019
426	EQX	LinStatic	0.1258	0.02
427	EQX	LinStatic	0.1138	0.019667
428	EQX	LinStatic	0.102	0.019333
429	EQX	LinStatic	0.0904	0.019833
430	EQX	LinStatic	0.0785	0.019667
431	EQX	LinStatic	0.0667	0.018667
432	EQX	LinStatic	0.0555	0.017833
583	EQX	LinStatic	0.0448	0.016333
584	EQX	LinStatic	0.035	0.0155
638	EQX	LinStatic	0.0257	0.012833
692	EQX	LinStatic	0.018	0.0115
583	EQX	LinStatic	0.0111	0.0085
584	EQX	LinStatic	0.006	0.007
638	EQX	LinStatic	0.0018	0.003

3.2.3 %40 Model

2D model (40% X-direction planar system) with PMM ratio values and colors are indicated in figure 3.11.

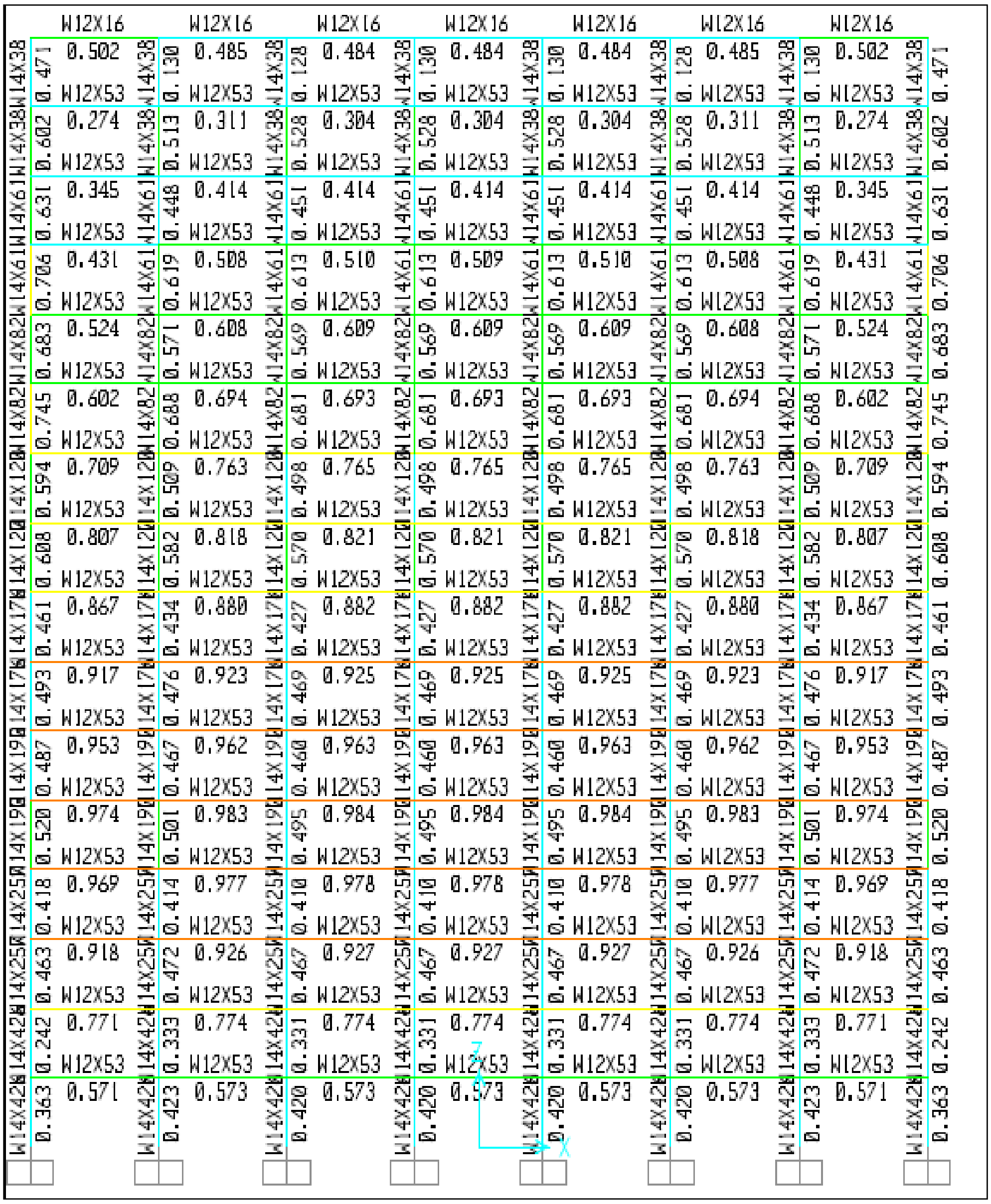

Figure 3.11 : PMM Ratios %40-MF-16 (SAP 2000).

After constituting the 3-D model with the frames of 2-d model, the actual base shear proportion of moment frames to whole system is calculated as %14. Even though, the whole members in two dimensional model are enough to carry loads, they must be checked in three dimensional model too. So that, they controlled in three model and 3D model with PMM ratio colors is indicated in figure 3.12 below.

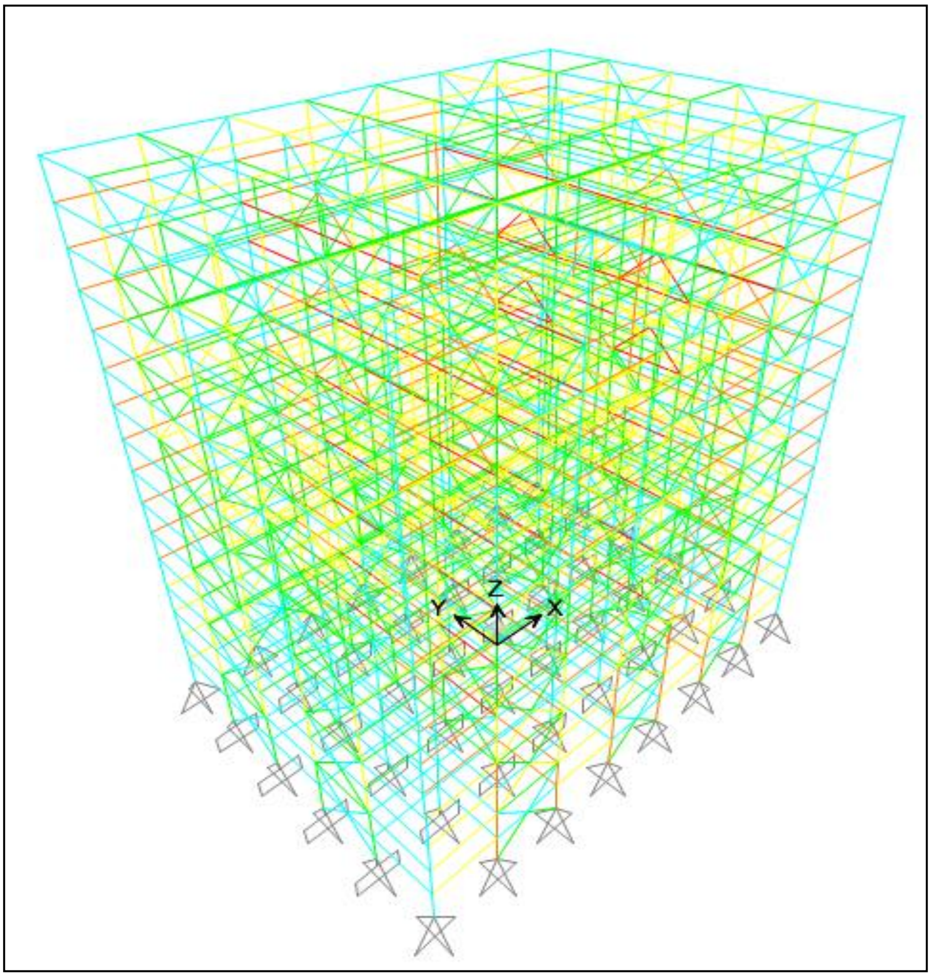

Figure 3.12 : PMM Ratios %40- 16 (SAP 2000).

The story drifts are smaller than 0.02 as shown in table 3.24.

Table 3.24 : Drift Check (16 storey %40 of base shear).

Joint	Output Case	Case Type	U1	
Text	Text	Text	m	
424	EQX	LinStatic	0.1358	0.015333
425	EQX	LinStatic	0.1266	0.017
426	EQX	LinStatic	0.1164	0.017333
427	EQX	LinStatic	0.106	0.018167
428	EQX	LinStatic	0.0951	0.0185
429	EQX	LinStatic	0.084	0.018833
430	EQX	LinStatic	0.0727	0.017833
431	EQX	LinStatic	0.062	0.017167
432	EQX	LinStatic	0.0517	0.0165
583	EQX	LinStatic	0.0418	0.015167
584	EQX	LinStatic	0.0327	0.014333
638	EQX	LinStatic	0.0241	0.012
692	EQX	LinStatic	0.0169	0.010833
583	EQX	LinStatic	0.0104	0.008
584	EQX	LinStatic	0.0056	0.0065
638	EQX	LinStatic	0.0017	0.002833

3.3 20-Storey Building

S_s S_1 (mapped acceleration parameters) are taken from maps ASCE 7-05 figure 22-1 through 22-14 as shown in Table 3.25. According to geotechnical information, the site class is D. Note: These values are site specific and are based on MCE values for 2% in 50 year probability (≈2,500 year recurrence) Occupancy category are determined with respect to description of Hazard Represented by Building Collapse. It is chosen as "II" as indicated in Table 3.26.

$$S_{ms} = S_s \times F_a \quad \textbf{(3.11)}$$

$$S_{m1} = S_1 \times F_v \quad \textbf{(3.12)}$$

Table 3.25 : Mapped Acceleration Parameters (ASCE 7-05 figures 22-1).

Parameter		Period	
S_s=	1.5 g	T=	0.2 sec
S_1=	0.6 g	T=	1 sec

Table 3.26 : Occupancy Category (ASCE 7-05 table 1-1).

Occupancy Category	2

F_a and F_v the site coefficients are taken from ASCE 7-05 as shown in table 3.27. In addition the design spectral responses are calculated with respect to equation **(3.11)** and **(3.12)** as shown in table 3.28. Seismic Parameters are shown in table 3.29.

Table 3.27 : Site Coefficients (ASCE 7-05 11-4-1).

Parameter	Description
Fa=	1
Fv=	1.5

Table 3.28 : Design Spectral Response (ASCE 7-05 11-4-1).

Parameter	Value		Parameter	Value	
S_{ms}=	S_s*F_a	1.5	S_{ds}=	2/3*S_{ms}	1
S_{m1}=	S_1*F_v	0.9	S_{d1}=	2/3*S_{m1}	0.6

Table 3.29 : Seismic Ground Motion Parameters (ASCE 7-05 11-4-5).

		Period	
T_0=	0.2*S_{d1}/S_{ds}	0.12	Sec
T_s=	S_{d1}/S_{ds}	0.6	Sec

For the dual system with the special moment frame, the coefficients R, C_d and Ω are determined. "ρ" redundancy factor must be determined. It is for usage of more lateral-load resisting elements. The factor varies from 1.0 to 1.5. These parameters are taken from ASCE 7-05 12.3.4.2**.**

R=7, Ω=2,5, C_d=5, ρ=1,3

The approximate period is calculated as 0.72 sec. with the equation **(3.13)** below

$$T_a = C_t \times H_n^{\;x} \tag{3.13}$$

h_n=	60
C_t=	0.0488
x=	0.75

(ASCE 7-05 eq. 12.8-7)

The approximate fundamental building period can be computed from the building height. But from the table, the metric equivalents are used. In addition to this, the upper limits are figured out with respect to equation **(3.13)**. However, while calculating the base shear, the periods from computer analysis are used.

Upper Limit

T<	C_u*T_a
T_{max}=	3.130
T_x=	2.962 sec
T_y=	1.844 sec

ASCE 7-05 eq. 12.8-2

T_{max}= 2.962

S_{DS}/(R/1)=1.0g/(7/1.0)=0.14286 (ASCE 7-05 eq. 12.8-3)

Cs need not exceed S_{DS}/(T*(R/1)) for T≤TL=(0.6g)/(0.53*(7/1.0)=0.0686g

Seismic base shear per ASCE 7-05 12.8.1 V=Cs*W

Vertical distribution:

$$F_x = C_{vx} \times V \tag{3.14}$$

$$C_{vx} = \left(W_x \times h_x^k\right) / \left(\sum w_i h_i^k\right) \tag{3.15}$$

Where

F_x is horizontal force at each level X

W_x is the story weight

h_x is the story height

$V_x = \Sigma f_i$ is story shear sum of of levels above.

Exponent related to building period

k 1 for $T \leq 0.5s$

k 2 for $T \geq 2.5s$

Use linear interpolation between 0.5 and 2.5 for T=0.53s, k=1.15

Example is based on rigid diaphragm. For this reason all the static forces are added to the system from centre of mass, however in this way the torsion would be neglected. To take torsion effects into consideration, after distribution of forces per stiffness and location, torsional moments to include both natural and accidental torsion must be calculated where:

Mt= %5

$M_t = 0.05*42*F_x = 2.1\ F_x$ N-S

$M_t = 0.05*30*F_x = 1.5\ F_x$ E-W

During analysis procedure, 3-D model assumed that resist 15% of base shear is made initially. 3-D model is used to determine force distribution to frames. Seismic weight is calculated by taking 100% of dead loads and wall loads plus 25% of roof and normal floor live loads into consideration. After that, the base shear calculated is distributed to stories. In order to test 25% rule, three different models are created. Then all of them are divided into two with respect to X and Y directions. The models in y direction are neglected. Both models are planar systems that consist only moment frames. Successively, the models adjusted to resist 15%, 25% and 40% of seismic design force. The members are determined. After that for linear static analysis, the equivalent seismic force is calculated with the equation **(3.14)** and distributed to story levels with respect to story feight and story weight as indicated in equation **(3.15)**. Here, in table 3.30, is the equivalent seismic force distribution of story levels:

Table 3.30 : Equivalent Static Force Distribution (20 storey).

Storey	Wx	hx	hx^k	$Wx*hx^k$	C	Fx	Fy	Mx	My
1	7168	3	5.05538	36236.97	0.00159	12.4221	12.4221	26.0864	18.6332
2	7168	6	14.0531	100732.8	0.00442	34.5314	34.5314	72.516	51.7972
3	7168	9	25.5569	183191.7	0.00804	62.7985	62.7985	131.877	94.1977
4	7168	12	39.0654	280020.8	0.01228	95.9917	95.9917	201.583	143.988
5	7168	15	54.2919	389164	0.01707	133.406	133.406	280.153	200.109
6	7108	18	71.0439	504980.2	0.02215	173.108	173.108	363.527	259.663
7	7048	21	89.1812	628549.3	0.02757	215.468	215.468	452.483	323.202
8	6995	24	108.595	759625.1	0.03332	260.401	260.401	546.842	390.602
9	6941	27	129.2	896775.2	0.03934	307.417	307.417	645.575	461.125
10	6922	30	150.923	1044685	0.04582	358.12	358.12	752.053	537.181
11	6904	33	173.703	1199248	0.0526	411.105	411.105	863.32	616.657
12	6837	36	197.491	1350242	0.05923	462.866	462.866	972.019	694.299
13	6769	39	222.239	1504336	0.06599	515.69	515.69	1082.95	773.534
14	6719	42	247.909	1665702	0.07306	571.006	571.006	1199.11	856.509
15	6669	45	274.466	1830413	0.08029	627.47	627.47	1317.69	941.204
16	6635	48	301.878	2002958	0.08786	686.618	686.618	1441.9	1029.93
17	6604	51	330.116	2180083	0.09563	747.337	747.337	1569.41	1121.01
18	6573	54	359.154	2360720	0.10355	809.26	809.26	1699.45	1213.89
19	6562	57	388.969	2552417	0.11196	874.974	874.974	1837.45	1312.46
20	3165	60	419.54	1327843	0.05824	455.188	455.188	955.894	682.781
	134291			22797924					

Note that the Torsional moments for both directions are taken into account in order to ignore ±5% eccentricity. To calculate these moments the whole length of each dimension is multiplied with story seismic load and 0.05. The seismic force is divided with the number of braces. These loads are figured based on assumption that there is a main model which has section members calculated approximately. Then the seismic load divided into four due to existence of four moment frame in three dimensional model. Here, in table 3.31, are the forces for only one special moment frame system:

Table 3.31 : Equivalent Static Force Distribution for Single SMRF (20 storey).

FOR 15%, 25% 40% MODEL

	0.15	0.25	0.4
20	17.06953	28.44922	45.51875
19	32.81153	54.68588	87.4974
18	30.34724	50.57874	80.92598
17	28.02515	46.70858	74.73372
16	25.74818	42.91363	68.66182
15	23.53011	39.21685	62.74696
14	21.41273	35.68789	57.10063
13	19.33836	32.2306	51.56896
12	17.35748	28.92913	46.2866
11	15.41642	25.69404	41.11046
10	13.42951	22.38252	35.81203
9	11.52812	19.21353	30.74165
8	9.765042	16.27507	26.04011
7	8.080052	13.46675	21.54681
6	6.491561	10.81927	17.31083
5	5.002734	8.33789	13.34062
4	3.59969	5.999484	9.599174
3	2.354944	3.924906	6.279849
2	1.294929	2.158215	3.453143
1	0.465829	0.776382	1.242211

After the analysis is completed, every member capacity is checked carefully. Some of the elements changed due to drift check. For some of them, a few times trial and error method is applicated between two dimensional and three dimensional models. Finally all the member sections are determined by considering economy. The profiles are chosen as in table 3.32:

Table 3.32 : Column and Beam Sections (20 storey).

	15% model		25% model		40% model	
STOREY	Column	Beam	Column	Beam	Column	Beam
1	W14X398	W12X35	W14X455	W12X40	W14X500	W12X53
2	W14X398	W12X35	W14X455	W12X40	W14X500	W12X53
3	W14X311	W12X35	W14X311	W12X40	W14X342	W12X53
4	W14X311	W12X35	W14X311	W12X40	W14X342	W12X53
5	W14X283	W12X35	W14X283	W12X40	W14X283	W12X53
6	W14X283	W12X35	W14X283	W12X40	W14X283	W12X53
7	W14X233	W12X35	W14X233	W12X40	W14X233	W12X53
8	W14X233	W12X35	W14X233	W12X40	W14X233	W12X53
9	W14X193	W12X35	W14X193	W12X40	W14X193	W12X53
10	W14X193	W12X35	W14X193	W12X40	W14X193	W12X53
11	W14X176	W12X35	W14X176	W12X40	W14X176	W12X53
12	W14X176	W12X35	W14X176	W12X40	W14X176	W12X53
13	W14X132	W12X35	W14X132	W12X40	W14X132	W12X53
14	W14X132	W12X35	W14X132	W12X40	W14X132	W12X53
15	W14X99	W12X35	W14X109	W12X40	W14X109	W12X53
16	W14X99	W12X16	W14X109	W12X16	W14X109	W12X53
17	W14X74	W12X35	W14X82	W12X40	W14X82	W12X53
18	W14X74	W12X35	W14X82	W12X40	W14X82	W12X53
19	W14X48	W12X35	W14X53	W12X40	W14X53	W12X53
20	W14X48	W12X22	W14X53	W12X22	W14X53	W12X22

After the initial analysis is completed, as beams and columns, the brace sections are also determined. In fact the brace member sections do not differ from model to model. They are all same in main model and the other three model. Because in this paper, the moment frame shear force capacities or in other words the moment frame member sizes are more important. The braces are chosen as in following table 3.33:

Table 3.33 : Brace (X-Y Directions) Sections (20 storey)

Storey	X	Y	Storey	X	Y
20	100x100x10	100x100x10	10	200x200x14	200x200x14
19	100x100x10	100x100x10	9	200x200x14	200x200x14
18	120x120x10	120x120x10	8	200x200x16	200x200x16
17	120x120x10	120x120x10	7	200x200x16	200x200x16
16	140x140x10	140x140x10	6	200x200x20	200x200x20
15	140x140x10	140x140x10	5	200x200x20	200x200x20
14	160x160x12	160x160x12	4	220x220x20	220x220x20
13	160x160x12	160x160x12	3	220x220x20	220x220x20
12	180x180x12	180x180x12	2	220x220x20	220x220x20
11	180x180x12	180x180x12	1	220x220x20	220x220x20

3.3.1 %15 Model

2D model (15% X-direction planar system) with PMM ratio values and colors are indicated in figure 3.13.

Figure 3.13 : PMM Ratios %15-MF-20 (SAP 2000).

After constituting the 3-D model with the frames of 2-d model, the actual base shear proportion of moment frames to whole system is calculated as %9. 3D model with PMM ratio colors is indicated in figure 3.14 below.

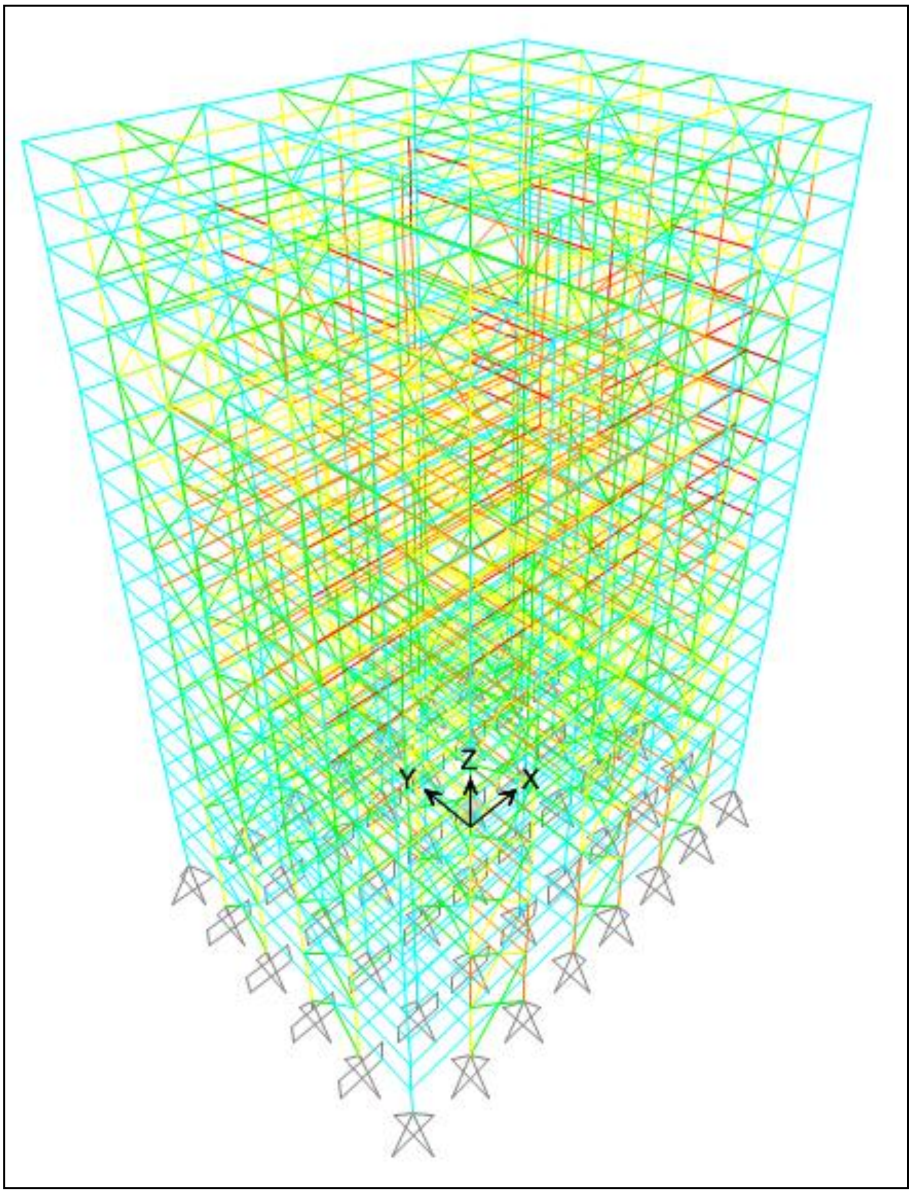

Figure 3.14 : PMM Ratios %15- 20 (SAP 2000).

The story drifts are normalized by story heights. For each model, the story drifts are calculated with respect to story numbers. During linear static analysis, some of the elements are changed due to the fact that they do not satisfy the drift limits as mentioned in the previous part. Until the drift limit satisfaction is supplied, some of the stories drift ratios become critical. However the story drifts are smaller than 0.02 as shown in table 3.34.

Table 3.34 : Drift Check (20 storey-%15 of base shear).

Joint	Output Case	Case Type	U1	
Text	Text	Text	m	
424	EQX	LinStatic	0.1779	0.019333
425	EQX	LinStatic	0.1663	0.019333
426	EQX	LinStatic	0.1547	0.02
427	EQX	LinStatic	0.1427	0.019667
428	EQX	LinStatic	0.1309	0.018333
429	EQX	LinStatic	0.1199	0.017167
430	EQX	LinStatic	0.1096	0.017
431	EQX	LinStatic	0.0994	0.001833
432	EQX	LinStatic	0.0983	0.019667
583	EQX	LinStatic	0.0865	0.019167
584	EQX	LinStatic	0.075	0.02
638	EQX	LinStatic	0.063	0.018333
692	EQX	LinStatic	0.052	0.011667
583	EQX	LinStatic	0.045	0.021333
584	EQX	LinStatic	0.0322	0.014167
638	EQX	LinStatic	0.0237	0.011833
692	EQX	LinStatic	0.0166	0.010667
583	EQX	LinStatic	0.0102	0.007667
584	EQX	LinStatic	0.0056	0.0065
638	EQX	LinStatic	0.0017	0.002833

3.3.2 %25 Model

2D model (15% X-direction planar system) with PMM ratio values and colors are indicated in figure 3.15. Then 3-D model is created again the frames which are determined with the analysis of 2-d model, the actual base shear proportion of moment frames to whole system is calculated as %13. Compare to the 12 storey and 16 storey models, the base shear ratios are greater. This change is not significant. The important thing that matters here is the base shear ratios are lower than the values which are assumed initially.

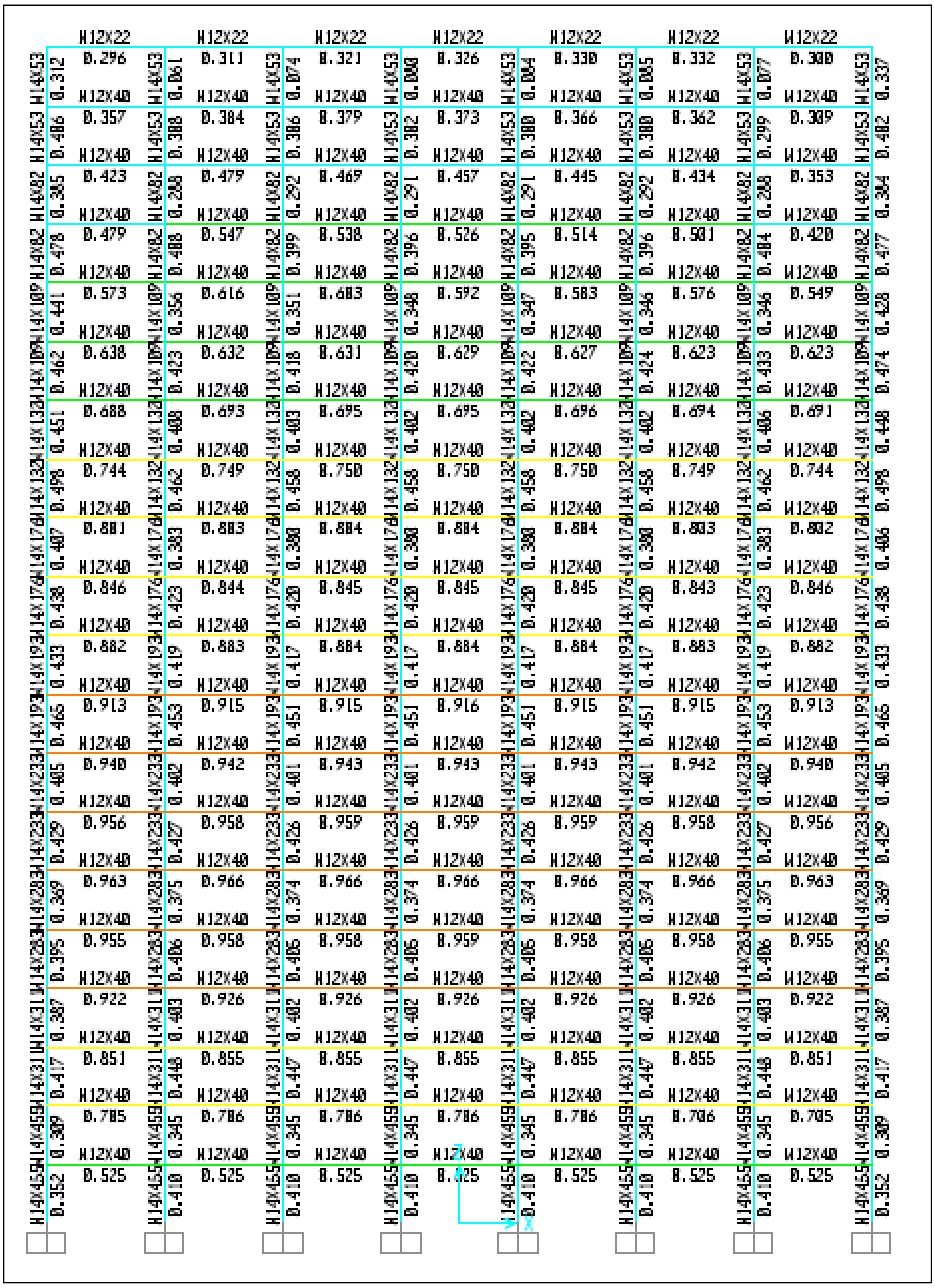

Figure 3.15 : PMM Ratios %25-MF-20 (SAP 2000).

After the completion of the three dimensional analysis, the whole member section sizes are determined. 3D model with PMM ratio colors is indicated in figure 3.16 below. The story drifts are normalized by story heights. During linear static analysis, some of the elements are changed because they do not satisfy the drift limits as mentioned in the previous part. For each model, the story drifts are calculated with respect to story numbers. the story drifts are smaller than 0.02 as shown in table 3.35 successively.

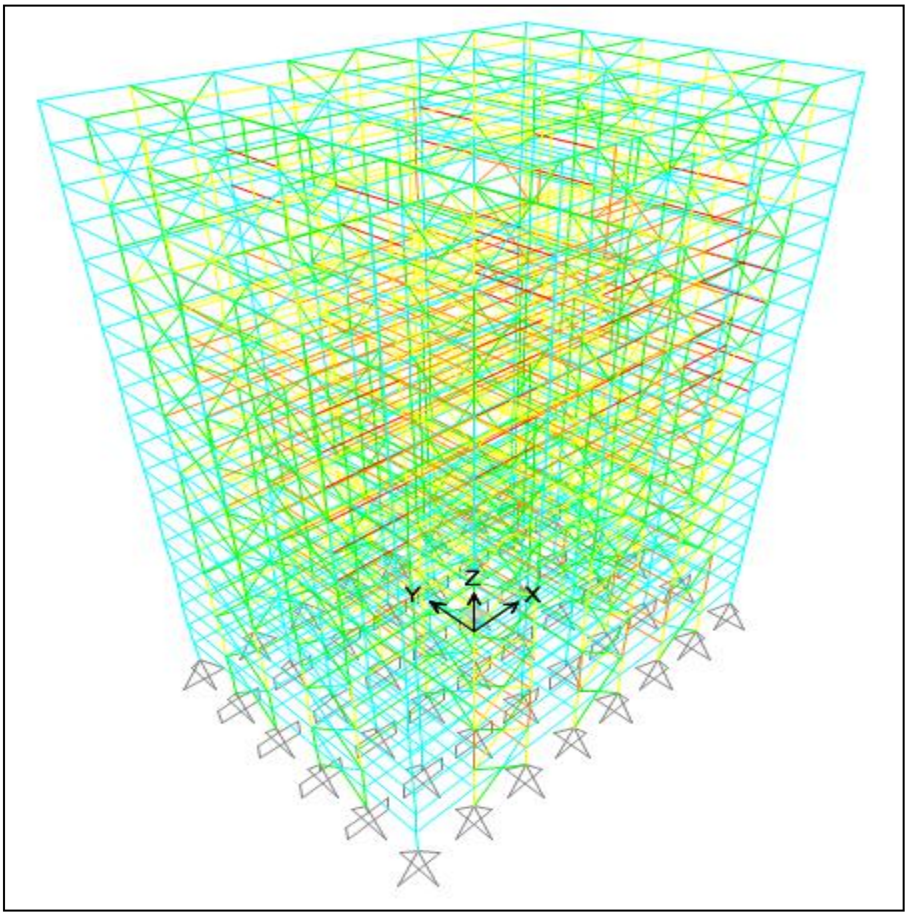

Figure 3.16 : PMM Ratios %25- 20 (SAP 2000).

Table 3.35 : Drift Check (20 storey-%25 of base shear).

Joint	Output Case	Case Type	U1	
Text	Text	Text	m	
424	EQX	LinStatic	0.1893	0.019167
425	EQX	LinStatic	0.1778	0.018833
426	EQX	LinStatic	0.1665	0.0195
427	EQX	LinStatic	0.1548	0.019167
428	EQX	LinStatic	0.1433	0.02
429	EQX	LinStatic	0.1313	0.019833
430	EQX	LinStatic	0.1194	0.02
431	EQX	LinStatic	0.1074	0.019
432	EQX	LinStatic	0.096	0.019667
583	EQX	LinStatic	0.0842	0.019833
584	EQX	LinStatic	0.0723	0.019167
638	EQX	LinStatic	0.0608	0.018
692	EQX	LinStatic	0.05	0.017
583	EQX	LinStatic	0.0398	0.015167
584	EQX	LinStatic	0.0307	0.013833
638	EQX	LinStatic	0.0224	0.011333
692	EQX	LinStatic	0.0156	0.010167
583	EQX	LinStatic	0.0095	0.007167
584	EQX	LinStatic	0.0052	0.006
638	EQX	LinStatic	0.0016	0.002667

3.3.3 %40 Model

2D model (40% X-direction planar system) with PMM ratio values and colors are indicated in figure 3.13.

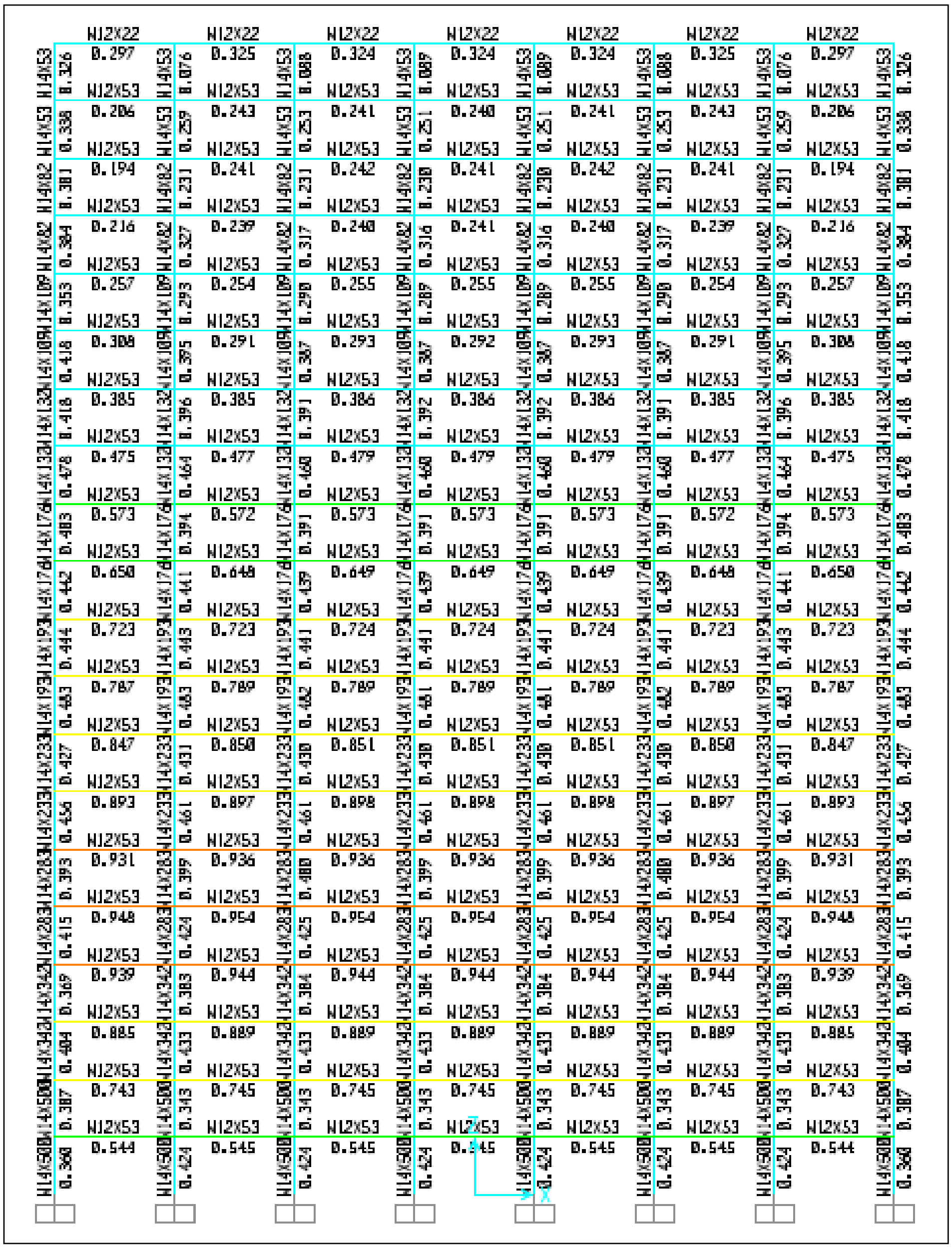

Figure 3.17 : PMM Ratios %40-MF-20 (SAP 2000).

After constituting the 3-D model with the frames of 2-d model, the actual base shear proportion of moment frames to whole system is calculated as %16. After the completion of the three dimensional analysis, the whole section sizes are determined. 3D model with PMM ratio colors are indicated in figure 3.18 below. In the table 3.36, it can be easily seen that story drifts are smaller than 0.02.

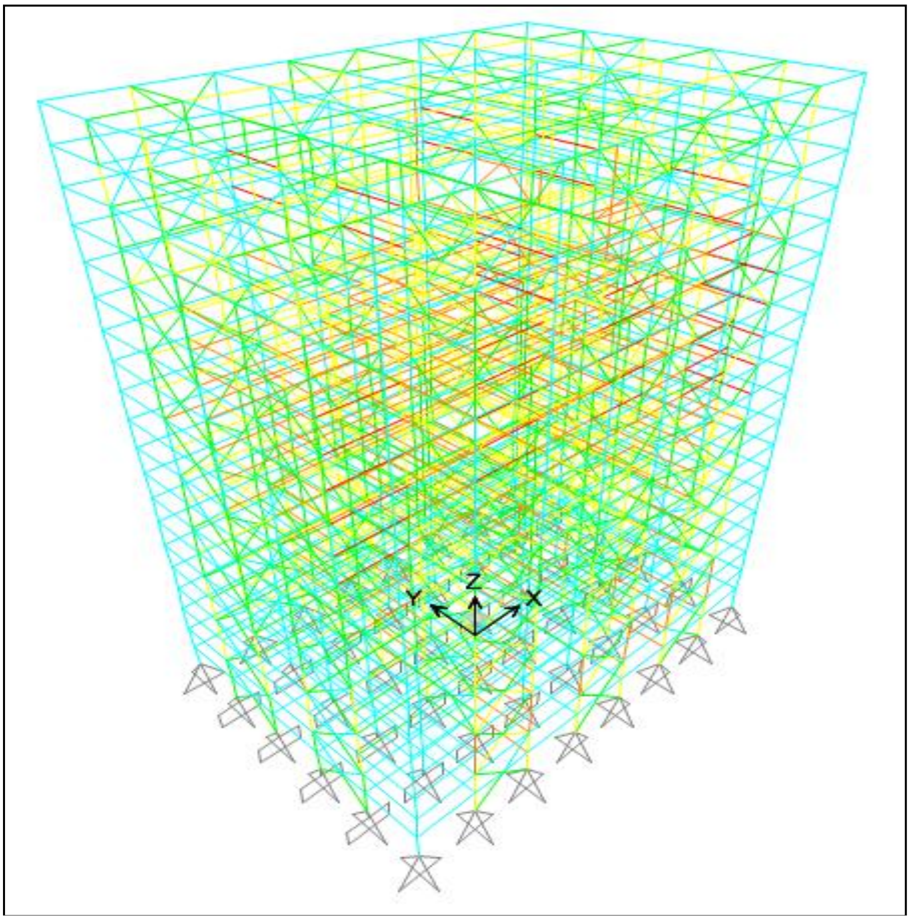

Figure 3.18 : PMM Ratios %40- 20 (SAP 2000).

Table 3.36 : Drift Check (20 storey-%40 of base shear).

Joint	Output Case	Case Type	U1	
Text	Text	Text	m	
424	EQX	LinStatic	0.1907	0.017167
425	EQX	LinStatic	0.1804	0.018667
426	EQX	LinStatic	0.1692	0.019167
427	EQX	LinStatic	0.1577	0.02
428	EQX	LinStatic	0.1457	0.02
429	EQX	LinStatic	0.1337	0.019833
430	EQX	LinStatic	0.1218	0.019667
431	EQX	LinStatic	0.11	0.019333
432	EQX	LinStatic	0.0984	0.019
583	EQX	LinStatic	0.087	0.02
584	EQX	LinStatic	0.075	0.019167
638	EQX	LinStatic	0.0635	0.019167
692	EQX	LinStatic	0.052	0.02
583	EQX	LinStatic	0.04	0.017833
584	EQX	LinStatic	0.0293	0.013333
638	EQX	LinStatic	0.0213	0.010833
692	EQX	LinStatic	0.0148	0.0095
583	EQX	LinStatic	0.0091	0.006833
584	EQX	LinStatic	0.005	0.005667
638	EQX	LinStatic	0.0016	0.002667

Table 3.37 : Base Shear Distribution.

	BF(kN)	MF(kN)	MF/TS (%)
Model 15-12	6317	617	8
Model 25-12	6089	841	11
Model 40-12	5814	1101	15
Model 15-16	6490	377	5
Model 25-16	6870	568	8
Model 40-16	6339	1028	14
Model 15-20	6551	653	9
Model 25-20	6189	889	13
Model 40-20	5952	1115	16

Briefly, the base shear distribution between BF and MF is not like as it is assumed. Moment frames are designed apart from the 3D model and they are designed according to proportions %15, 25 and 40 but in the 3d models they share different level of lateral forces as shown above in table 3.37. The proportions are lower than assumption.

4. NONLINEAR STATIC ANALYSIS

Before modelling whole structure, a push-over analysis was carried out in to test whether the assumptions are true or not. For this reason, two separate models in SAP 2000 are examined. In the figure 4.1, it can be seen that modelling assumptions are available. ASCE 41-06 was used to determine the nonlinear behaviour of elements and to make assessments in the end. Firstly, according to ASCE 41-06 there is a certain distinction between primary and secondary elements. The definition in ASCE 41-06 indicates that secondary elements carry only axial loads and do not support any lateral force like earthquake or wind. This causes moment frames and braces are resisting together against the lateral forces so that we made an assumption that all the elements are primary elements. For that reason, all the performance criteria are assigned elements as they are primary elements instead of secondary elements.

4.1 Preliminary Studies on Modelling

The dead load on the beam is 6 kN/m, live load on the beam is 4 kN/m and lateral load load is 5 kN acting on the joint which we will monitor during pushover analysis. W12/22 profile was chosen as beam element and W14/48 was chosen as column element. Tube 200x200x20 was assigned to braces. System represents a single story of concentrically braces. Monitored displacement is calculated as the %4 of storey height. So the system was pushed 3*0.04=0.12.

In the figure 4.1 there are hinge places in SAP 2000 model. PMM Hinges are assigned to the columns at the bottom part. Moment-rotation hinges are assigned to the beam near the brace connection. Also axial hinges are assigned to the brace in the middle part. All hinges are auto hinges, however all the nonlinear properties are calculated according to the ASCE 41-06. Even though, the hinge properties that are used in SAP 2000 are with respect to FEMA.

The hand calculations are done according to ASCE 41-06. As expected, plastic hinge properties are very close to each other. For this reason, the analysis can be expected true. In the 4.2 part, all the graphs from AISC 41-06 are shown and the required hand calculation is done. All types of plastic hinge (moment hinge, PMM hinge and axial hinge) are examined separately.

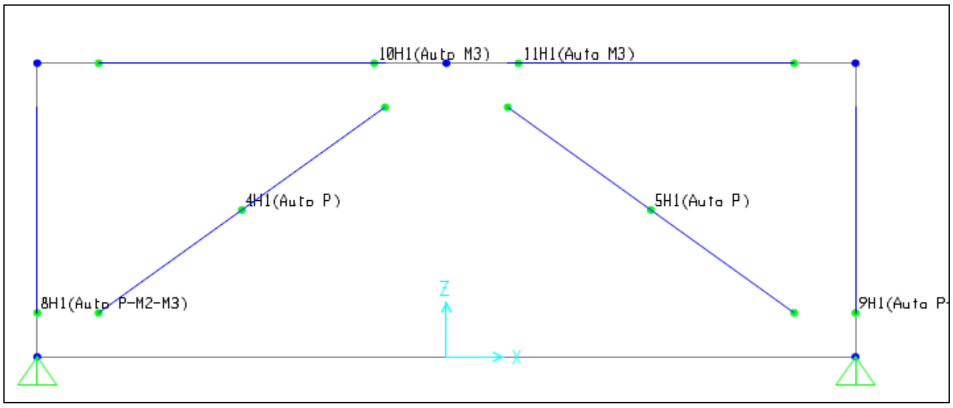

Figure 4.1 : Hinge places For Push-Over Analysis.

4.2 Plastic Hinges Definition

4.2.1 Moment Hinge

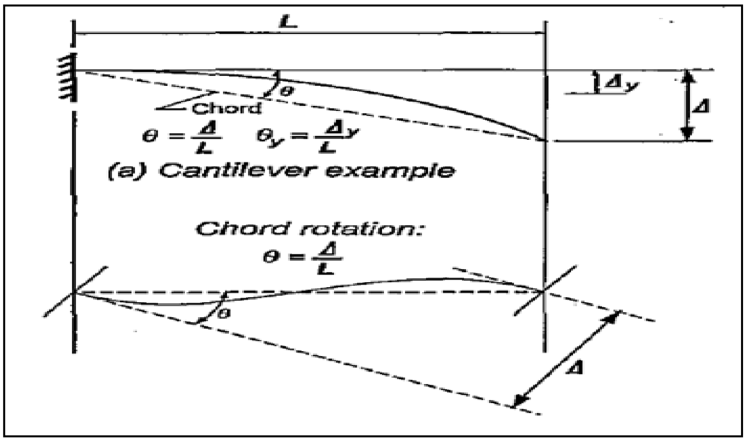

Figure 4.2 : Definition of Chord Rotation (ASCE41-06, figure 5-2).

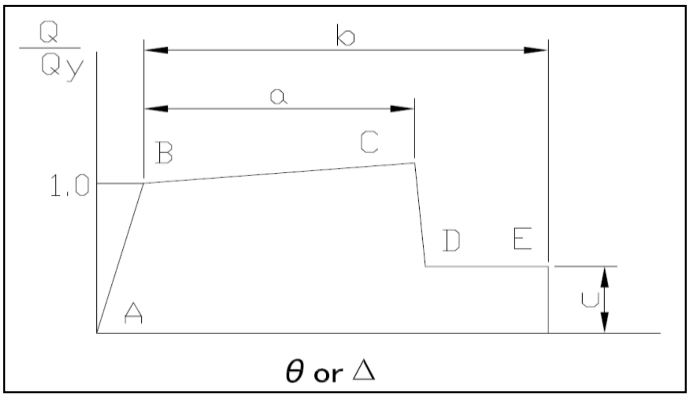

Figure 4.3 : Generalized Force-Deformation Relation for Steel Elements (ASCE41-06, figure 5-1).

Definition of Chord Rotation is shown in figure 4.2; Generalized Force-Deformation Relation for Steel Elements is indicated in the figure 4.3. The rotation angle is determined with respect to the equation **(4.1)**. In addition to them, modelling parameters and acceptance criteria for nonlinear procedures are taken from the table 4.1. $M_p = ZxF_{ye}$ is the moment capacity of element. P_{ye} is the axial load capacity. For Beam W12/22:

W12/22 Geometric Specifications

h	**b**	**t_w**	**t_f**	**A**	**L**	**Z_x**	**I_x**
mm	mm	mm	mm	cm^2	cm	mm^3	cm^4
312,7	102,4	6,6	21.5	41,81	400	480141	6493,2

$$\theta_y = \frac{Z \times F_y \times L_b}{6EI_b} = 8{,}21 \times 10^{-3} \qquad \textbf{(4.1)}$$

Table 4.1 : Modelling Parameters and Acceptance Criteria for Nonlinear Procedures (ASCE41-06, figure 5-1).

Componenet/Action	Modeling Parameters: Plastic Rotation Angle, Radians		Modeling Parameters: Residual Strength Ratio	Acceptance Criteria: Plastic Rotation Angle, Radians: Primay			Secondary	
Beams-Flexure	a	b	c	IO	LS	CP	LS	CP
a) $b_f/(2t_f) \leq 52/\sqrt{(F_{ye})}$ and $h_w/t_w \leq 418/\sqrt{(F_{ye})}$	$9\theta_y$	$11\theta_y$	0.6	$6\theta_y$	$8\theta_y$	$9\theta_y$	$9\theta_y$	$11\theta_y$
b) $b_f/(2t_f) \geq 65/\sqrt{(F_{ye})}$ or $h_w/t_w \geq 640/\sqrt{(F_{ye})}$	$4\theta_y$	$6\theta_y$	0.2	$2\theta_y$	$3\theta_y$	$3\theta_y$	$3\theta_y$	$4\theta_y$
c) Other	Linear interpolation between the values on lines a and b for both flange slenderness (the first term) and web slenderness (second term) shall be performed, and the lower resulting value shall be used							

$$\frac{b_f}{2xt_f} \geq \frac{65}{\sqrt{F_{ye}}} = 8.995 \ or \ \frac{h_w}{t_w} \geq \frac{640}{\sqrt{F_{ye}}} = 88.57$$

W12/22 fits the requirements of b option. So the IO: 0.25 $\theta_{y,}$ LS: 2 θ_y, CP: 3 θ_y.

Plastic rotation angles (radian) are chosen as a=4 θ_y, b=6 θ_y, c=0.2.

4.2.2 PMM Hinge

Effect of Axial Force on Ductile Limit is shown in the figure 4.4. Modelling parameters and acceptance criteria for nonlinear procedures are indicated in the table 4.2. In addition to them, the rotation angle is determined with respect to the equation **(4.2)**.

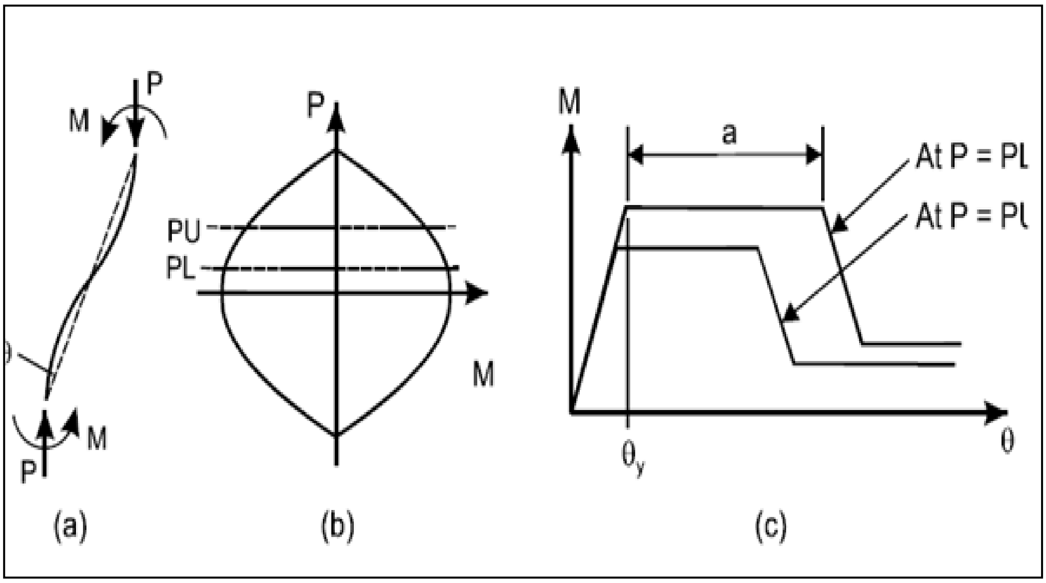

Figure 4.4 : Effect of Axial Force on Ductile Limit (ASCE41-06, figure 5-10).

On the contrary to beams, axial load has an effect on plastic rotation angle. We need to calculate the axial load capacity of columns. A*F_y can be accepted as axial load capacity. To take axial load effect into account, a nonlinear load case named "vertical-PUSH" was defined in SAP 2000. After that another nonlinear load case "horizontal-PUSH, which continued from zero condition "vertical-PUSH", was defined. "vertical-PUSH" contains dead load and 0.25 of live load. "0.25" coefficient represents here live load participitation factor here. Also, the hand calculations are made. Here is the table of hand calculations:

M_p=ZxF_{ye} is the moment capacity of element. P_y is the axial load capacity. For Beam W14/48

W14/48 Geometric Specifications

H	**b**	**t_w**	**t_f**	**A**	**L**	**Z_x**	**I_x**
Mm	mm	mm	mm	cm^2	cm	mm^3	cm^4
350,3	203,9	8,6	15.1	90,96	300	1284745	20190

$$\theta_y = \frac{Z \times F_y \times L_b}{6EI_b} \times \left(1 - \frac{P}{P_y}\right) \qquad \textbf{(4.2)}$$

P_y=A*F_y=9096*360=3274.56 kN

For each column plastic rotation angle values are calculated below:

column	L	I	P(kN)	Pc	Z	Fy	6EI/L	θ y
1st	3m	20190	13.553	3274.6	1284745	360	823308	0.5017
2nd	3m	20190	13.553	3274.6	1284745	360	823308	0.5017

After that, from table 5.6 in ASCE 41-06 the plastic rotation angle acceptance criteria are determined. For this reason, slenderness of flange and web are calculated. These values are compared to the values on table. Since P/Pc>0.2 we used the first part of table 4.2.

Table 4.2 : Modelling Parameters and Acceptance Criteria for Nonlinear Procedures.

	Modeling Parameters			Acceptance Criteria				
Columns-Flexure	Plastic Rotation Angle, Radians		Residual Strength Ratio	Plastic Rotation Angle, Radians				
				Primay			Secondary	
For P/Pcl<0.2	a	b	c	IO	LS	CP	LS	CP
a) $b_f/(2t_f) \leq 52/\sqrt{(F_{ye})}$ and $h_w/t_w \leq 300/\sqrt{(F_{ye})}$	9 θ_y	11 θ_y	0.6	1 θ_y	6 θ_y	8 θ_y	9 θ_y	11 θ_y
b) $b_f/(2t_f) \geq 65/\sqrt{(F_{ye})}$ or $h_w/t_w \geq 460/\sqrt{(F_{ye})}$	4 θ_y	6 θ_y	0.2	0.25 θ_y	2 θ_y	3 θ_y	3 θ_y	4 θ_y
c) Other	Linear interpolation between the values on lines a and b for both flange slenderness (the first term) and web slenderness (second term) shall be performed, and the lower resulting value shall be used							
For 0.2<P/Pcl<0.5	a	b	c	IO	LS	CP	LS	CP
a) $b_f/(2t_f) \leq 52/\sqrt{(F_{ye})}$ and $h_w/t_w \leq 260/\sqrt{(F_{ye})}$	-	-	0.6	6 θ_y	-	-	-	-
b) $b_f/(2t_f) \geq 65/\sqrt{(F_{ye})}$ or $h_w/t_w \geq 400/\sqrt{(F_{ye})}$	1 θ_y	1.5 θ_y	0.2	0.25 θ_y	0.5 θ_y	0.8 θ_y	1.2 θ_y	1.2 θ_y
c) Other	Linear interpolation between the values on lines a and b for both flange slenderness (the first term) and web slenderness (second term) shall be performed, and the lower resulting value shall be used							

$$\frac{b_f}{2xt_f} \geq \frac{65}{\sqrt{F_{ye}}} = 8.995 \; or \; \frac{h_w}{t_w} \geq \frac{460}{\sqrt{F_{ye}}} = 63.66$$

W14/48 fits the requirements of b option. So the IO: 0.25 θ_y, LS: 2 θ_y, CP: 3 θ_y.

Plastic rotation angles (radian) are chosen as a=4 θ_y, b=6 θ_y, c=0.2.

4.2.3 Axial Hinge

Axial hinge for steel components depends on compression or tension conditions. Another criterion is brace type. For this thesis Concentrically Braced Frame is used rather than EBF. The last factor effects acceptance criterion is whether the brace is slender or stocky. All the braces in Push-over analysis and Time History Analysis are tubes. Also plastic deformation angles defined in the ASCE 41- 06 as the multiplication of $\triangle_c$ and $\triangle_t$. $\triangle_c$ is the axial deformation at expected buckling load. $\triangle_t$ is the axial deformation at expected tensile yielding load. For axial hinge, modelling parameters and acceptance criteria for nonlinear procedures are shown in table 4.3 below:

Table 4.3 : Modelling Parameters and Acceptance Criteria for Nonlinear Procedures.

	Modeling Parameters			Acceptance Criteria				
Braces(except EBF) in Compression	Plastic Deformation		Residual Strength Ratio	Plastic Deformation				
a)Slender Kl/r≥4.2√E/Fy				Primay			Secondary	
	a	b	c	IO	LS	CP	LS	CP
1. W, I, 2L In-plane, 2C In-plane	$0.5\triangle_c$	$10\triangle_c$	0.3	$0.25\triangle_c$	$6\triangle_c$	$8\triangle_c$	$8\triangle_c$	$10\triangle_c$
2. 2L Out-of-Plane, 2C Out-of-Plane	$0.5\triangle_c$	$9\triangle_c$	0.3	$0.25\triangle_c$	$5\triangle_c$	$7\triangle_c$	$7\triangle_c$	$9\triangle_c$
3. HSS, Pipes, Tubes	$0.5\triangle_c$	$9\triangle_c$	0.3	$0.25\triangle_c$	$5\triangle_c$	$7\triangle_c$	$7\triangle_c$	$9\triangle_c$
Braces(except EBF) in Compression	Plastic Deformation		Residual Strength Ratio	Plastic Deformation				
b)Stocky Kl/r≤2.1√E/Fy				Primay			Secondary	
	a	b	c	IO	LS	CP	LS	CP
1. W, I, 2L In-plane, 2C In-plane	$1\triangle_c$	$8\triangle_c$	0.5	$0.25\triangle_c$	$5\triangle_c$	$7\triangle_c$	$7\triangle_c$	$8\triangle_c$
2. 2L Out-of-Plane, 2C Out-of-Plane	$1\triangle_c$	$7\triangle_c$	0.5	$0.25\triangle_c$	$4\triangle_c$	$6\triangle_c$	$6\triangle_c$	$7\triangle_c$
3. HSS, Pipes, Tubes	$1\triangle_c$	$7\triangle_c$	0.5	$0.25\triangle_c$	$4\triangle_c$	$6\triangle_c$	$6\triangle_c$	$7\triangle_c$
c)Intermediate	Linear interpolation between the values fort he slender and stocky braces (after application of all applicable modifiers) shall be used.							
Braces(except EBF) in Tension	$11\triangle_t$	$14\triangle_t$	0.8	$0.25\triangle_t$	$7\triangle_t$	$9\triangle_t$	$11\triangle_t$	$13\triangle_t$

KL/r=0.5*5/0.0739=33.83<49.5

For tension; IO: 0.25 $\triangle_y$, LS: 7 $\triangle_y$, CP: 9 $\triangle_y$.

For compression; IO: -0.25 $\triangle_c$, LS: 1 $\triangle_c$, CP: 2 $\triangle_c$.

After verifying all plastic hinge properties by hand, a prototype model analyzed in the next chapter.

4.3 Push-Over Results of Prototype Model

After push-over analysis is finished. Plastic hinges are appaered. In the first two steps, any plastic hinge did not appear. The first one is appaered in the brace in the third step as shown below. One of the brace is collapsed after the fourt step. Hinge Status of Push-Over Analysis is indicated in the table 4.4. after the step figures. Additionally, here are the steps of “horizontal-PUSH” step-1 in figure 4.5, step-2 in figure 4.6, step-3 in figure 4.7, step-4 in figure 4.8 and step-5 in figure 4.9 successively.

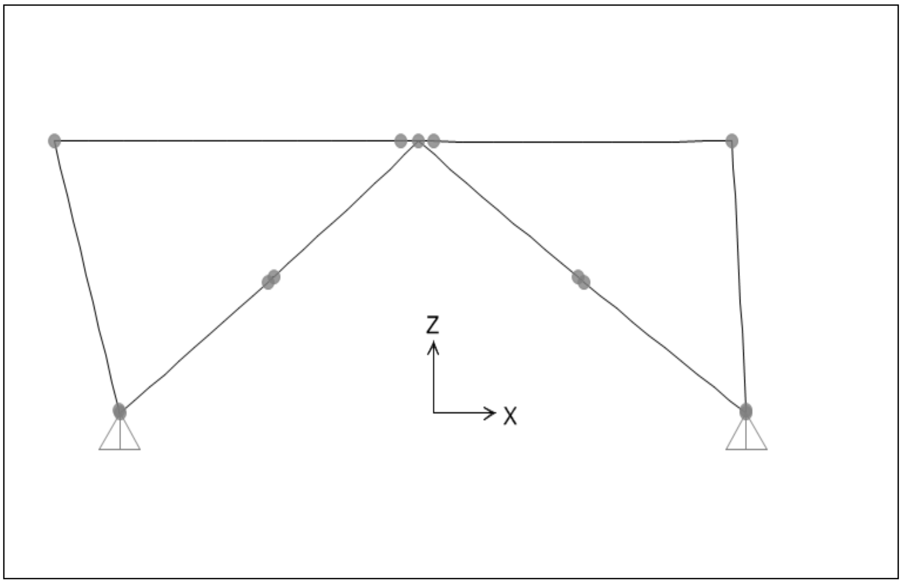

Figure 4.5 : Step-1

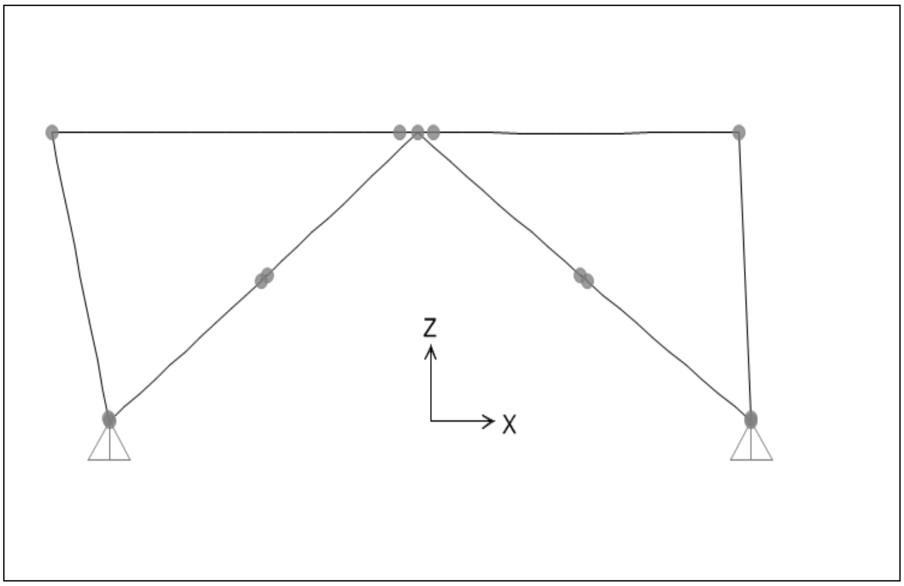

Figure 4.6 : Step-2

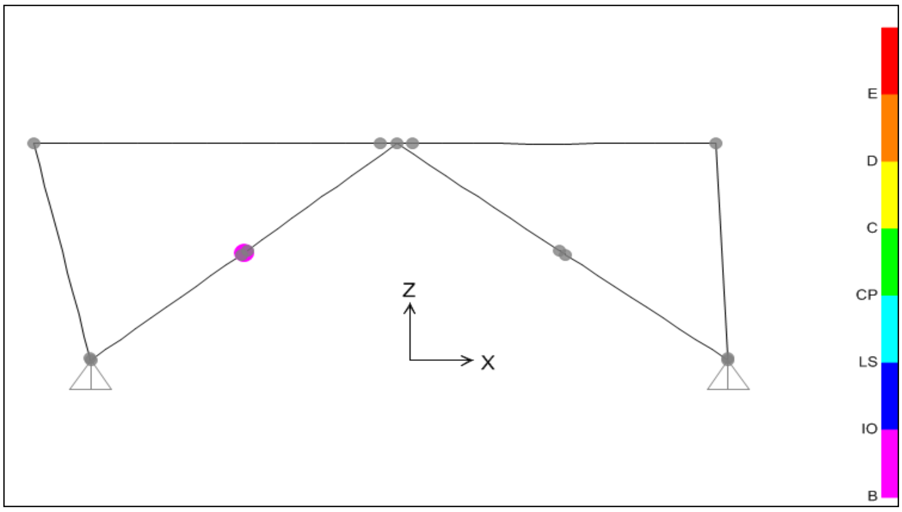

Figure 4.7 : Step-3

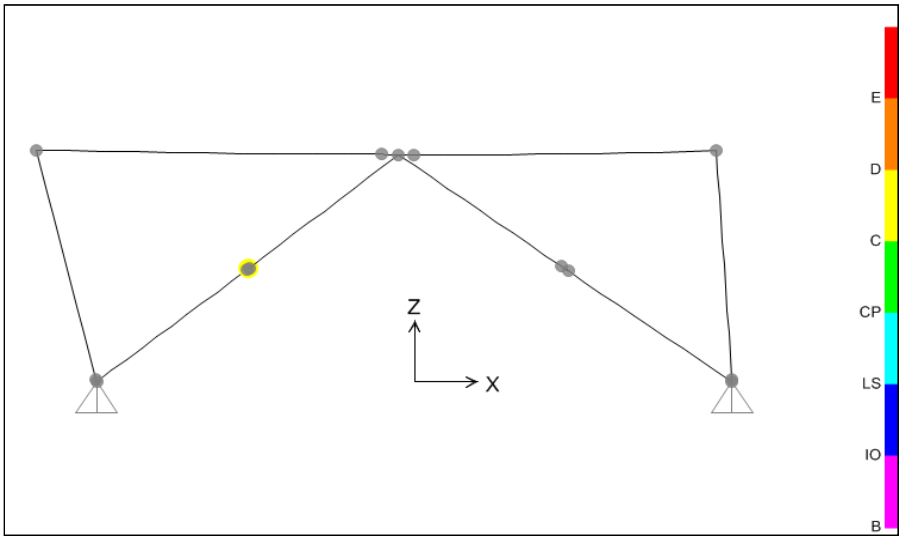

Figure 4.8 : Step-4

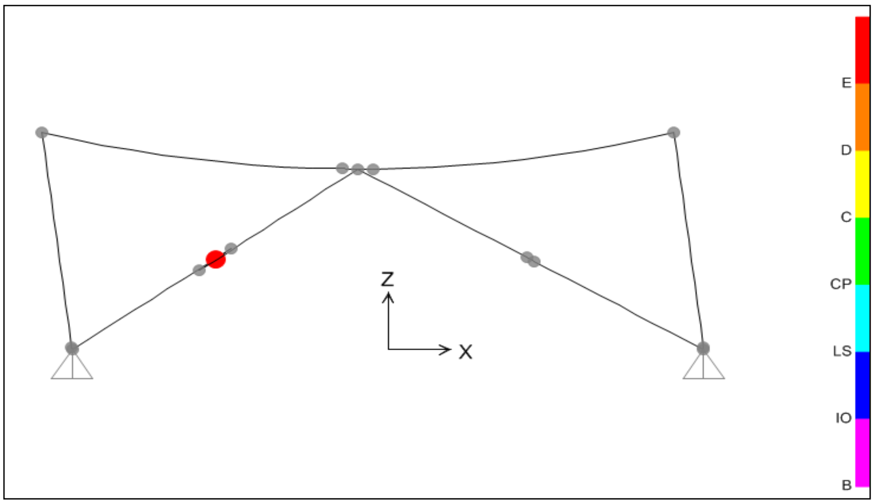

Figure 4.9 : Step-5

Table 4.4 : Hinge Status of Push-Over Analysis (SAP 2000).

Frame	OutputCase	AssignHinge	GenHinge	HingeState	HingeStatus
4	HORIZONTAL-PUSH	Auto P	4H1	A to B	A to IO
4	HORIZONTAL-PUSH	Auto P	4H1	>E	>CP
5	HORIZONTAL-PUSH	Auto P	5H1	A to B	A to IO
5	HORIZONTAL-PUSH	Auto P	5H1	A to B	A to IO
8	HORIZONTAL-PUSH	Auto P-M2-M3	8H1	A to B	A to IO
8	HORIZONTAL-PUSH	Auto P-M2-M3	8H1	A to B	A to IO
9	HORIZONTAL-PUSH	Auto P-M2-M3	9H1	A to B	A to IO
9	HORIZONTAL-PUSH	Auto P-M2-M3	9H1	A to B	A to IO
10	HORIZONTAL-PUSH	Auto M3	10H1	B to C	LS to CP
10	HORIZONTAL-PUSH	Auto M3	10H1	A to B	A to IO
11	HORIZONTAL-PUSH	Auto M3	11H1	B to C	LS to CP
11	HORIZONTAL-PUSH	Auto M3	11H1	A to B	A to IO

After careful examination of SAP 2000 model, we acknowledged that auto hinges values are very close to the handed-calculated hinge values with respect to ASCE 41-06. Also, the base shear force, the periods and the hinge status are very reasonable. So that it is decided to use SAP 2000 in the nonlinear static analysis.

During nonlinear static analysis, in the SAP 2000 process real model pushover curves are not as usual. Due to convergence problem, a suitable hinge unloading method should be used. There are three types of hinge unloading method: Unload entire structure, apply local redistribution and restart using secant stiffness. Only the third method restarting using stiffness solved convergence proble, however this method works in this way: When a hinge unloads , the program must find a way to remove the load that the hinge was carrying and possibly redistribute it to the remainder of the structure. Restart option using the secant stiffness. Any hinge reaches the negative slope of the stress-strain curve has become nonlinear All hinges are re-using the secant stiffness properties, and the analysis is restarted according to SAP 2000 manuel. As a result, this method cause sharp decreases and discontinuity in the push-over curves. All the assesments are done by taking this fact into account.

Base shear distribution is calculated at the target displacement point. In the next part, the method of target displacement calculation is shown.

4.4 Push-Over Results of Real Models

4.4.1 Target Displacement

For Pushover analysis, ASCE 41-06 (3.3.3.3.2) offers the calculation of target displacements with the equation defined below:

$$\delta_t = C_0 \times C_1 \times C_2 \times S_a \times \left(\frac{T_e^2}{4\pi^2} \right) \times g \qquad \textbf{(4.1)}$$

Where,

δ_t is the target displacement,

C_0 is the modification factor to relate spectral displacement. It is defined in table 3-2 in ASCE 41-06. According to the table 3-2, when the building has floor number over 10 and the any kind of loading type is used, C_0 is taken 1,5.

C_1 = modification factor to relate expected maximum inelastic displacements to displacements calculated for linear elastic response. According to ASCE 41-06, for periods less than 0.2 sec, C_1 need not be taken greater than the value at T = 0.2 sec. For periods greater than 1.0 sec, C_1 = 1.0.

C_2 = modification factor to represent the effect of pinched hysteresis shape, cyclic stiffness degradation, and strength deterioration on maximum displacement response. According to ASCE 41-06, for periods greater than 0.7 sec, C_2=1.0.

S_a = response spectrum acceleration, at the effective fundamental period and damping ratio of the building in the direction under consideration. (% g)

$S_a = S_{x1}/(B_1 x T)$, for $T > T_s$, $S_{x1}=F_v x S_1$=1,5*0,6=0,9>0,2 (for high seismicity)

B_1 = 4/[5.6 - In (100β)] β is the effective viscous damping. β=0.05, B_1=1,0024

T_e = the fundamental period (secs)

g=the gravity (k/in/s^2) = 386.220472441

The target displacements are calculated with the equation **(4.1)** and summarized below in the table 4.5. Initially the target displacements are calculated in inch unit, then they are converted into metric unit.

Table 4.5 : Target Displacements.

	Period(sec)	δ_t(inch)	δ_t(cm)
Model 15-12	1,33	17,523	44,509
Model 25-12	1,31	17,259	43,840
Model 40-12	1,26	16,601	42,167
Model 15-16	2,04	26,878	68,270
Model 25-16	2,02	26,678	67,763
Model 40-16	1,95	25,692	65,258
Model 15-20	2,53	33,332	84,664
Model 25-20	2,50	32,938	83,665
Model 40-20	2,47	32,543	82,661

4.4.2 12-Storey System

4.4.2.1 Push-Over Curves

After pushing the building about three percent of the height of the structure. The push-over curve and the plastic hinge distribution of the braces and the moment frame are illustrated below in figure 4.10.

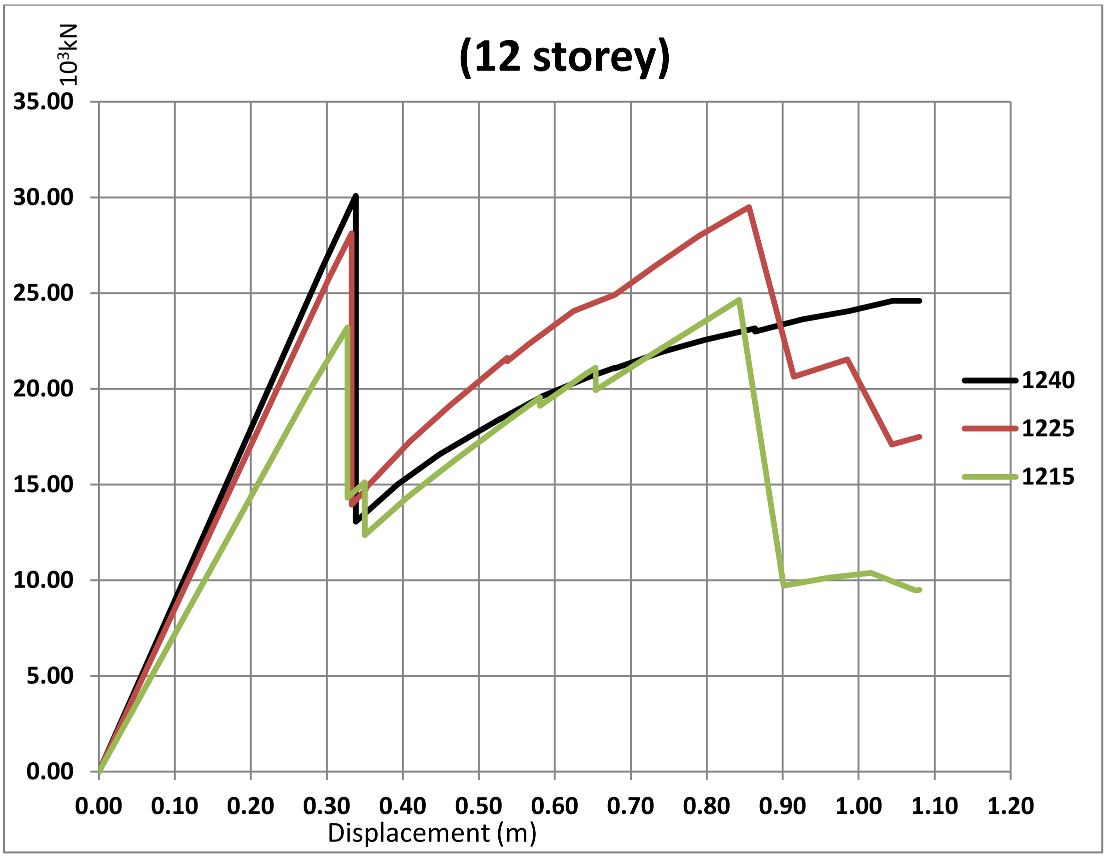

Figure 4.10 : Push-Over Curves (SAP 2000).

4.4.2.2 Plastic Hinge Distribution

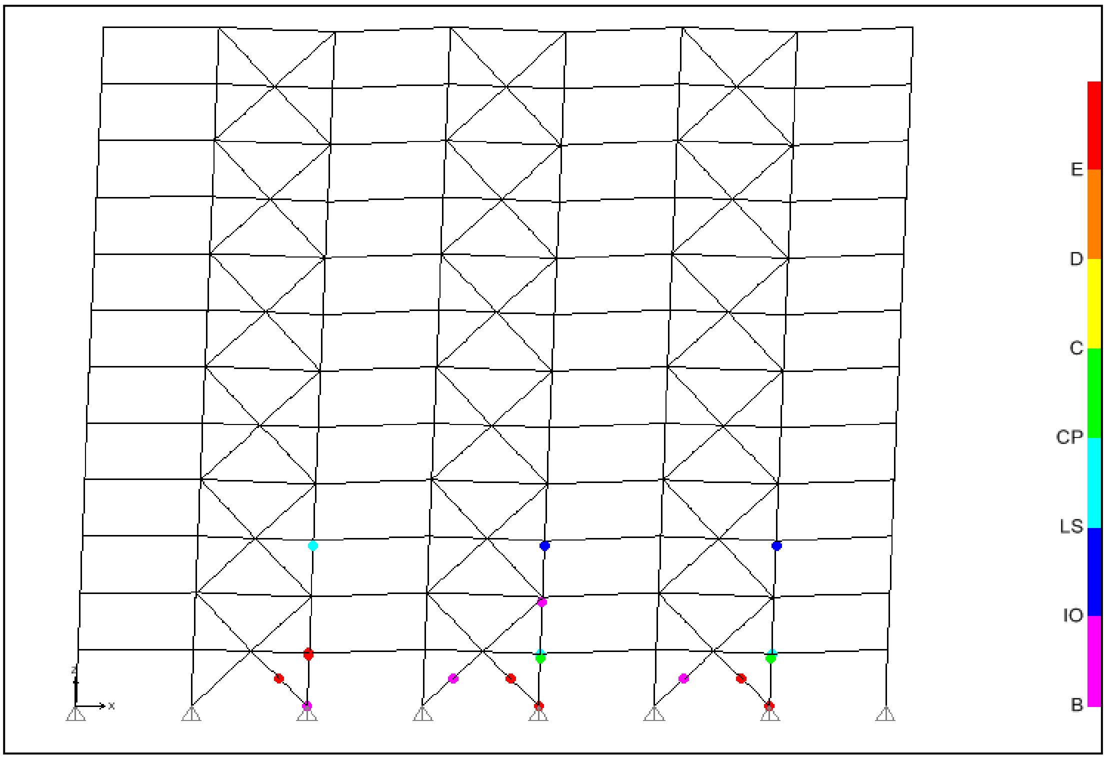

Figure 4.11 : Plastic Hinges in Braced Axis (SAP 2000).

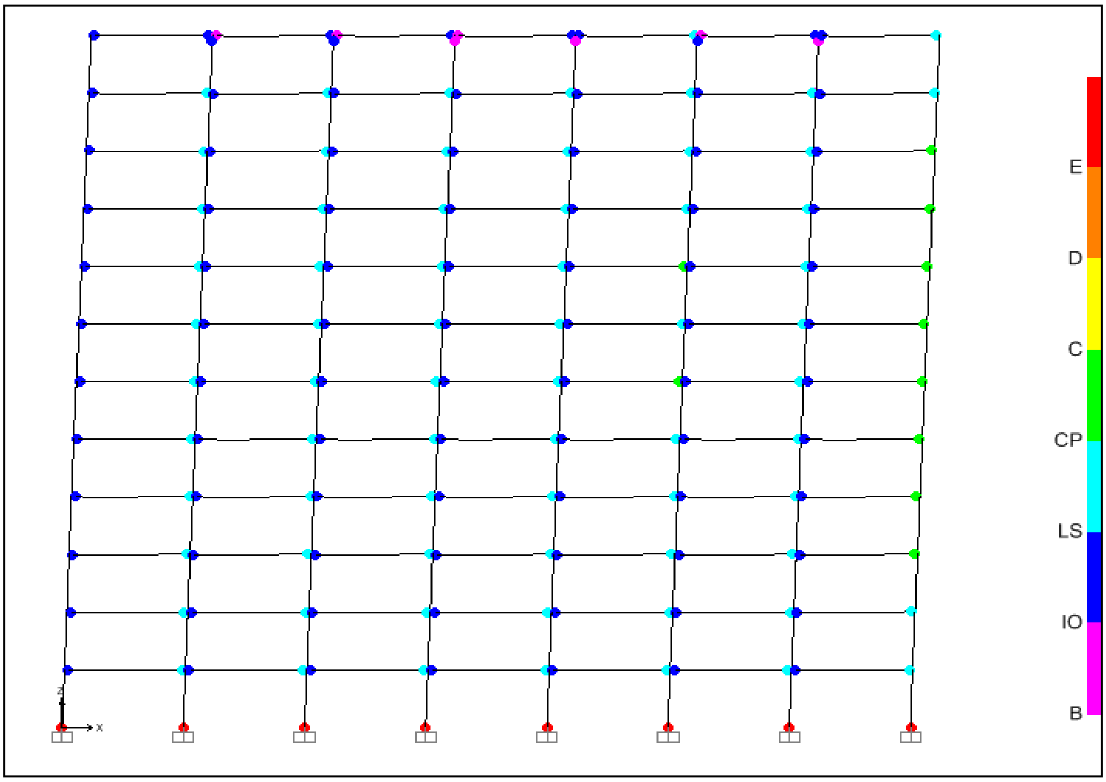

Figure 4.12 : Plastic Hinges in MF Axis (SAP 2000).

Plastic hinge distribution in the axis where braces exist is shown in the figure 4.11 and the plastic hinge distribution in moment frame axis is shown in the figure 4.12.

4.4.3 16-Storey System

4.4.3.1 Push-Over Curves

After pushing the building about three percent of the height of the structure. The push-over curve and the plastic hinge distribution of the braces and the moment frame are illustrated below in figure 4.13.

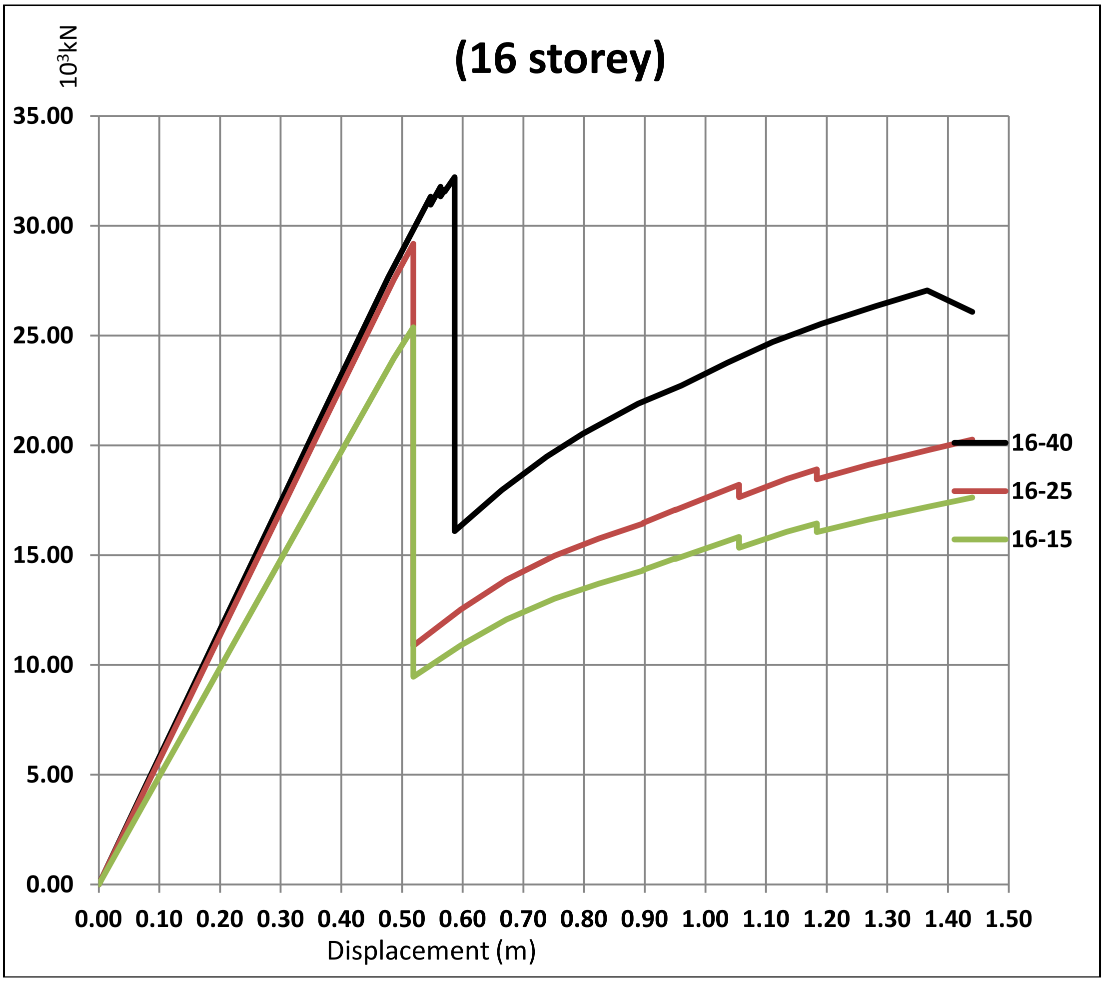

Figure 4.13 : Push-Over Curves (SAP 2000).

4.4.3.2 Plastic Hinge Distribution

Plastic hinge distribution in the axis where braces exist is shown in the figure 4.14 and the plastic hinge distribution in moment frame axis is shown in the figure 4.15 below:

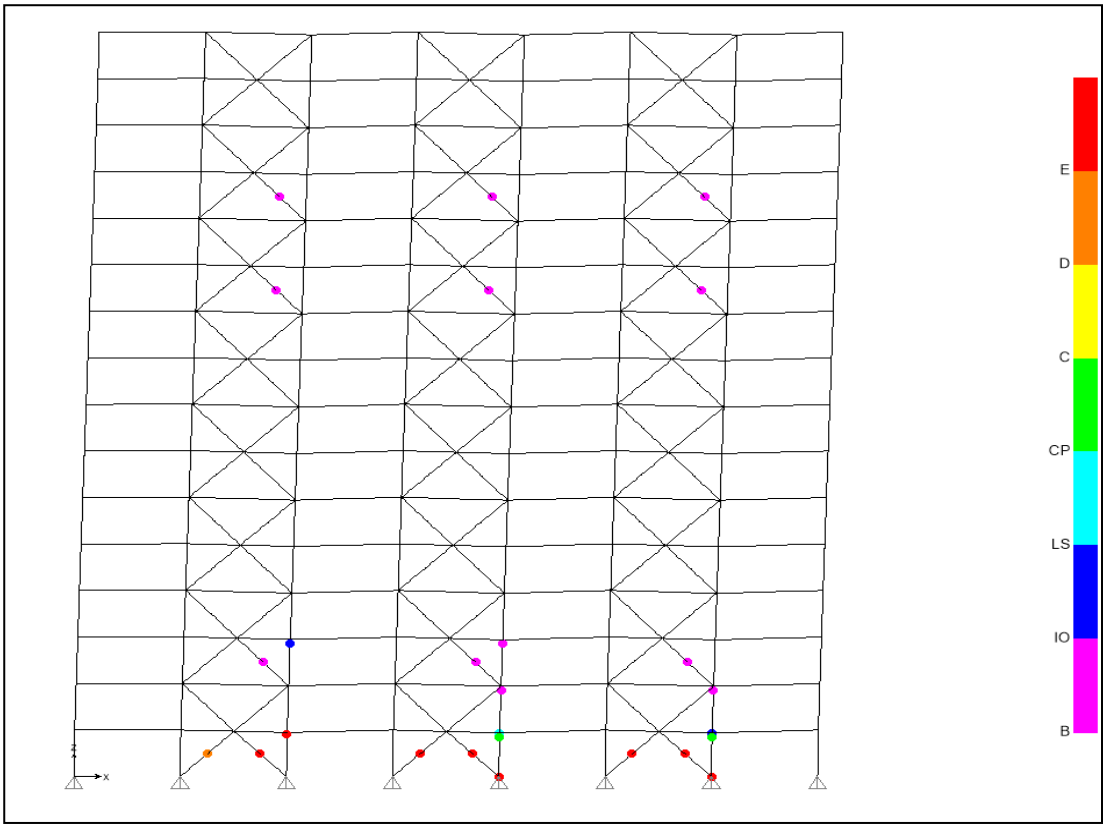

Figure 4.14 : Plastic Hinges in Braced Axis (SAP 2000).

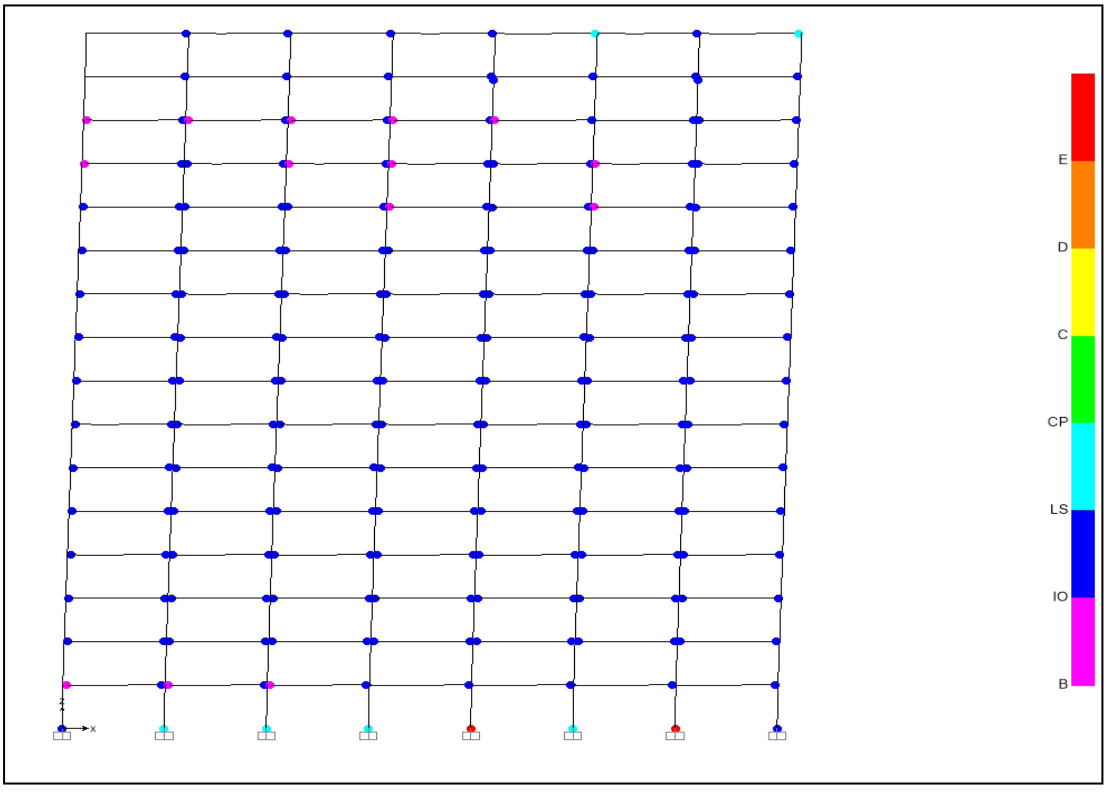

Figure 4.15 : Plastic Hinges in MF Axis (SAP 2000).

4.4.4 20-Storey System

4.4.4.1 Push-Over Curves

After pushing the building about three percent of the height of the structure. The push-over curve and the plastic hinge distribution of the braces and the moment frame are illustrated below in figure 4.13.

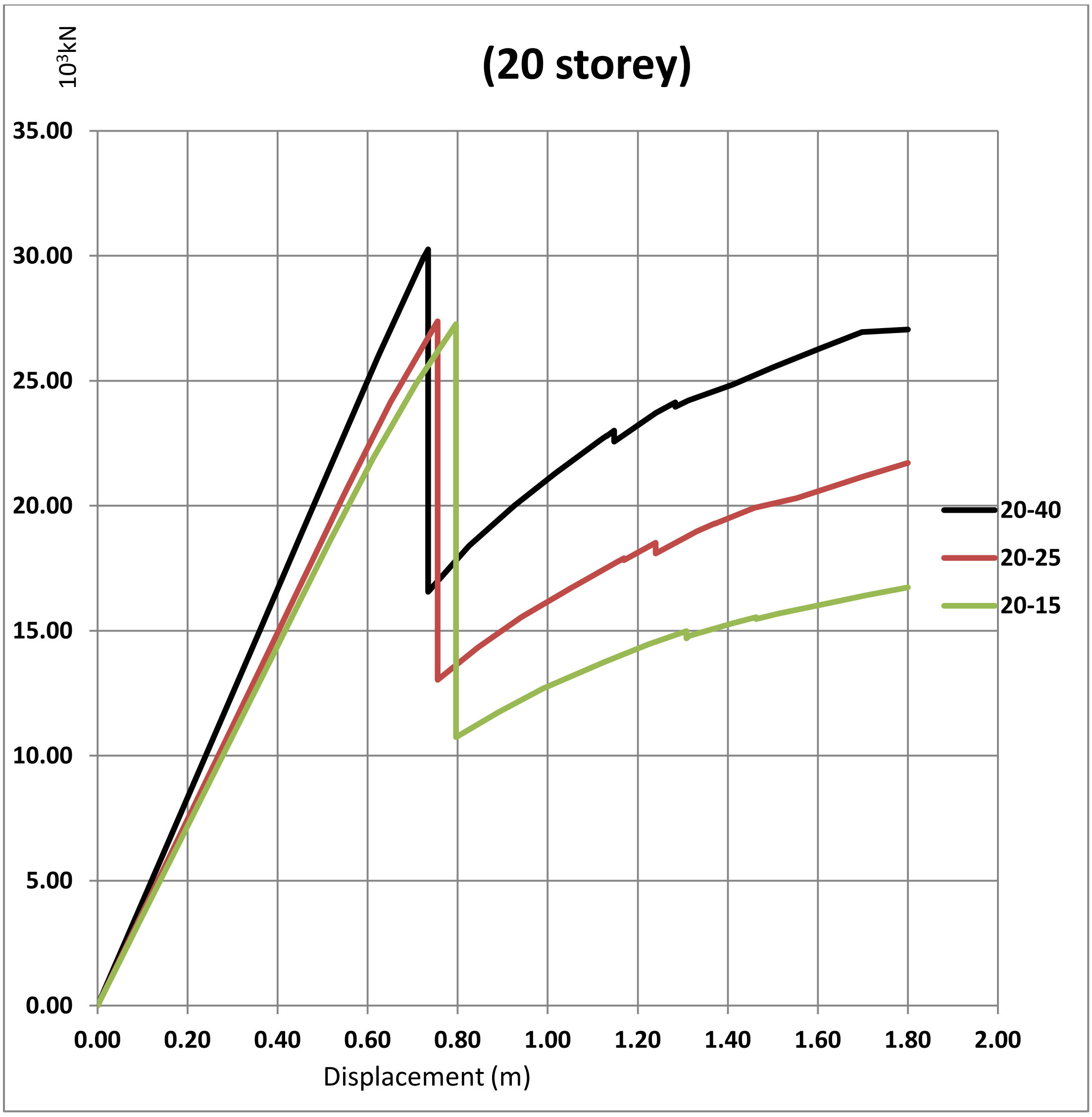

Figure 4.16 : Push-Over Curves (SAP 2000).

4.4.4.2 Plastic Hinge Distribution

Plastic hinge distribution in the axis where braces exist is shown in the figure 4.17 and the plastic hinge distribution in moment frame axis is shown in the figure 4.18 below:

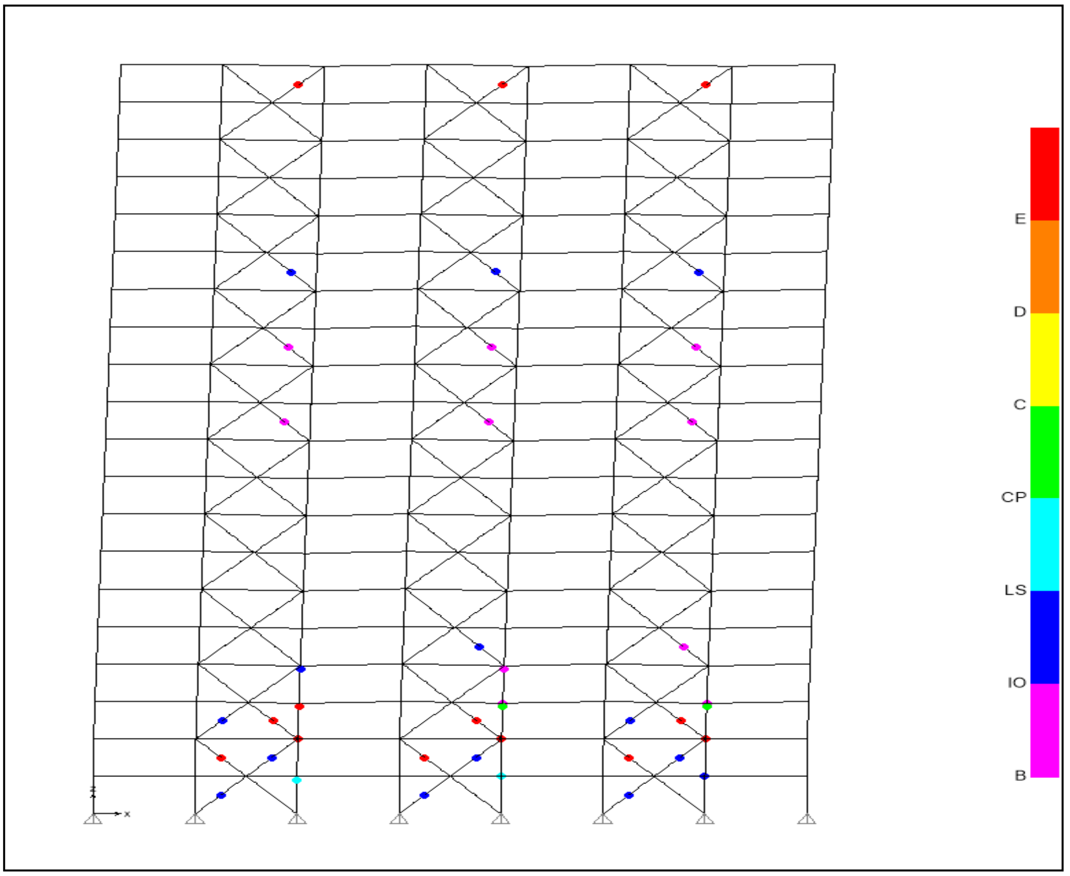

Figure 4.17 : Plastic Hinges in Braced Axis (SAP 2000).

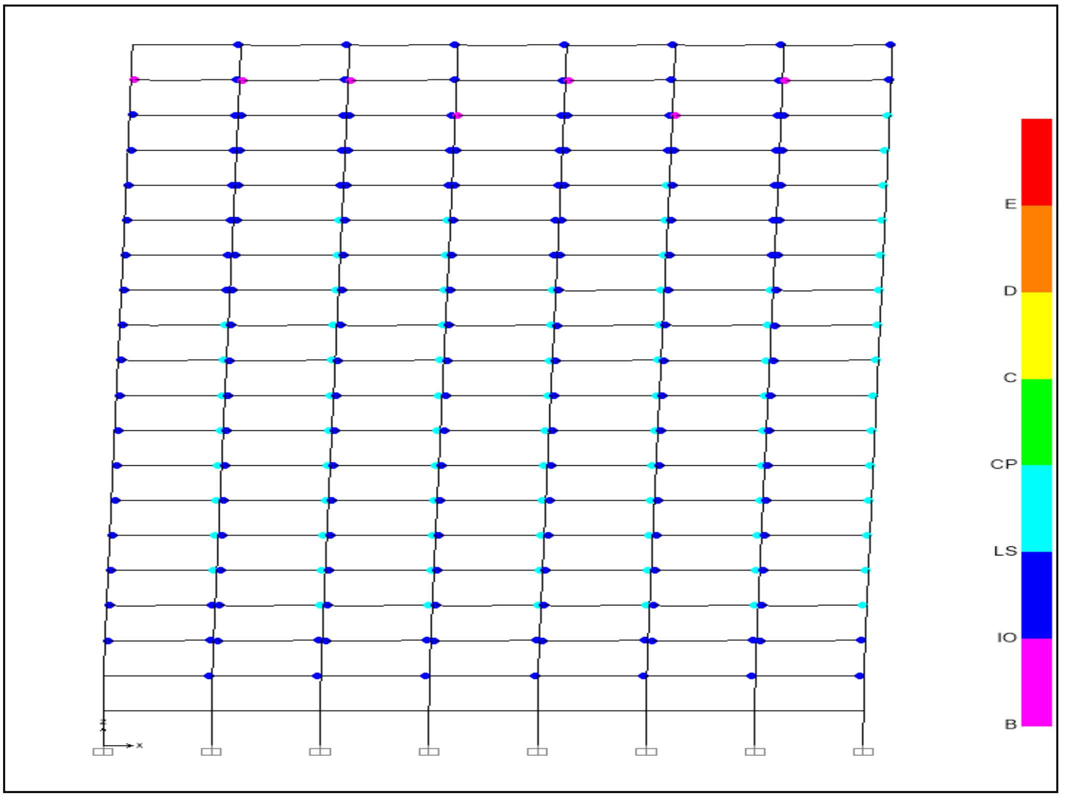

Figure 4.18 : Plastic Hinges in MF Axis (SAP 2000).

In order to compare the base shear distribution between MF and BF, the BF shear forces, MF base forces and the interaction of them at the target displacement is illustrated below in table 4.6.

Table 4.6 : Base Shear Distribution.

	BF(kN)	MF(kN)	MF/TS (%)
Model 15-12	17444	1713	9
Model 25-12	15134	2047	12
Model 40-12	12410	2587	17
Model 15-16	23460	1915	8
Model 25-16	18564	2774	13
Model 40-16	14024	3938	21
Model 15-20	14964	1723	10
Model 25-20	15777	2619	14
Model 40-20	14475	3915	21

First, it is expected that after the beginning of yielding of braces, the base shear capacity continue although the stiffness is changed. Because the low-level columns continue to be loaded until, they reach their interaction curve capacity. Due to elimination of safety factors and nonlinear behavior of material, the base shear capacity is higher compare to linear analysis results since no elements were designed to yield. This behavior is more realistic.

As a result, the total system base shear capacity is higher than the design strength. Also, it is remarkable that the relative lateral resistance of MF to BF at the target displacement in the pushover analysis is higher than for the elastic model. In the inelastic range, the MF base shear gets higher and shares more of the earthquake load.

5. NONLINEAR DYNAMIC ANALYSIS

5.1 Ground Motions

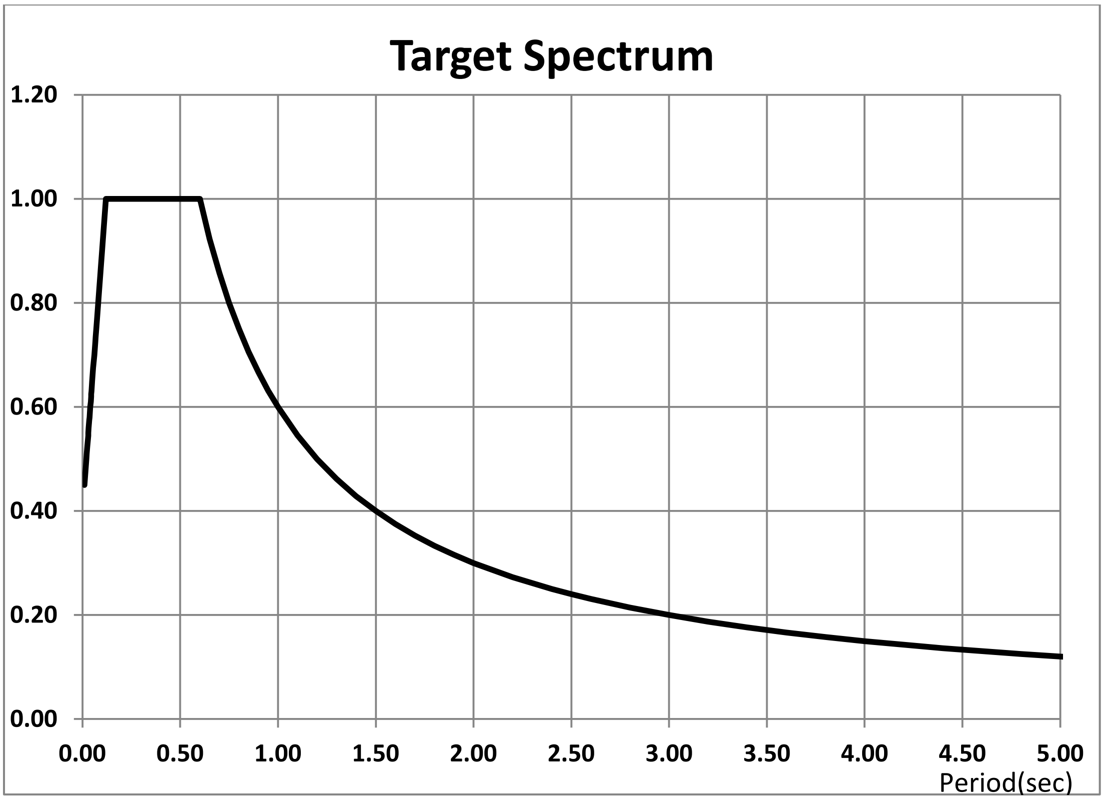

Figure 5.1 : DBE Target Spectrum.

According to AISC 41-06, time-history analysis should be carried out with at least three records. These records contain both x and y horizontal componenets and vertical component if required. Time histories must have source mechanisms, fault distances and magnitudes. All of these data should consist with DBE. In addition, according to AISC 41-06, the square root of the sum of the squares (SRSS) of the 5%-damped site-specific spectra of the scaled horizontal componenets shall be constructed for earthquake datas. The ground motion data must be scaled at more than 1.3 times the 5%-damped spectrum for the DBE for periods between 0.2T and 1.5T (where T is the fundamental period of the building). While choosing earthquake datas, PEER ground motion database is used and ground motions are determined according to the criteria defined in DBE Target Spectrum above in the figure 5.1.

Earthquake Record Data of DBE is shown in Table 5.1; Summary of PEER Ground Motion Database Search Criteria is shown in Table 5.2. Also the scaled spectra from PEER is illustrated in the figure 5.2.

Table 5.1 : Earthquake Record Data (DBE).

Earthquake Name	Year	Scale Factor	Duration (sec)	Station Name	Magnitude	Mechanism
Imperial Valley-06	1979	2.0319	36.4	Cerro Prieto	6.53	Strike slip
Northridge-01	1994	2.5256	15.9	Gleason Ave	6.69	Reverse
Irpinia, Italy	1980	2.8227	27.0	Bisaccia	6.9	Normal

Table 5.2 : Summary of PEER Ground Motion Database Search Criteria (DBE).

	Magnitude	Rrup (km)	Vs30 (m/sec)	D9-95 (sec)	Scale Factor
Min	6,5	10	360	15	0,1
Max	7,5	30	760	60	10

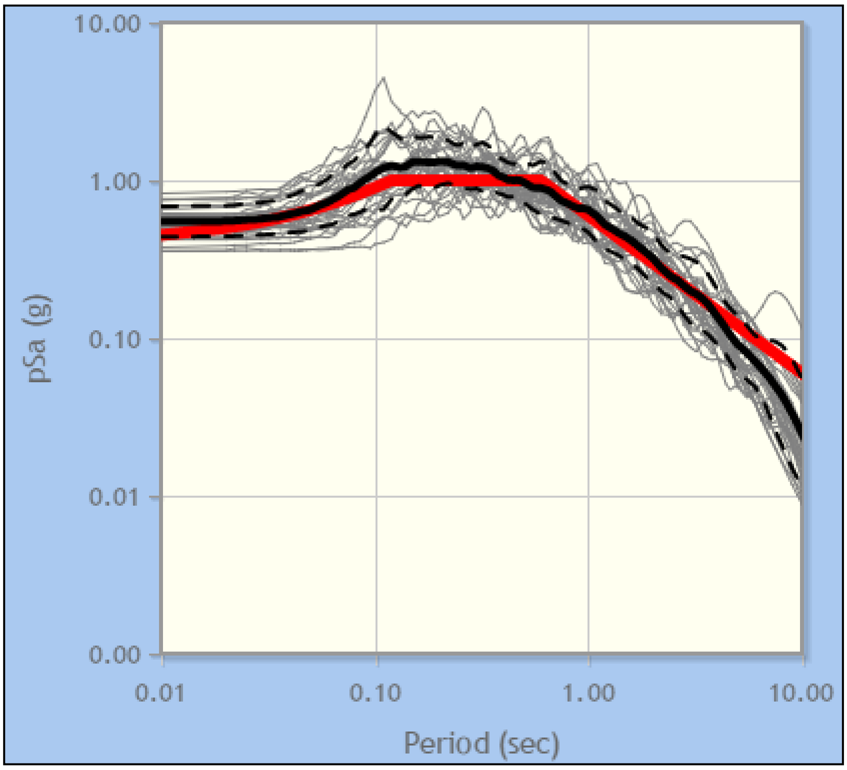

Figure 5.2 : Scaled Spectra (PEER).

Earthquake Record Data of MCE is shown in Table 5.3; Summary of PEER Ground Motion Database Search Criteria is shown in Table 5.4. Also the MCE Target Spectrum is illustrated in the figure 5.3.

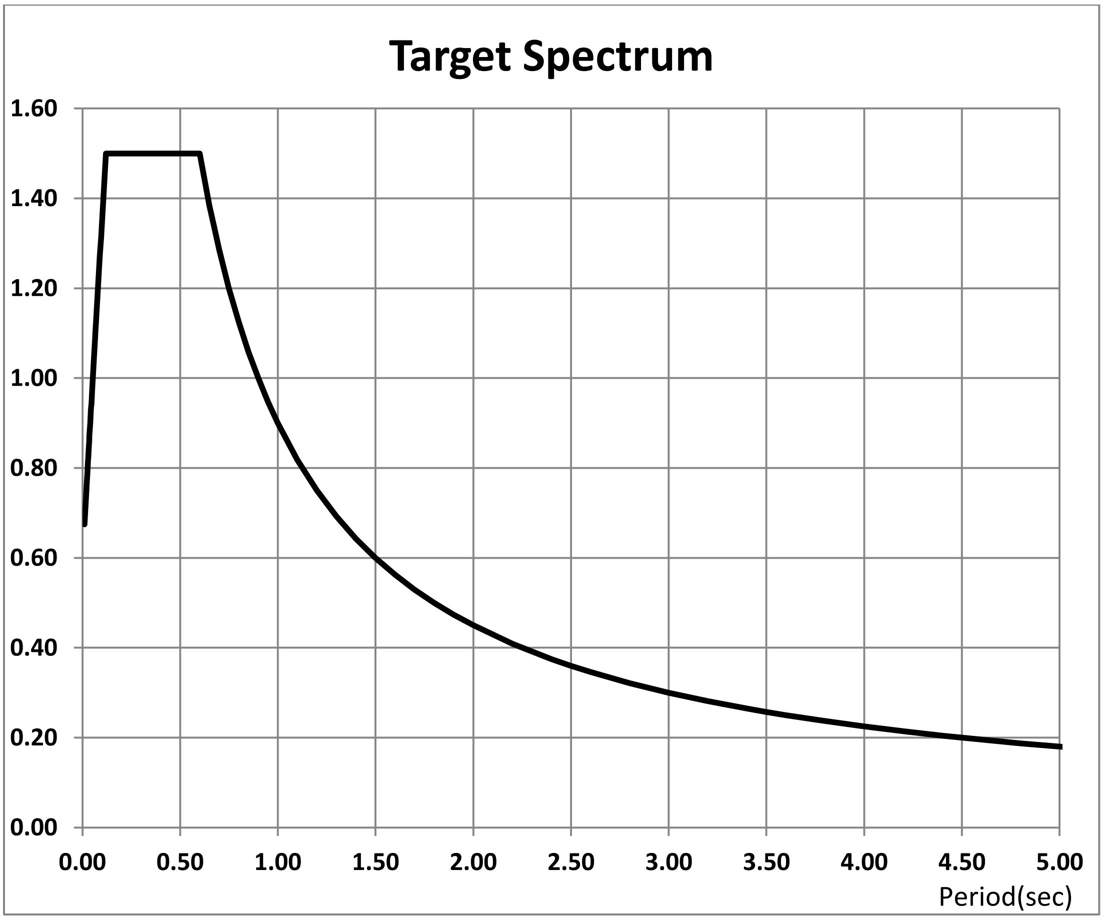

Figure 5.3 : MCE Target Spectrum.

Table 5.3 : Earthquake Record Data (MCE).

Earthquake Name	Year	Scale Factor	Duration (sec)	Station Name	Magnitude	Mechanism
Landers	1992	2.3	27.1	Joshua Tree	7.28	strike slip

Table 5.4 : Summary of PEER Ground Motion Database Search Criteria (MCE).

	Magnitude	Rrup (km)	Vs30 (m/sec)	D9-95 (sec)	Scale Factor
Min	6,5	10	360	15	0,1
Max	8,0	30	760	60	10

5.1.1 Graphical Display of DBEs

Successively, the graphical display of Irpinia, Imperial Valley and Northridge Records are shown in the figure 5.4, 5.5 and 5.6.

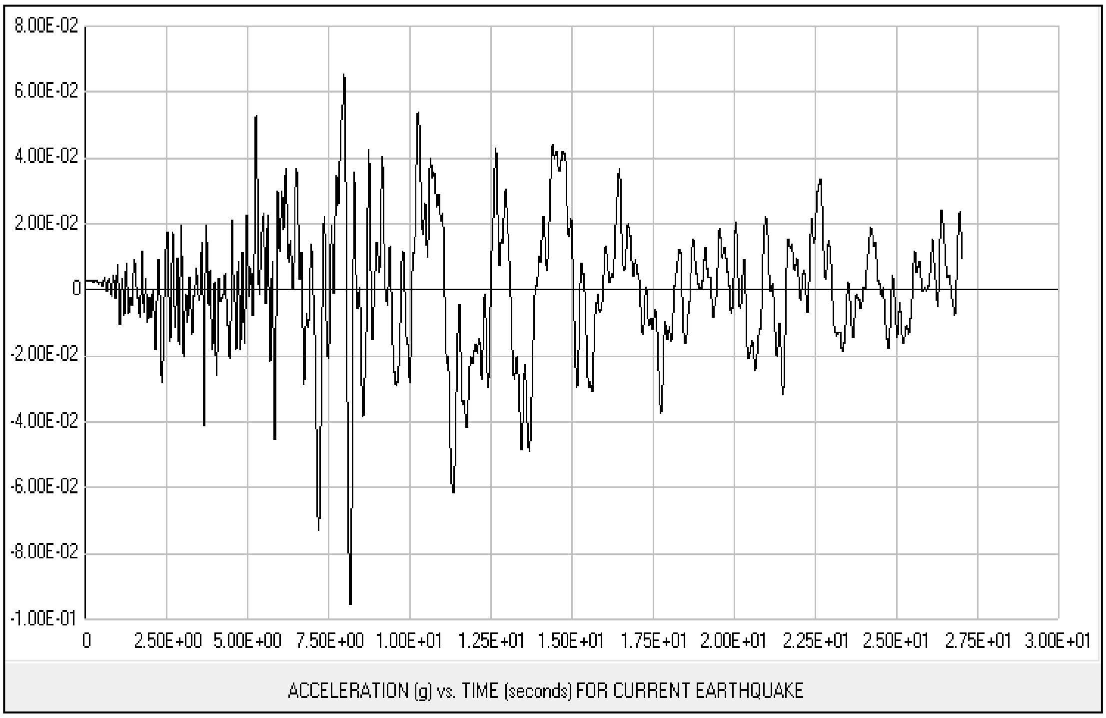

Figure 5.4 : Irpinia E-W EQ Record.

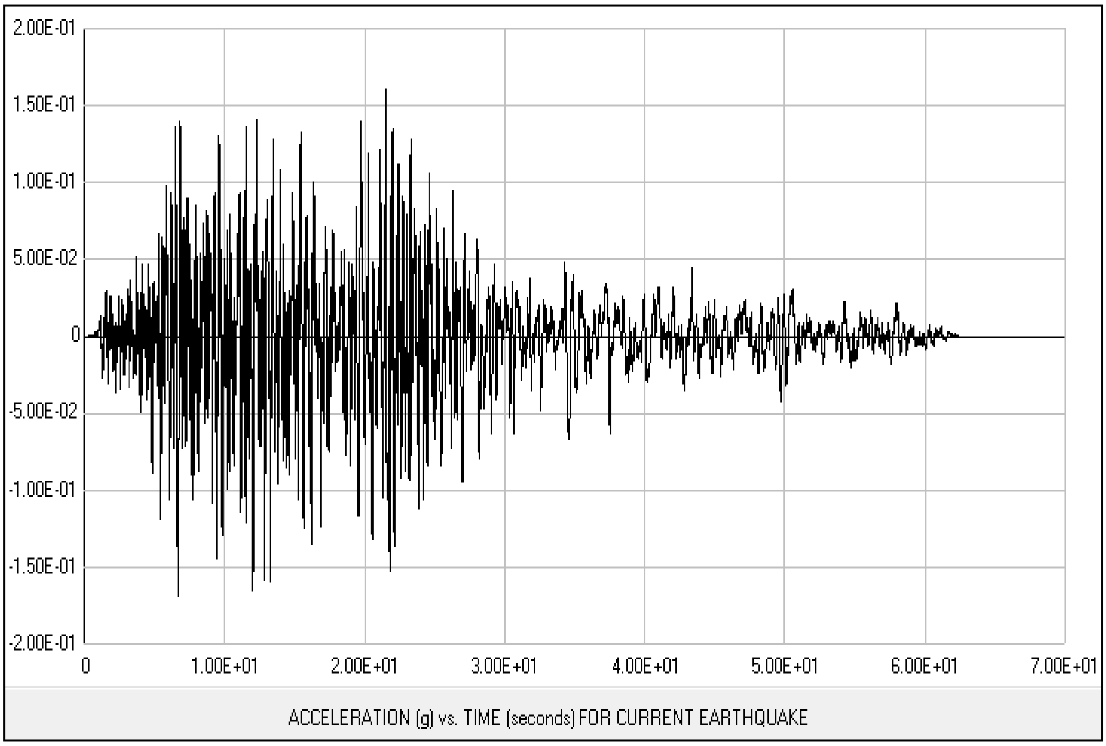

Figure 5.5 : Imperial Valley E-W EQ Record.

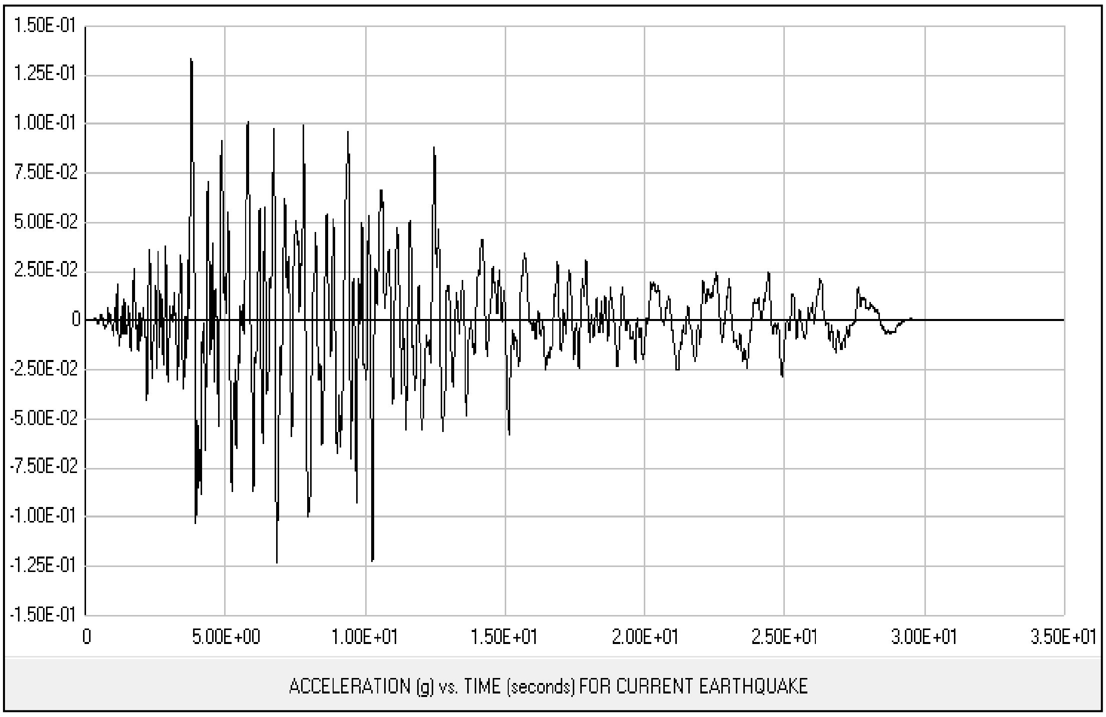

Figure 5.6 : Northridge E-W EQ Record.

5.1.2 Graphical Display of MCEs

As the maximum considered earthquake Landers is chosen. In the figure 5.7, the graphical display of the record is shown.

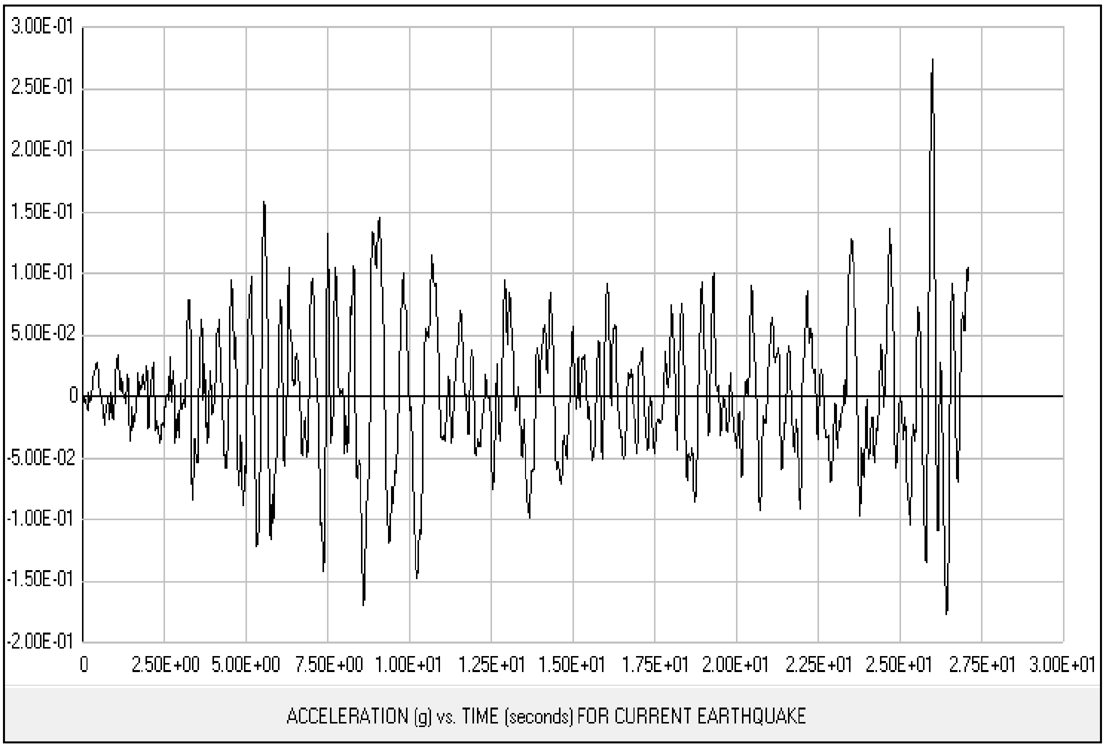

Figure 5.7 : Landers E-W EQ Record.

5.2 OpenSEES Models

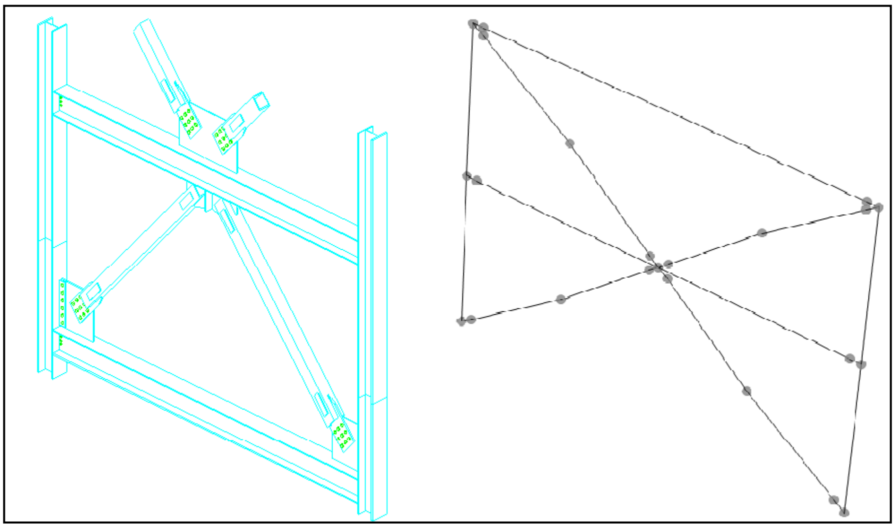

Figure 5.8 : Opensees Representation of Braces.

In opensees models, the brace system is modeled as shown above in the figure 5.8. In the mid part of brace, there is an imperfection to supply brace buckling in analysis. All the gusset plates are also modeled in the opensees. For hinge behavior, the zero length elements are defined between gusset plates and braces.In addition only the half of the models is constructed in the software and the structures consist only the elements in the analysis direction. Instead of other elements, the loads they carry and their self-weights are imposed on models as point loads. To prove that opensees models represent the real models, the element internal forces and natural vibration periods are compared with SAP 2000 as shown below. There is an expected situation that periods of Opensees model are lower than SAP 2000 models as shown in the table 5.5. The internal forces are very close to each other. In the figure 5.9, 5.10 and 5.10, the OpenSEES Represantation of Push-over Analysis are shown.

Table 5.5 : Period Comparison Between SAP2000 and Opensees.

	SAP2000	Opensees
Model 15-12	1,68	1,68
Model 25-12	1,55	1,54
Model 40-12	1,46	1,39
Model 15-16	2,68	2,35
Model 25-16	2,39	2,18
Model 40-16	2,20	1,99
Model 15-20	3,13	2,57
Model 25-20	3,07	2,55
Model 40-20	2,97	2,52

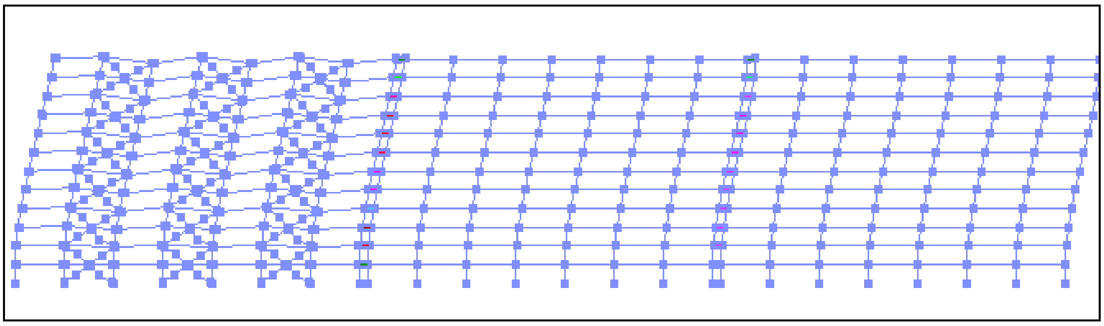

Figure 5.9 : OpenSEES Representation of Push-over Analysis(12 storey).

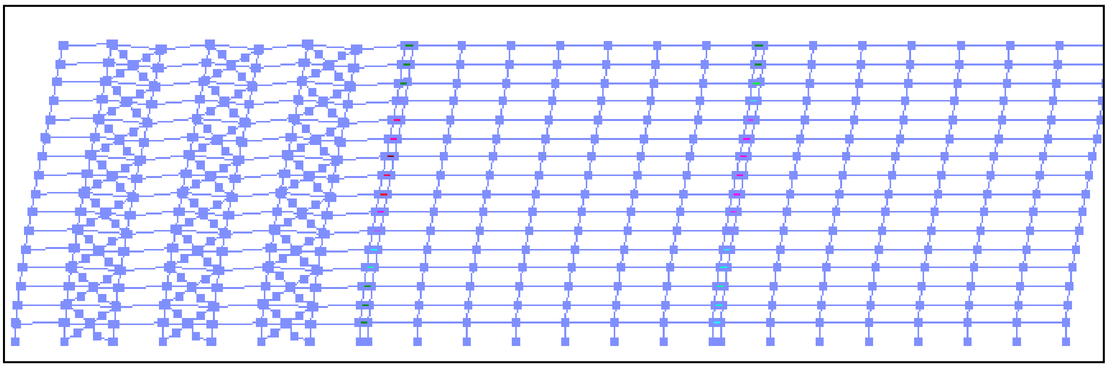

Figure 5.10 : OpenSEES Representation of Push-over Analysis(16 storey).

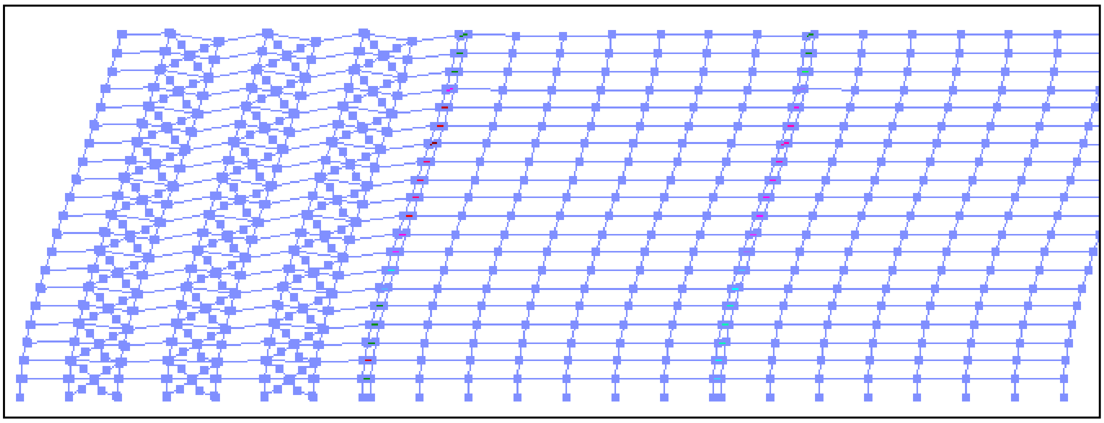

Figure 5.11 : OpenSEES Representation of Push-over Analysis(20 storey).

In opensees models, corotational transformation is used. According to Opensees Manuel, “This command is used to construct the Corotational Coordinate Transformation (CorotCrdTransf) object. Corotational transformation can be used in large displacement-small strain problems. The element coordinate system is specified as follows: The x-axis is the axis connecting the two element nodes; the y- and z-axes are then defined using a vector that lies on a plane parallel to the local x-z plane -- vecxz. The local y-axis is defined by taking the cross product of the vecxz vector and the x-axis. The z-axis by taking cross product of x and new y. The section is attached to the element such that the y-z coordinate system used to specify the section corresponds to the y-z axes of the element.”

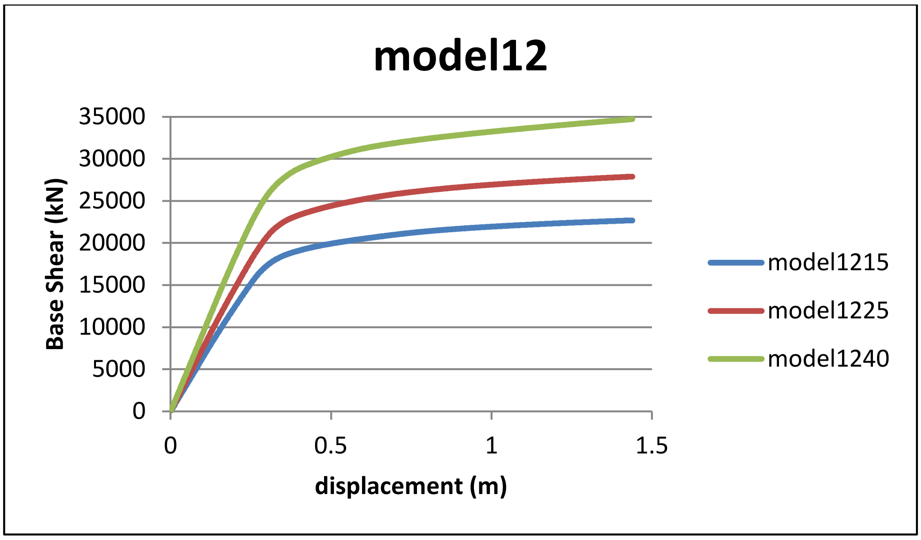

Figure 5.12 : Push-over Curve of 12 Storey (OpenSEES).

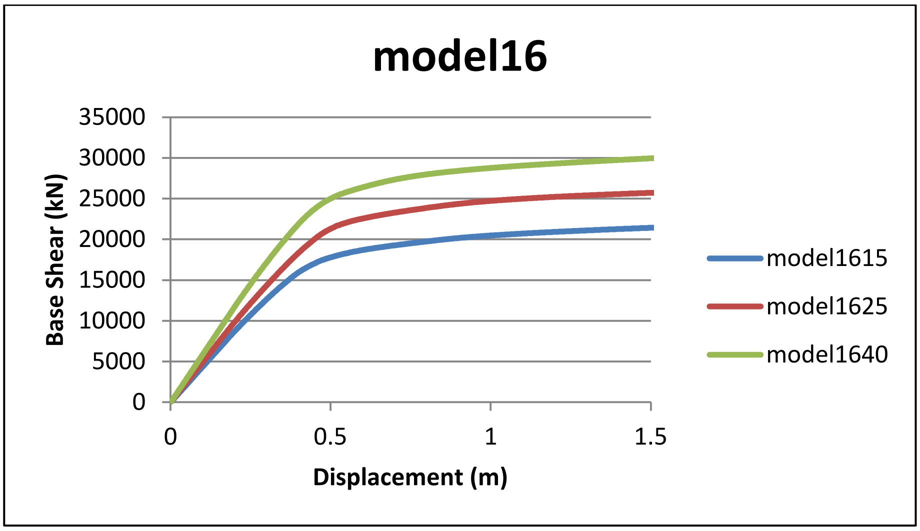

Figure 5.13 : Push-over Curve of 16 Storey (OpenSEES).

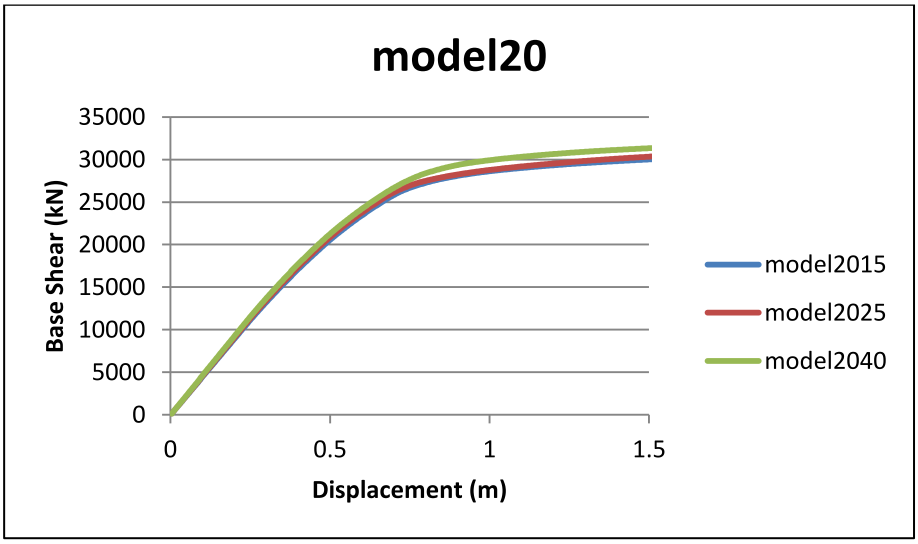

Figure 5.14 : Push-over Curve of 20 Storey (OpenSEES).

Table 5.6 : Base Shear Distribution.

	BF(kN)	MF(kN)	MF/TS (%)
Model 15-12	9451	2823	23
Model 25-12	9628	3561	27
Model 40-12	8262	4085	36
Model 15-16	8020	2818	26
Model 25-16	9387	4836	34
Model 40-16	12099	7416	38
Model 15-20	19459	6145	24
Model 25-20	15567	6994	31
Model 40-20	12431	7301	37

In the figure 5.12, 5.13 and 5.14, the push-over curves of structures are shown with respect to the base shear distribution. In the table 5.6 the base shear distribution after push-over analysis is indicated.

5.2.1 Nonlinear Dynamic Analysis Results

5.2.1.1 Story Drift Calculation

The story drifts are normalized by story heights. For each model, the story drifts are calculated with respect to story numbers. For DBE and maximum of MCEs, the graphs are illustrated separately. The drifts are calculated with the equation **(5.1)** below:

$$\theta_y = \frac{\Delta_i - \Delta_{i-1}}{h_i} \tag{5.1}$$

where θ is the story drift angle (radians),

Δ is the absolute floor displacement (m),

h is the story height (m), and

i is the story level of interest (dimensionless).

Graphs are prepared with respect to earthquake types. Firstly, for each model, the story drifts for Design Based Earthquake and Maximum Considered Earthquake were drawn as shown in the figure 5.15, 5.17 and 5.19 respectively. After that to make a better comparison, the graphs were drawn by taking into record type into consideration as indicated in figure 5.16, 5.18 and 5.20. In each earthquake type, the structures are compared. This detail comparison is shown below:

5.2.1.2 Story Drift Graphs

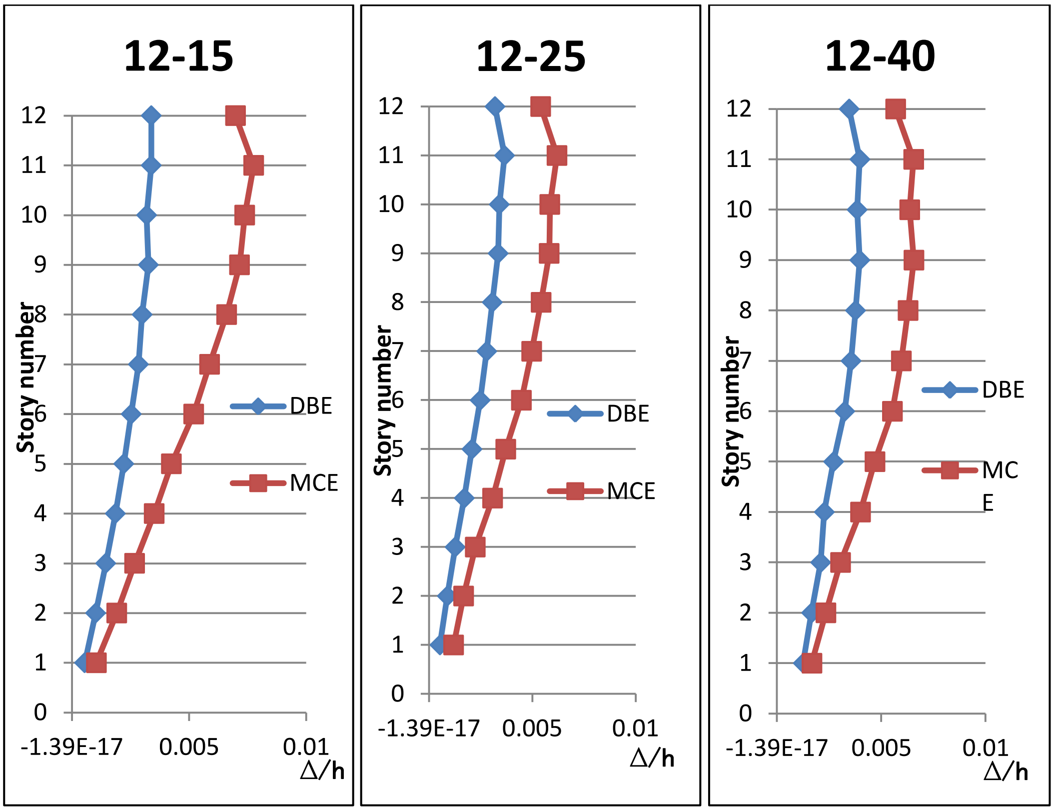

Figure 5.15 : Story Drift Max. of DBE and MCE (12 storey).

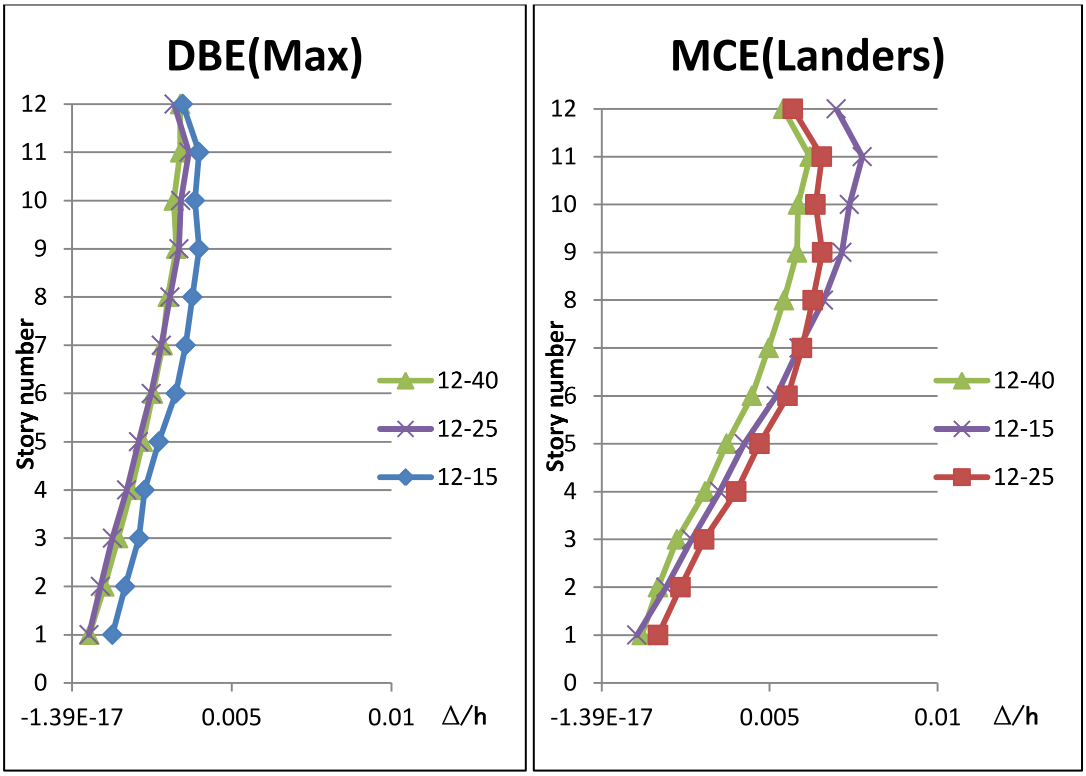

Figure 5.16 : Story Drift Comparison (12 storey).

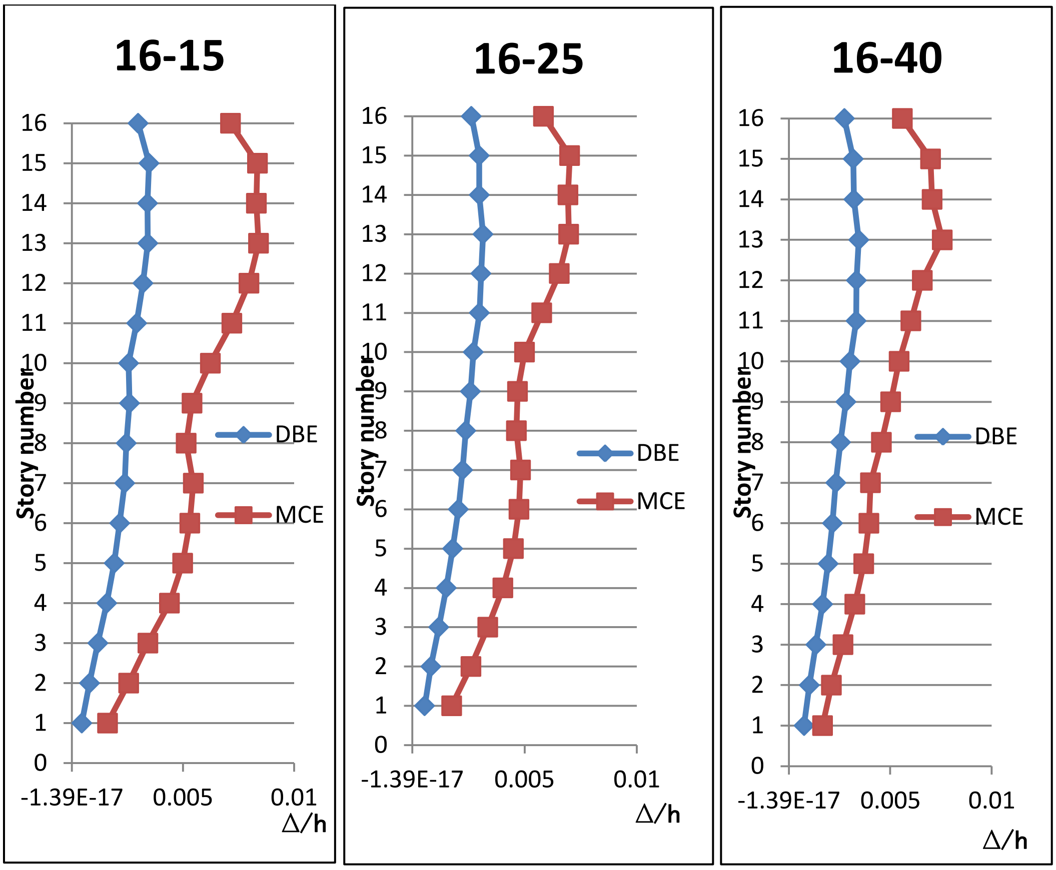

Figure 5.17 : Story Drift Max. of DBE and MCE (16 storey).

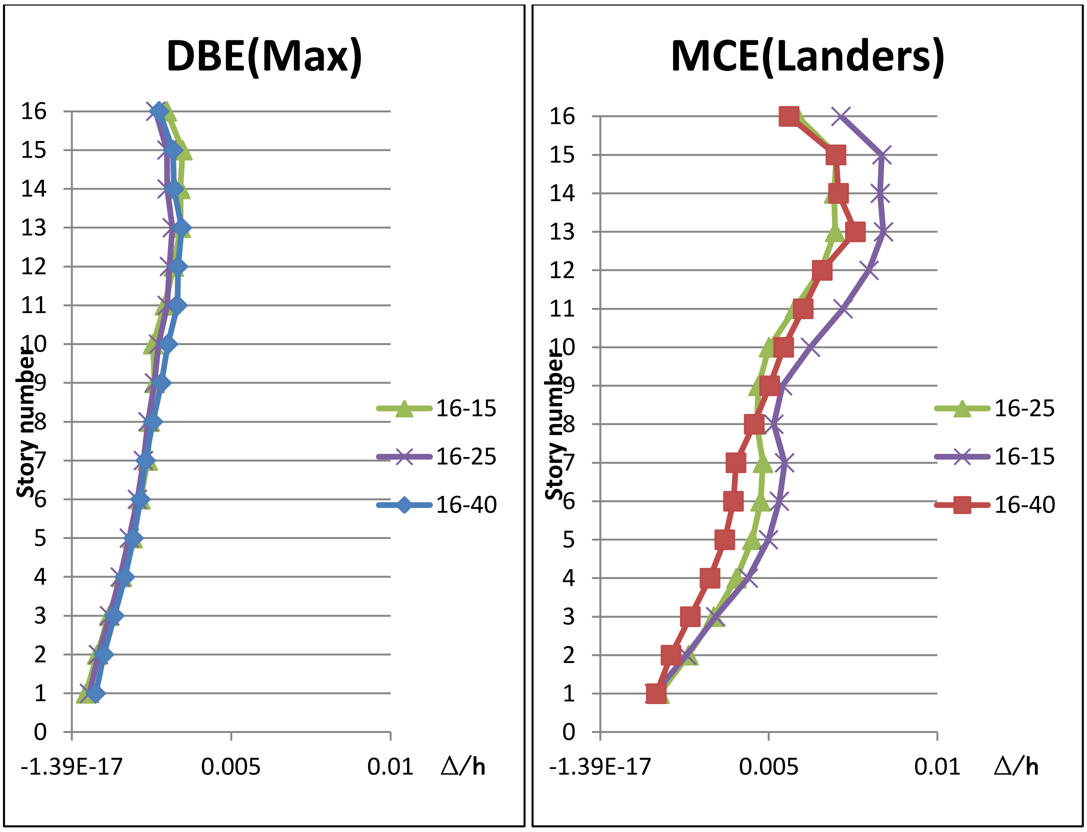

Figure 5.18 : Story Drift Comparison (16 storey).

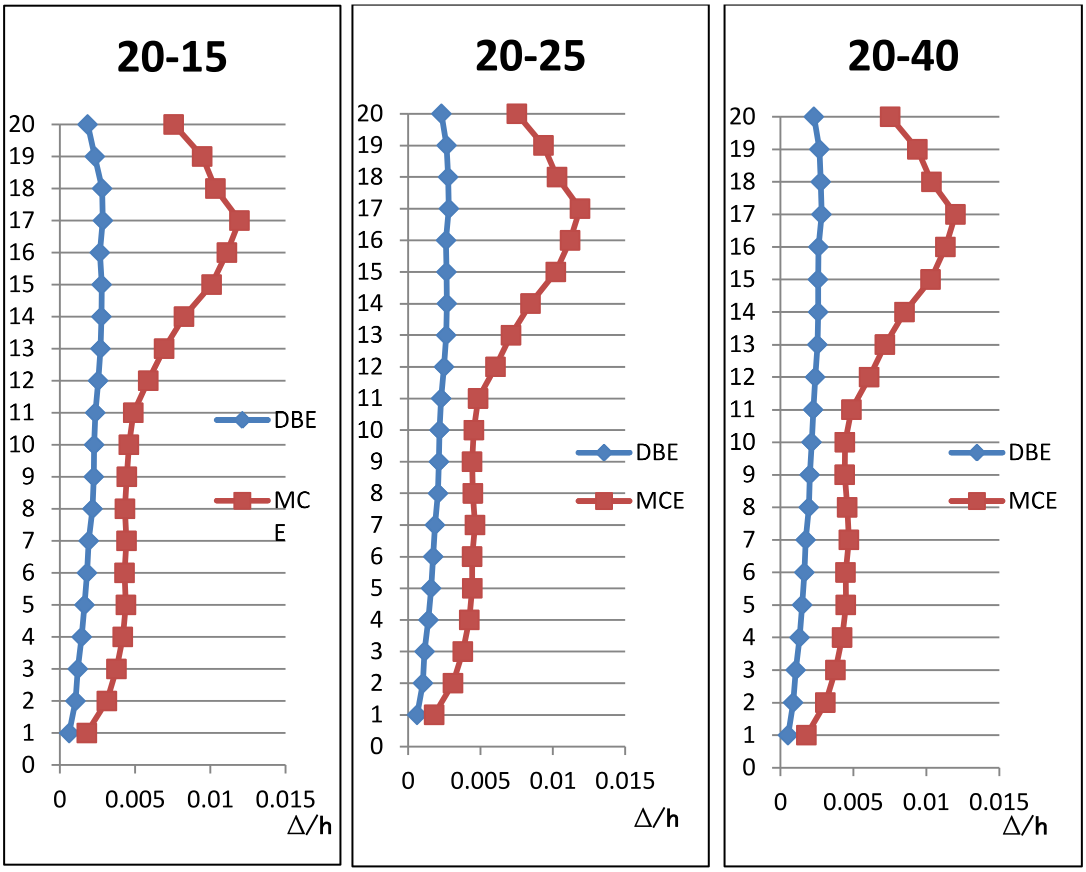

Figure 5.19 : Story Drift Max. of DBE and MCE (20 storey).

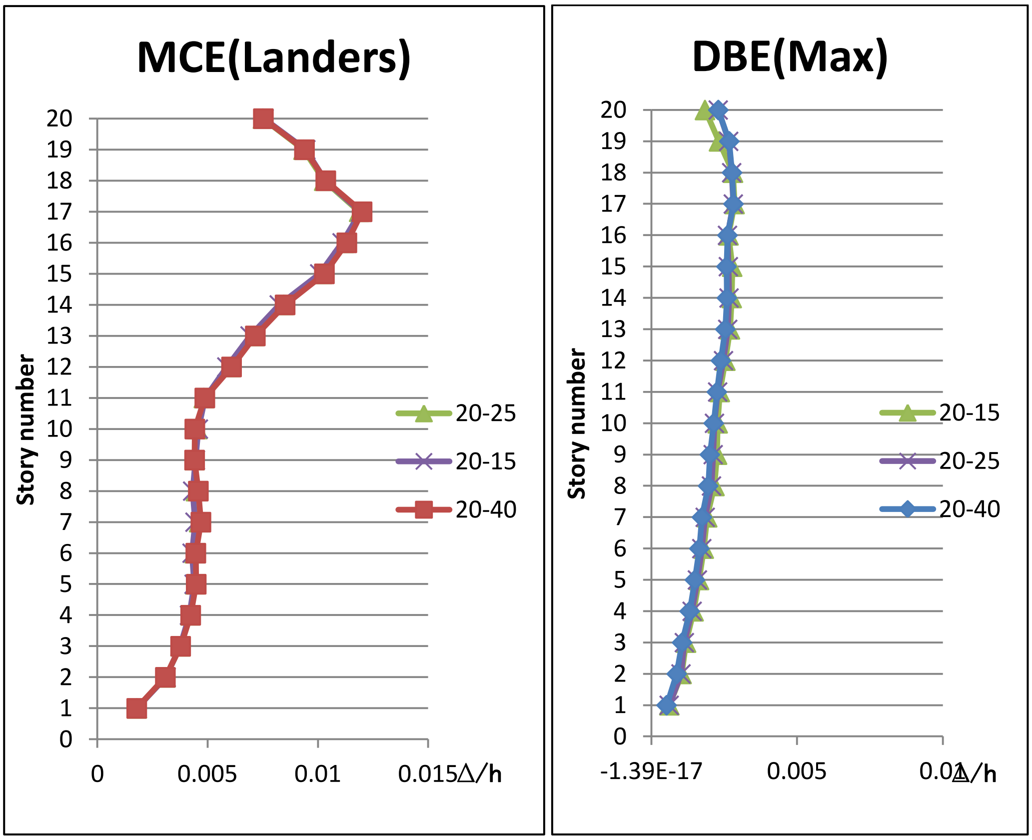

Figure 5.20 : Story Drift Comparison (20 storey).

6. CONCLUSIONS AND RECOMMENDATIONS

After the analysis, general assessment and the comments about story shear, base shear distribution and recommendations are given below:

6.1 General Assesment

In the linear static analysis, the size of the overall structural member is determined. In non-linear static analysis, the distribution of the base shear is examined and the plastic hinge formation at the target displacement point is observed in the building. In nonlinear dynamic analysis, story drifts and base shear force distribution are controlled for assessment.The detailed explanation is given below.

6.2 Story Shears

To sum up, according to the linear static analysis the base shear distribution of 12 storey building is %8, 11 and 15, the base shear distribution of 16 storey building is %5, 8 and 14 and the base shear distribution of 20 storey building is %9, 13 and 16. according to the nonlinear static analysis the base shear distribution of 12 storey building is %9, 12 and 17, the base shear distribution of 16 storey building is %8, 13 and 21 and the base shear distribution of 20 storey building is %10, 14 and 21 respectively.

6.3 Story Drifts

There is no clear evidence that one model is more suitable for better performance when we examine the story drift results. In general story drift ratios over the heigth of the buildings are found to be less than 0,02. Additionally, the story drift figures show that all drift ratios are nearly 0,01 for DBE. Finally, only drift demands are not adequate to show one model as performing well than another.

6.4 Recommendations

Firstly, apart from base shear distributions, all structures satisfy the drift limits. It is hard to determine the exact role of moment frames in the structurtes due to variation of their strength. ASCE 7-05 sets this 25% rule for dual systems, but the all results show that there is no significant performance gap between Model 15, Model 25 or Model40 similarly to the Model 25. For this reason, it is difficult to say that this rule is a necessity. In this paper, it is shown that only linear analysis with the application of 25% rule is not a sufficient method. The moment frame strength requirement should de determined according to performance based design. This supplies more efficient and economic MF system design.

REFERENCES

Abrahart, R. J., and See, L. (1998). Neural Network vs. ARMA Modelling: **[1] ASCE 7-05.** (2006). Minimum Design Loads for Buildings and Other Structures. *American Society of Civil Engineers/Structural Engineering Institute,* Reston, VA, USA.

[2] ASCE 41-06. (2007). Seismic Rehabilitation of Existing Buildings. *American Society of Civil Engineers/Structural Engineering Institute,* Reston, VA, USA.

[3] Aukeman, L. J. et. al. (2011). *Evaluation of the ASCE 7-05 Design Rule for Relative Strength in a Tall Buckling-Restrained Braced Frame Dual System,* San Luis Obispo, CA, USA.

[4] CSI. (2013). ETABS Analysis Reference Manual Version 13. *Computers and Structures, Inc. (CSI),* Berkeley, CA, USA.

[5] CSI. (2014). SAP 2000 Analysis Reference Manual Version 17. *Computers and Structures, Inc. (CSI),* Berkeley, CA, USA.

[6] Hutchinson, D. (1997). Seismic Design Manual Design Example 3 Steel Special Moment Resisting Frame, *Buehler & Buehler Structural Engineers, Inc.,* Sacremento, CA.

[7] Magnuson, J. D. (1997). ”Earthquake-Resisting Dual Systems and the 25% Rule.”, *Building to Last: Proceedings of Structural Congress:* Vol. 1. ASCE, NY.

[8] Nabin, R. J., & Elavenil, S. (2012). Analytical Study on Seismic Performance of Hybrid (DUAL) Structural System Subjected To Earthquake, *International Journal of Modern Engineering Research (IJMER):* Vol2. . (pp. 2358-2363). Chennai: SRM University Press.

[9] Opensees. (2015). Opensees Analysis Reference Manual Version 2.4.5. *University of California,* Berkeley, CA, USA.

[10] Qiang, X. (2008). Dual System Design of Steel Frames Incorporating Buckling-Restrained Braces, *The 14th World Conference on Earthquake Engineering,* Shanghai, China.

Url-1 <*http://www.ijmer.com*>, date retrieved 21.03.2014.

[11] SEAOC Seismology Committee. (2007). *the SEAOC Blue Book: SeismicDesign Recommendations*, Jan.2007.

Url-1 <*http://www.seaoc.org/bluebook/index.html*>, date retrieved 25.05.2014.

[12] UBC (1988). Uniform Building Code, *International Conference of Building Officials*, Whittier, CA.

[13] Wakabayashi, M., Matsu, C., Minami, K. and Mitani, I. (1974). Inelastic Behaviour of Full-Scale Steel Frames with and without Bracings. *JBulletin of the Disaster Prevention Research Institute,* Vol. ***24***, no. 1, pp. 1-23.

Url-1 <*http://hdl.handle.net/2433/124840*>, date retrieved 17.02.2015.

[14] Zandi, Y. (2013). Comparison of Dual System of Steel Moment frame and Thin steel Plate shear walls with Dual system of Steel moment frame and cross Barcings or Chevron with a design Method based on Performance levels, *Bulletin of Environment, Pharmacology and Life Sciences* Vol2. . (pp. 51-57). Tabriz, Iran.

Url-1 <*http://www.bepls.com*>, date retrieved 22.03.2014.

APPENDICES

APPENDIX A: PMM Deatils

Table A.1 : Steel Design (12-Storey Main) - PMM Details - AISC360-05-IBC2006.

Frame	Section	Type	Combo	P_r (kN)	M_{33} (kNm)	M_{22} (kNm)	Ratio
1	W14X283	Column	COMB11-O	-765.251	190.912	-6.3757	0.141208
41	W14X283	Column	COMB22O	-765.251	-172.483	6.3705	0.131577
49	W14X283	Column	COMB22O	-7432.62	-180.829	-4.7099	0.766396
57	W14X211	Column	COMB23O	-2773.29	-103.089	2.8298	0.410823
65	W14X211	Column	COMB23O	-2737.86	-100.781	2.3897	0.404422
73	W14X211	Column	COMB23O	-2721.58	-98.5898	2.3865	0.401004
81	W14X211	Column	COMB23O	-2778.52	-96.2817	2.0267	0.406053
89	W14X283	Column	COMB22O	-6641.39	-168.965	12.5772	0.695925
97	W14X283	Column	COMB11-O	-7509.15	179.7328	-3.8959	0.772121
137	W14X283	Column	COMB11-O	-6688.15	168.7028	-0.5111	0.688988
145	W14X283	Column	COMB22O	-7468.83	-180.343	-7.7453	0.772261
153	W14X211	Column	COMB23O	-2758.83	-103.198	0.9233	0.406694
161	W14X211	Column	COMB12-O	-2721.73	100.8099	-0.4911	0.400045
169	W14X211	Column	COMB12-O	-2726.47	98.6037	-0.4734	0.399181
177	W14X211	Column	COMB23O	-2756.32	-96.4056	0.1101	0.400969
185	W14X283	Column	COMB22O	-6662.24	-168.86	9.3705	0.694833
193	W14X283	Column	COMB11-O	-7469.01	180.341	-7.7521	0.772283
201	W14X211	Column	COMB12-O	-2758.93	103.1981	0.9197	0.406702
209	W14X211	Column	COMB23O	-2721.63	-100.808	-0.4875	0.400027
217	W14X211	Column	COMB23O	-2726.37	-98.6016	-0.4698	0.399164
225	W14X211	Column	COMB12-O	-2756.41	96.4061	0.1064	0.400976
233	W14X283	Column	COMB11-O	-6662.43	168.8601	9.3633	0.694844
241	W14X283	Column	COMB22O	-7508.96	-179.735	-3.8889	0.772099
281	W14X283	Column	COMB22O	-6687.97	-168.703	-0.5036	0.688964
289	W14X283	Column	COMB11-O	-7432.81	180.8267	-4.7168	0.766418
297	W14X211	Column	COMB12-O	-2773.54	103.0643	2.8262	0.410833
305	W14X211	Column	COMB12-O	-2738.11	100.7565	2.386	0.404432
313	W14X211	Column	COMB12-O	-2721.84	98.5651	2.3828	0.401015
321	W14X211	Column	COMB12-O	-2778.76	96.2577	2.023	0.406063
329	W14X283	Column	COMB11-O	-6641.58	168.9647	12.57	0.695935
337	W14X283	Column	COMB22O	-765.251	-190.911	-6.3682	0.1412
377	W14X283	Column	COMB11-O	-765.251	172.4839	6.3629	0.13157
1102	220x220x20	Brace	COMB22O	-1392.69	0	1.1265	0.93926
1108	250x250x20	Brace	COMB22O	-1647.69	0	1.4369	0.782613
1116	250x250x20	Brace	COMB11-O	-1647.74	0	-1.4377	0.782638
1126	220x220x20	Brace	COMB11-O	-1392.75	0	-1.1272	0.939307
1132	250x250x20	Brace	COMB11-O	-1659.78	0	-1.6535	0.788904
1134	220x220x20	Brace	COMB22O	-1405.53	0	1.2893	0.948677
1140	250x250x20	Brace	COMB22O	-1659.74	0	1.6526	0.78888
1142	220x220x20	Brace	COMB11-O	-1405.59	0	-1.29	0.948724
1150	220x220x20	Brace	COMB22O	-1249.08	0	-1.2479	0.838209
1156	250x250x20	Brace	COMB22O	-1482.46	0	-1.4996	0.703602
1164	250x250x20	Brace	COMB11-O	-1482.5	0	1.4988	0.703622
1174	220x220x20	Brace	COMB11-O	-1249.14	0	1.2472	0.83825
1182	220x220x20	Brace	COMB22O	-1259.42	0	-1.0047	0.844281
1190	220x220x20	Brace	COMB11-O	-1259.48	0	1.0039	0.844322
1212	250x250x20	Brace	COMB15-O	-1216.19	0	1.668	0.57864
1214	220x220x20	Brace	COMB26O	-1066.95	0	-1.6685	0.718885
1220	250x250x20	Brace	COMB26O	-1216.25	0	-1.6677	0.578668
1222	220x220x20	Brace	COMB15-O	-1066.98	0	1.6691	0.718913
1228	250x250x20	Brace	COMB26O	-1217.87	0	-1.8288	0.579854
1230	220x220x20	Brace	COMB15-O	-1065.4	0	1.4903	0.717231
1236	250x250x20	Brace	COMB15-O	-1217.81	0	1.8291	0.579826
1238	220x220x20	Brace	COMB26O	-1065.37	0	-1.4898	0.717203
1340	250x250x20	Brace	COMB15-O	-1361.05	0	-2.0712	0.648997
1342	220x220x20	Brace	COMB26O	-1191.6	0	1.5949	0.805351
1348	250x250x20	Brace	COMB26O	-1361.1	0	2.0715	0.649027
1350	220x220x20	Brace	COMB15-O	-1191.64	0	-1.5943	0.805376
1356	250x250x20	Brace	COMB26O	-1359.36	0	1.8955	0.647727
1358	220x220x20	Brace	COMB15-O	-1193.35	0	-1.7972	0.807301
1364	250x250x20	Brace	COMB15-O	-1359.3	0	-1.8952	0.647697
1366	220x220x20	Brace	COMB26O	-1193.31	0	1.7977	0.807276

1509	180x180x10	Brace	COMB22O	-248.265	0	2.49	0.595517
1511	180x180x10	Brace	COMB11-O	-248.263	0	-2.4899	0.595512
1515	180x180x10	Brace	COMB11-O	-252.214	0	-2.4721	0.603472
1517	180x180x10	Brace	COMB22O	-252.216	0	2.4722	0.603477
1521	180x180x10	Brace	COMB22O	-213.538	0	-3.7434	0.523412
1522	180x180x10	Brace	COMB14-O	-30.531	0	1.8064	0.052053
1523	180x180x10	Brace	COMB11-O	-213.536	0	3.7435	0.523408
1527	180x180x10	Brace	COMB11-O	-217.096	0	2.973	0.52338
1529	180x180x10	Brace	COMB22O	-217.098	0	-2.9729	0.523384
1717	200X200X20	Brace	COMB22O	-1097.65	0	1.1734	0.920999
1723	200X200X20	Brace	COMB11-O	-1097.62	0	-1.1736	0.920969
1725	200X200X20	Brace	COMB22O	-1109.39	0	1.3948	0.935574
1727	200X200X20	Brace	COMB11-O	-1109.37	0	-1.395	0.935542
1729	200X200X20	Brace	COMB22O	-975.311	0	-1.3834	0.894827
1735	200X200X20	Brace	COMB11-O	-975.283	0	1.3832	0.894798
1737	200X200X20	Brace	COMB22O	-985.188	0	-1.1961	0.904056
1739	200X200X20	Brace	COMB11-O	-985.16	0	1.1959	0.904027
1927	200x200x16	Brace	COMB22O	-762.708	0	2.3038	0.858585
1933	200x200x16	Brace	COMB11-O	-762.707	0	-2.3037	0.858584
1935	200x200x16	Brace	COMB22O	-772.191	0	3.1851	0.878781
1937	200x200x16	Brace	COMB11-O	-772.19	0	-3.1851	0.87878
1939	200x200x16	Brace	COMB22O	-676.089	0	-3.1837	0.757811
1945	200x200x16	Brace	COMB11-O	-676.089	0	3.1838	0.757811
1947	200x200x16	Brace	COMB22O	-683.992	0	-3.2976	0.770464
1949	200x200x16	Brace	COMB11-O	-683.992	0	3.2977	0.770464
2029	180x180x10	Brace	COMB15-O	-248.062	0	1.9076	0.586952
2031	180x180x10	Brace	COMB26O	-248.062	0	-1.9076	0.586952
2033	180x180x10	Brace	COMB26O	-247.925	0	-2.2063	0.589385
2035	180x180x10	Brace	COMB15-O	-247.925	0	2.2063	0.589385
2061	180x180x10	Brace	COMB15-O	-279.403	0	-1.6256	0.661677
2063	180x180x10	Brace	COMB26O	-279.403	0	1.6255	0.661676
2065	180x180x10	Brace	COMB26O	-278.804	0	1.2539	0.656553
2067	180x180x10	Brace	COMB15-O	-278.804	0	-1.2539	0.656553
2149	200X200X20	Brace	COMB26O	-874.96	0	-2.175	0.815093
2151	200X200X20	Brace	COMB15-O	-874.967	0	2.175	0.8151
2153	200X200X20	Brace	COMB15-O	-873.679	0	1.945	0.812906
2155	200X200X20	Brace	COMB26O	-873.672	0	-1.945	0.812899
2181	200X200X20	Brace	COMB26O	-971.633	0	1.7983	0.912601
2183	200X200X20	Brace	COMB15-O	-971.64	0	-1.7983	0.912609
2185	200X200X20	Brace	COMB15-O	-973.197	0	-2.0732	0.915513
2187	200X200X20	Brace	COMB26O	-973.19	0	2.0732	0.915505
2269	200x200x16	Brace	COMB26O	-608.508	0	-3.3382	0.691988
2271	200x200x16	Brace	COMB15-O	-608.508	0	3.3382	0.691988
2273	200x200x16	Brace	COMB15-O	-607.896	0	2.948	0.689366
2275	200x200x16	Brace	COMB26O	-607.896	0	-2.9481	0.689366
2301	200x200x16	Brace	COMB26O	-673.594	0	2.2965	0.765561
2303	200x200x16	Brace	COMB15-O	-673.594	0	-2.2966	0.765561
2305	200x200x16	Brace	COMB15-O	-674.883	0	-2.7761	0.769685
2307	200x200x16	Brace	COMB26O	-674.883	0	2.7761	0.769684
8	W12X26	Beam	COMB22O	-71.229	-7.2751	-0.0114	0.346576
16	W12X26	Beam	COMB22O	-178.686	-7.3892	0.0119	0.803741
24	W12X26	Beam	COMB22O	-144.822	-7.4539	0.006	0.665118
32	W12X26	Beam	COMB22O	-70.831	-7.276	-0.0792	0.347011
40	W12X26	Beam	COMB22O	-178.164	-7.3936	-0.0623	0.803143
48	W12X26	Beam	COMB22O	-144.35	-7.4633	-0.0821	0.665522
56	W12X26	Beam	COMB22O	-71.092	-7.2767	-0.0819	0.348185
64	W12X26	Beam	COMB22O	-178.496	-7.3968	-0.0852	0.805269
72	W12X26	Beam	COMB22O	-144.67	-7.4696	-0.1011	0.667503
80	W12X26	Beam	COMB22O	-64.87	-7.2758	0.0237	0.320446
88	W12X26	Beam	COMB22O	-161.424	-7.3913	0.0246	0.731383
96	W12X26	Beam	COMB22O	-130.505	-7.457	0.0231	0.604911
104	W12X26	Beam	COMB22O	-64.444	-7.2763	0.0734	0.320197
112	W12X26	Beam	COMB22O	-160.883	-7.3942	0.0513	0.729941
120	W12X26	Beam	COMB22O	-130.027	-7.4634	0.0753	0.604535
128	W12X26	Beam	COMB22O	-64.731	-7.2766	0.0593	0.320963
136	W12X26	Beam	COMB22O	-161.234	-7.3958	0.0265	0.730668
144	W12X26	Beam	COMB22O	-130.353	-7.4667	0.054	0.605286
152	W12X26	Beam	COMB26O	-73.667	-7.3681	0.099	0.362817
160	W12X26	Beam	COMB26O	-116.164	-7.4498	0.0756	0.54465
168	W12X26	Beam	COMB26O	-107.604	-7.5405	0.1791	0.515012
176	W12X26	Beam	COMB26O	-73.674	-7.3677	0.0917	0.362622

184	W12X26	Beam	COMB26O	-116.17	-7.449	0.0576	0.544117
192	W12X26	Beam	COMB26O	-107.602	-7.5389	0.1608	0.514427
200	W12X26	Beam	COMB26O	-84.922	-7.3669	-0.1015	0.410243
208	W12X26	Beam	COMB26O	-131.672	-7.4482	-0.0676	0.610065
216	W12X26	Beam	COMB26O	-123.044	-7.5381	-0.1754	0.580668
224	W12X26	Beam	COMB26O	-84.929	-7.3672	-0.1089	0.410502
232	W12X26	Beam	COMB26O	-131.678	-7.449	-0.0858	0.610655
240	W12X26	Beam	COMB26O	-123.041	-7.5398	-0.1941	0.581244
248	W12X26	Beam	COMB22O	-129.607	-9.8255	-0.017	0.620557
256	W12X26	Beam	COMB22O	-129.6	-9.8351	-0.3118	0.629593
264	W12X26	Beam	COMB22O	-129.884	-9.8643	-0.2936	0.630442
272	W12X26	Beam	COMB22O	-113.377	-9.8319	-0.0042	0.550843
280	W12X26	Beam	COMB22O	-113.384	-9.8351	0.2986	0.559936
288	W12X26	Beam	COMB22O	-113.654	-9.8578	0.2945	0.561116
296	W12X26	Beam	COMB22O	-129.12	-7.5156	-0.0236	0.601732
304	W12X26	Beam	COMB22O	-128.903	-7.5302	-0.2379	0.607506
312	W12X26	Beam	COMB22O	-129.213	-7.5393	-0.2497	0.609251
320	W12X26	Beam	COMB22O	-116.711	-7.5201	0.0419	0.549451
328	W12X26	Beam	COMB22O	-116.504	-7.5302	0.2208	0.554145
336	W12X26	Beam	COMB22O	-116.804	-7.5349	0.1939	0.554631
344	W12X26	Beam	COMB22O	-131.186	-7.7317	-0.0824	0.616506
352	W12X26	Beam	COMB22O	-131.22	-7.7475	-0.9932	0.644802
360	W12X26	Beam	COMB22O	-131.819	-7.7703	-0.9838	0.647228
368	W12X26	Beam	COMB22O	-113.796	-7.7385	0.0947	0.542466
376	W12X26	Beam	COMB22O	-113.859	-7.7475	0.9345	0.568659
384	W12X26	Beam	COMB22O	-114.429	-7.7635	0.8471	0.568517
392	W12X26	Beam	COMB26O	-103.65	-9.8356	0.3408	0.519668
395	W12X26	Beam	COMB26O	-103.613	-9.8321	0.3444	0.519598
399	W12X26	Beam	COMB26O	-119.063	-9.8318	-0.3621	0.58612
407	W12X26	Beam	COMB26O	-119.026	-9.836	-0.3615	0.585972
409	W12X26	Beam	COMB26O	-97.49	-7.6185	0.4541	0.481477
413	W12X26	Beam	COMB26O	-97.447	-7.616	0.4307	0.480555
416	W12X26	Beam	COMB26O	-113.023	-7.6158	-0.4554	0.547775
424	W12X26	Beam	COMB26O	-112.98	-7.6186	-0.4805	0.548382
427	W12X26	Beam	COMB26O	-93.399	-7.7487	0.6703	0.472938
431	W12X26	Beam	COMB26O	-93.284	-7.7454	0.6476	0.471723
439	W12X26	Beam	COMB26O	-105.29	-7.7451	-0.6865	0.524319
447	W12X26	Beam	COMB26O	-105.175	-7.749	-0.7133	0.524678
808	W12X26	Beam	COMB26O	-76.031	-12.1939	0.0034	0.40242
815	W12X26	Beam	COMB26O	-119.546	-12.2619	0.0067	0.586953
823	W12X26	Beam	COMB26O	-110.664	-12.4404	0.0055	0.554915
831	W12X26	Beam	COMB26O	-76.043	-12.1939	-0.0044	0.402502
839	W12X26	Beam	COMB26O	-119.564	-12.262	-0.0118	0.587184
847	W12X26	Beam	COMB26O	-110.702	-12.4405	-0.0109	0.555243
856	W12X26	Beam	COMB26O	-80.818	-12.1912	0.0034	0.422538
864	W12X26	Beam	COMB26O	-126.142	-12.259	0.0067	0.614731
879	W12X26	Beam	COMB26O	-117.21	-12.4371	0.0062	0.582755
887	W12X26	Beam	COMB26O	-80.83	-12.1912	-0.0046	0.422627
896	W12X26	Beam	COMB26O	-126.159	-12.259	-0.0119	0.614963
904	W12X26	Beam	COMB26O	-117.248	-12.4373	-0.0102	0.583037
919	W12X26	Beam	COMB26O	-106.658	-15.859	-0.0037	0.593786
927	W12X26	Beam	COMB26O	-106.651	-15.86	0.0046	0.593794
929	W12X26	Beam	COMB26O	-113.178	-15.8589	-0.0017	0.623461
933	W12X26	Beam	COMB26O	-113.172	-15.8601	0.0065	0.623588
936	W12X26	Beam	COMB26O	-100.108	-13.0717	0.003	0.531854
944	W12X26	Beam	COMB26O	-100.146	-13.072	-0.009	0.532212
947	W12X26	Beam	COMB26O	-106.661	-13.0703	0.0052	0.560933
951	W12X26	Beam	COMB26O	-106.699	-13.0707	-0.0067	0.56115
959	W12X26	Beam	COMB26O	-94.172	-13.4689	-9.3E-05	0.515756
967	W12X26	Beam	COMB26O	-94.123	-13.4696	-0.0059	0.515705
976	W12X26	Beam	COMB26O	-99.109	-13.4687	0.0043	0.538133
984	W12X26	Beam	COMB26O	-99.06	-13.4696	-0.0016	0.537833

Table A.2 : Steel Design 16-Storey Main) - PMM Details - AISC360-05-IBC2006.

Frame	Section	Type	Combo	P_r (kN)	M_{33} (kNm)	M_{22} (kNm)	Ratio
1	W14X283	Column	COMB11-O	-764.296	187.805	-6.5234	0.139695
9	W14X283	Column	COMB26O	-5550.129	-130.5656	10.2684	0.585861
17	W14X283	Column	COMB15-O	-5543.762	130.5574	7.898	0.583089
25	W14X283	Column	COMB26O	-5543.593	-130.5671	7.8998	0.583079
33	W14X283	Column	COMB15-O	-5550.055	130.556	10.2662	0.585848
41	W14X283	Column	COMB22O	-764.296	-169.2477	6.5193	0.129998
49	W14X283	Column	COMB22O	-7269.268	-182.996	-4.4921	0.764999
57	W14X283	Column	COMB23O	-2804.57	-144.4208	3.7657	0.330599
65	W14X283	Column	COMB23O	-2761.617	-141.1519	3.2481	0.324622
73	W14X283	Column	COMB23O	-2744.272	-137.9875	3.2434	0.32154
81	W14X283	Column	COMB23O	-2810.99	-134.7184	2.792	0.325795
89	W14X283	Column	COMB22O	-6547.903	-168.7155	12.5983	0.698739
97	W14X283	Column	COMB11-O	-7343.258	182.0464	-3.9836	0.758141
105	W14X283	Column	COMB26O	-6548.811	-4.5332	-50.7987	0.656083
113	W14X283	Column	COMB15-O	-6552.626	1.5448	50.7884	0.65504
121	W14X283	Column	COMB26O	-6550.811	1.5399	-50.7954	0.654875
129	W14X283	Column	COMB15-O	-6549.668	-4.5283	50.7932	0.656155
137	W14X283	Column	COMB11-O	-6594.786	168.4948	-0.5784	0.680435
145	W14X283	Column	COMB22O	-7301.249	-182.5922	-7.6411	0.770677
153	W14X283	Column	COMB23O	-2780.617	-144.5027	1.1721	0.326033
161	W14X283	Column	COMB12-O	-2735.685	141.1937	-0.6601	0.31986
169	W14X283	Column	COMB12-O	-2740.94	138.0159	-0.6445	0.318858
177	W14X283	Column	COMB23O	-2779.657	-134.8139	0.189	0.320543
185	W14X283	Column	COMB22O	-6565.884	-168.6327	9.3052	0.697348
193	W14X283	Column	COMB11-O	-7301.318	182.5986	-7.6401	0.770685
201	W14X283	Column	COMB12-O	-2780.673	144.513	1.1729	0.326044
209	W14X283	Column	COMB23O	-2735.629	-141.1854	-0.6609	0.319852
217	W14X283	Column	COMB23O	-2740.887	-138.0076	-0.6453	0.31885
225	W14X283	Column	COMB12-O	-2779.709	134.8241	0.1898	0.320554
233	W14X283	Column	COMB11-O	-6565.953	168.6398	9.3062	0.697359
241	W14X283	Column	COMB22O	-7343.19	-182.04	-3.9845	0.758133
249	W14X283	Column	COMB26O	-6851.039	-4.499	-53.5694	0.686639
257	W14X283	Column	COMB15-O	-6855.501	1.5144	53.5536	0.685653
265	W14X283	Column	COMB26O	-6853.563	1.5097	-53.5627	0.685479
273	W14X283	Column	COMB15-O	-6852.019	-4.4938	53.5628	0.686722
281	W14X283	Column	COMB22O	-6594.718	-168.4878	-0.5793	0.680426
289	W14X283	Column	COMB11-O	-7269.336	183.0025	-4.4912	0.765007
297	W14X283	Column	COMB12-O	-2804.632	144.432	3.7665	0.33061
305	W14X283	Column	COMB12-O	-2761.68	141.1631	3.2489	0.324634
313	W14X283	Column	COMB12-O	-2744.337	137.9987	3.2442	0.321552
321	W14X283	Column	COMB12-O	-2811.051	134.7295	2.7928	0.325807
329	W14X283	Column	COMB11-O	-6547.972	168.7226	12.5992	0.698749
337	W14X283	Column	COMB22O	-764.296	-187.7983	-6.5242	0.139692
345	W14X283	Column	COMB26O	-6250.034	-151.046	-6.6346	0.65708
353	W14X283	Column	COMB15-O	-6258.062	151.0225	-9.0055	0.659992
361	W14X283	Column	COMB26O	-6257.822	-151.0325	-9.0038	0.659973
369	W14X283	Column	COMB15-O	-6250.03	151.0365	-6.6359	0.657076
377	W14X283	Column	COMB11-O	-764.296	169.2552	6.5202	0.130002
1102	220x220x20	Brace	COMB22O	-1362.301	0	1.067	0.916544
1108	250x250x20	Brace	COMB22O	-1617.254	0	1.3635	0.767565
1116	250x250x20	Brace	COMB11-O	-1617.314	0	-1.3633	0.767593
1126	220x220x20	Brace	COMB11-O	-1362.331	0	-1.0674	0.916567
1134	220x220x20	Brace	COMB22O	-1373.765	0	1.2189	0.924854
1142	220x220x20	Brace	COMB11-O	-1373.796	0	-1.2193	0.924877
1150	220x220x20	Brace	COMB22O	-1231.092	0	-1.198	0.825148
1156	250x250x20	Brace	COMB22O	-1472.205	0	-1.4559	0.698432
1164	250x250x20	Brace	COMB11-O	-1472.265	0	1.456	0.698461
1174	220x220x20	Brace	COMB11-O	-1231.122	0	1.1977	0.825168
1182	220x220x20	Brace	COMB22O	-1240.274	0	-0.9661	0.830441
1190	220x220x20	Brace	COMB11-O	-1240.304	0	0.9657	0.83046
1214	220x220x20	Brace	COMB26O	-1043.71	0	-1.5501	0.701399
1222	220x220x20	Brace	COMB15-O	-1043.827	0	1.5497	0.701478
1230	220x220x20	Brace	COMB15-O	-1042.505	0	1.3718	0.699972
1238	220x220x20	Brace	COMB26O	-1042.311	0	-1.3715	0.699838
1342	220x220x20	Brace	COMB26O	-1175.531	0	1.4476	0.791711
1350	220x220x20	Brace	COMB15-O	-1175.67	0	-1.4461	0.791803

1358	220x220x20	Brace	COMB15-O	-1177.504	0	-1.6364	0.793738
1366	220x220x20	Brace	COMB26O	-1177.286	0	1.6371	0.793589
1509	180x180x10	Brace	COMB22O	-257.304	0	2.6222	0.620751
1511	180x180x10	Brace	COMB11-O	-257.303	0	-2.6222	0.62075
1515	180x180x10	Brace	COMB11-O	-260.287	0	-2.6244	0.626755
1517	180x180x10	Brace	COMB22O	-260.288	0	2.6244	0.626757
1521	180x180x10	Brace	COMB22O	-223.178	0	-3.8639	0.548992
1523	180x180x10	Brace	COMB11-O	-223.177	0	3.8639	0.548991
1527	180x180x10	Brace	COMB11-O	-225.767	0	3.1276	0.547128
1529	180x180x10	Brace	COMB22O	-225.768	0	-3.1276	0.54713
1717	200X200X20	Brace	COMB22O	-1068.539	0	1.1026	0.987387
1723	200X200X20	Brace	COMB11-O	-1068.526	0	-1.1027	0.987373
1725	200X200X20	Brace	COMB22O	-1078.875	0	1.3064	0.999586
1727	200X200X20	Brace	COMB11-O	-1078.862	0	-1.3065	0.999572
1729	200X200X20	Brace	COMB22O	-955.079	0	-1.3061	0.873652
1735	200X200X20	Brace	COMB11-O	-955.066	0	1.306	0.873639
1737	200X200X20	Brace	COMB22O	-963.733	0	-1.1264	0.881516
1739	200X200X20	Brace	COMB11-O	-963.72	0	1.1263	0.881502
1927	200x200x16	Brace	COMB22O	-743.161	0	2.2472	0.833266
1933	200x200x16	Brace	COMB11-O	-743.16	0	-2.2472	0.833265
1935	200x200x16	Brace	COMB22O	-750.902	0	3.1479	0.85114
1937	200x200x16	Brace	COMB11-O	-750.902	0	-3.1479	0.85114
1939	200x200x16	Brace	COMB22O	-661.69	0	-3.099	0.739889
1945	200x200x16	Brace	COMB11-O	-661.69	0	3.099	0.739889
1947	200x200x16	Brace	COMB22O	-668.065	0	-3.2652	0.750971
1949	200x200x16	Brace	COMB11-O	-668.065	0	3.2652	0.750971
2029	180x180x10	Brace	COMB15-O	-257.326	0	1.8262	0.609962
2031	180x180x10	Brace	COMB26O	-256.979	0	-1.8022	0.609038
2033	180x180x10	Brace	COMB26O	-256.821	0	-1.9729	0.609832
2035	180x180x10	Brace	COMB15-O	-256.741	0	2.1602	0.611916
2061	180x180x10	Brace	COMB15-O	-289.805	0	-1.5025	0.688201
2063	180x180x10	Brace	COMB26O	-289.39	0	1.4698	0.687031
2065	180x180x10	Brace	COMB26O	-288.687	0	0.8615	0.67891
2067	180x180x10	Brace	COMB15-O	-288.613	0	-1.0761	0.681389
2149	200X200X20	Brace	COMB26O	-855.182	0	-2.0598	0.792958
2151	200X200X20	Brace	COMB15-O	-855.279	0	2.0578	0.793047
2153	200X200X20	Brace	COMB15-O	-854.312	0	1.8197	0.791109
2155	200X200X20	Brace	COMB26O	-854.102	0	-1.8199	0.790904
2181	200X200X20	Brace	COMB26O	-956.702	0	1.6717	0.893101
2183	200X200X20	Brace	COMB15-O	-956.824	0	-1.6692	0.893221
2185	200X200X20	Brace	COMB15-O	-958.566	0	-1.9317	0.896154
2187	200X200X20	Brace	COMB26O	-958.325	0	1.9323	0.895905
2269	200x200x16	Brace	COMB26O	-605.059	0	-3.3653	0.687229
2271	200x200x16	Brace	COMB15-O	-605.13	0	3.3517	0.687238
2273	200x200x16	Brace	COMB15-O	-604.892	0	2.9234	0.684795
2275	200x200x16	Brace	COMB26O	-604.594	0	-2.9255	0.684443
2301	200x200x16	Brace	COMB26O	-673.091	0	2.2784	0.763843
2303	200x200x16	Brace	COMB15-O	-673.189	0	-2.2616	0.763869
2305	200x200x16	Brace	COMB15-O	-674.873	0	-2.7333	0.768342
2307	200x200x16	Brace	COMB26O	-674.524	0	2.7375	0.767921
248	W12X26	Beam	COMB22O	-145.237	-6.9786	-0.0343	0.670003
256	W12X26	Beam	COMB22O	-145.364	-6.9825	-0.4321	0.682562
264	W12X26	Beam	COMB22O	-145.71	-7.0382	-0.4053	0.683596
272	W12X26	Beam	COMB22O	-127.655	-6.9878	0.0094	0.594241
280	W12X26	Beam	COMB22O	-127.801	-6.9825	0.4142	0.606859
288	W12X26	Beam	COMB22O	-128.129	-7.029	0.4021	0.608202
352	W12X26	Beam	COMB22O	-134.752	-5.2525	-1.0309	0.644033
360	W12X26	Beam	COMB22O	-135.348	-5.2887	-1.0177	0.646422
368	W12X26	Beam	COMB22O	-118.218	-5.2402	0.1001	0.544564
376	W12X26	Beam	COMB22O	-118.42	-5.2525	0.9725	0.57233
384	W12X26	Beam	COMB22O	-118.986	-5.2789	0.8839	0.572204
392	W12X26	Beam	COMB26O	-104.339	-6.9742	0.4675	0.508045
395	W12X26	Beam	COMB26O	-104.372	-6.9686	0.4851	0.508691
399	W12X26	Beam	COMB26O	-120.137	-6.9678	-0.4986	0.576562
407	W12X26	Beam	COMB26O	-120.192	-6.9749	-0.5371	0.578031
409	W12X26	Beam	COMB26O	-95.268	-5.1501	0.4406	0.454254
413	W12X26	Beam	COMB26O	-95.229	-5.1461	0.4179	0.453359
416	W12X26	Beam	COMB26O	-110.783	-5.1443	-0.4474	0.520517
424	W12X26	Beam	COMB26O	-110.745	-5.1485	-0.4723	0.52115
427	W12X26	Beam	COMB26O	-93.751	-5.1965	0.7498	0.459503
431	W12X26	Beam	COMB26O	-93.657	-5.191	0.7233	0.458244

439	W12X26	Beam	COMB26O	-106.594	-5.1906	-0.7693	0.515032
447	W12X26	Beam	COMB26O	-106.506	-5.1967	-0.7987	0.515601
815	W12X26	Beam	COMB26O	-114.295	-8.0805	0.0061	0.536057
823	W12X26	Beam	COMB26O	-106.082	-7.6699	0.005	0.502619
839	W12X26	Beam	COMB26O	-114.309	-8.0805	-0.0107	0.536257
847	W12X26	Beam	COMB26O	-106.115	-7.6701	-0.0099	0.502913
919	W12X26	Beam	COMB26O	-106.322	-11.8275	-0.007	0.565024
927	W12X26	Beam	COMB26O	-106.656	-11.8285	-0.0082	0.566587
929	W12X26	Beam	COMB26O	-112.905	-11.8274	0.0079	0.595066
933	W12X26	Beam	COMB26O	-113.277	-11.8285	0.0074	0.59675
936	W12X26	Beam	COMB26O	-97.712	-7.5394	0.0027	0.483291
944	W12X26	Beam	COMB26O	-97.754	-7.5396	-0.0091	0.483679
947	W12X26	Beam	COMB26O	-104.239	-7.5258	0.0053	0.512152
951	W12X26	Beam	COMB26O	-104.283	-7.5263	-0.0064	0.512383

Table A.3 : Steel Design 20-Storey Main) - PMM Details - AISC360-05-IBC2006.

Frame	Section	Type	Combo	P_r (kN)	M_{33} (kNm)	M_{22} (kNm)	Ratio
1	W14X283	Column	COMB11-O	-764.953	183.005	-6.5521	0.137247
9	W14X342	Column	COMB26O	-5537.83	-163.5362	10.6189	0.486743
17	W14X342	Column	COMB15-O	-5527.173	163.5296	7.5751	0.483671
25	W14X342	Column	COMB26O	-5527.192	-163.5392	7.5772	0.483678
33	W14X342	Column	COMB15-O	-5537.811	163.5266	10.6168	0.486737
41	W14X283	Column	COMB22O	-764.953	-164.5983	6.5485	0.127629
49	W14X283	Column	COMB22O	-6816.521	-182.5907	-4.4012	0.722629
57	W14X342	Column	COMB23O	-2816.679	-180.9957	4.5213	0.283523
65	W14X342	Column	COMB23O	-2785.832	-176.8133	3.9962	0.27924
73	W14X342	Column	COMB23O	-2759.812	-172.7716	3.9927	0.275762
81	W14X342	Column	COMB23O	-2833.024	-168.5888	3.5226	0.279366
89	W14X283	Column	COMB22O	-6147.773	-165.0703	12.646	0.659885
97	W14X283	Column	COMB11-O	-6888.338	182.0093	-4.0561	0.716685
105	W14X342	Column	COMB26O	-6557.011	-5.8456	-64.2331	0.544421
113	W14X342	Column	COMB15-O	-6556.995	1.9837	64.2295	0.542971
121	W14X342	Column	COMB26O	-6557.012	1.9783	-64.234	0.542973
129	W14X342	Column	COMB15-O	-6556.993	-5.8403	64.2286	0.544414
137	W14X283	Column	COMB11-O	-6192.247	165.0099	-0.6062	0.642117
145	W14X283	Column	COMB22O	-6847.4	-182.3542	-7.6345	0.72836
153	W14X342	Column	COMB23O	-2805.268	-181.111	1.3279	0.280328
161	W14X342	Column	COMB23O	-2760.073	-176.954	0.7982	0.27497
169	W14X342	Column	COMB12-O	-2768.262	172.8194	-0.7961	0.274037
177	W14X342	Column	COMB23O	-2807.688	-168.7201	0.3233	0.275123
185	W14X283	Column	COMB22O	-6164.546	-165.0517	9.3249	0.658386
193	W14X283	Column	COMB11-O	-6847.448	182.3555	-7.6343	0.728365
201	W14X342	Column	COMB12-O	-2805.353	181.1142	1.3281	0.280336
209	W14X342	Column	COMB12-O	-2760.156	176.9572	0.7985	0.274977
217	W14X342	Column	COMB23O	-2768.181	-172.8179	-0.7963	0.274031
225	W14X342	Column	COMB12-O	-2807.766	168.7233	0.3235	0.27513
233	W14X283	Column	COMB11-O	-6164.594	165.0532	9.3252	0.658392
241	W14X283	Column	COMB22O	-6888.291	-182.008	-4.0563	0.716681
249	W14X342	Column	COMB26O	-6865.841	-5.8699	-68.5244	0.570911
257	W14X342	Column	COMB15-O	-6866.34	1.9592	68.5208	0.569482
265	W14X342	Column	COMB26O	-6866.358	1.9539	-68.5252	0.569484
273	W14X342	Column	COMB15-O	-6865.822	-5.8645	68.5199	0.570904
281	W14X283	Column	COMB22O	-6192.2	-165.0083	-0.6064	0.642112
289	W14X283	Column	COMB11-O	-6816.567	182.592	-4.4009	0.722634
297	W14X342	Column	COMB12-O	-2816.703	180.9997	4.5215	0.283526
305	W14X342	Column	COMB12-O	-2785.856	176.8173	3.9964	0.279244
313	W14X342	Column	COMB12-O	-2759.84	172.7756	3.9929	0.275766
321	W14X342	Column	COMB12-O	-2833.046	168.5927	3.5228	0.279369
329	W14X283	Column	COMB11-O	-6147.819	165.0719	12.6462	0.65989
337	W14X283	Column	COMB22O	-764.953	-183.0042	-6.5523	0.137247
345	W14X342	Column	COMB26O	-6250.25	-189.6834	-5.9534	0.546784
353	W14X342	Column	COMB15-O	-6260.785	189.6761	-8.9978	0.549842
361	W14X342	Column	COMB26O	-6260.802	-189.6857	-8.9957	0.549845
369	W14X342	Column	COMB15-O	-6250.233	189.6739	-5.9555	0.546781
377	W14X283	Column	COMB11-O	-764.953	164.5999	6.5487	0.12763

1102	220x220x20	Brace	COMB22O	-1295.057	0	1.0804	0.86883
1108	250x250x20	Brace	COMB22O	-1555.233	0	1.3437	0.73765
1116	250x250x20	Brace	COMB11-O	-1555.246	0	-1.3436	0.737656
1126	220x220x20	Brace	COMB11-O	-1295.118	0	-1.0805	0.868872
1134	220x220x20	Brace	COMB22O	-1306.043	0	1.2324	0.876755
1142	220x220x20	Brace	COMB11-O	-1306.104	0	-1.2325	0.876798
1150	220x220x20	Brace	COMB22O	-1172.771	0	-1.2336	0.785024
1174	220x220x20	Brace	COMB11-O	-1172.831	0	1.2335	0.785065
1182	220x220x20	Brace	COMB22O	-1181.375	0	-1.01	0.789954
1190	220x220x20	Brace	COMB11-O	-1181.436	0	1.0099	0.789996
1214	220x220x20	Brace	COMB26O	-1048.333	0	-1.1351	0.702068
1222	220x220x20	Brace	COMB15-O	-1048.358	0	1.1352	0.702085
1230	220x220x20	Brace	COMB15-O	-1046.111	0	0.9202	0.699823
1238	220x220x20	Brace	COMB26O	-1046.087	0	-0.92	0.699806
1342	220x220x20	Brace	COMB26O	-1183.817	0	0.9101	0.79405
1350	220x220x20	Brace	COMB15-O	-1183.842	0	-0.91	0.794066
1358	220x220x20	Brace	COMB15-O	-1186.153	0	-1.1282	0.796414
1366	220x220x20	Brace	COMB26O	-1186.128	0	1.1284	0.796397
1509	180x180x10	Brace	COMB22O	-201.798	0	2.4445	0.480769
1511	180x180x10	Brace	COMB11-O	-201.797	0	-2.4445	0.480767
1515	180x180x10	Brace	COMB11-O	-204.74	0	-2.4061	0.486355
1517	180x180x10	Brace	COMB22O	-204.741	0	2.406	0.486356
1521	180x180x10	Brace	COMB22O	-171.731	0	-3.595	0.421502
1523	180x180x10	Brace	COMB11-O	-171.73	0	3.595	0.4215
1527	180x180x10	Brace	COMB11-O	-174.348	0	2.8696	0.419913
1529	180x180x10	Brace	COMB22O	-174.349	0	-2.8696	0.419915
1717	200X200X20	Brace	COMB22O	-994.738	0	1.1535	0.911567
1723	200X200X20	Brace	COMB11-O	-994.722	0	-1.1536	0.911551
1725	200X200X20	Brace	COMB22O	-1004.807	0	1.3597	0.922719
1727	200X200X20	Brace	COMB11-O	-1004.791	0	-1.3598	0.922704
1729	200X200X20	Brace	COMB22O	-885.763	0	-1.3594	0.80707
1735	200X200X20	Brace	COMB11-O	-885.747	0	1.3593	0.807054
1737	200X200X20	Brace	COMB22O	-894.044	0	-1.1941	0.814394
1739	200X200X20	Brace	COMB11-O	-894.029	0	1.194	0.814379
1927	200x200x16	Brace	COMB22O	-672.976	0	2.1695	0.746428
1933	200x200x16	Brace	COMB11-O	-672.976	0	-2.1695	0.746428
1935	200x200x16	Brace	COMB22O	-680.651	0	2.9724	0.762013
1937	200x200x16	Brace	COMB11-O	-680.651	0	-2.9724	0.762013
1939	200x200x16	Brace	COMB22O	-596.998	0	-3.0329	0.663222
1945	200x200x16	Brace	COMB11-O	-596.998	0	3.0329	0.663221
1947	200x200x16	Brace	COMB22O	-603.238	0	-3.1085	0.672617
1949	200x200x16	Brace	COMB11-O	-603.238	0	3.1085	0.672617
2029	180x180x10	Brace	COMB15-O	-245.287	0	0.7152	0.559862
2031	180x180x10	Brace	COMB26O	-245.287	0	-0.7152	0.559862
2033	180x180x10	Brace	COMB26O	-245.184	0	-1.0824	0.563181
2035	180x180x10	Brace	COMB15-O	-245.184	0	1.0824	0.56318
2061	180x180x10	Brace	COMB15-O	-278.428	0	-0.3946	0.63611
2063	180x180x10	Brace	COMB26O	-278.428	0	0.3946	0.63611
2065	180x180x10	Brace	COMB26O	-277.771	0	0.0392	0.631234
2067	180x180x10	Brace	COMB15-O	-277.771	0	-0.0392	0.631234
2149	200X200X20	Brace	COMB26O	-834.601	0	-0.943	0.760976
2151	200X200X20	Brace	COMB15-O	-834.601	0	0.943	0.760976
2153	200X200X20	Brace	COMB15-O	-832.913	0	0.6979	0.758341
2155	200X200X20	Brace	COMB26O	-832.914	0	-0.6979	0.758341
2181	200X200X20	Brace	COMB26O	-935.778	0	0.5239	0.856643
2183	200X200X20	Brace	COMB15-O	-935.778	0	-0.5239	0.856642
2185	200X200X20	Brace	COMB15-O	-937.688	0	-0.7718	0.859566
2187	200X200X20	Brace	COMB26O	-937.688	0	0.7718	0.859566
2269	200x200x16	Brace	COMB26O	-574.17	0	-1.6081	0.629926
2271	200x200x16	Brace	COMB15-O	-574.17	0	1.6081	0.629926
2273	200x200x16	Brace	COMB15-O	-573.417	0	1.1997	0.626987
2275	200x200x16	Brace	COMB26O	-573.417	0	-1.1998	0.626987
2301	200x200x16	Brace	COMB26O	-642.98	0	0.686	0.703747
2303	200x200x16	Brace	COMB15-O	-642.98	0	-0.686	0.703747
2305	200x200x16	Brace	COMB15-O	-644.386	0	-1.0923	0.707398
2307	200x200x16	Brace	COMB26O	-644.386	0	1.0923	0.707398
248	W12X26	Beam	COMB22O	-126.567	-6.7958	-0.0227	0.587049
256	W12X26	Beam	COMB22O	-126.636	-6.803	-0.2664	0.594827
264	W12X26	Beam	COMB22O	-126.895	-6.8461	-0.2391	0.595386
272	W12X26	Beam	COMB22O	-111.138	-6.8043	-0.0009874	0.520649
280	W12X26	Beam	COMB22O	-111.223	-6.803	0.2587	0.528792

288	W12X26	Beam	COMB22O	-111.467	-6.8376	0.2546	0.52994
344	W12X26	Beam	COMB22O	-128.878	-5.2799	-0.0835	0.589898
352	W12X26	Beam	COMB22O	-129.023	-5.3006	-0.9087	0.616075
360	W12X26	Beam	COMB22O	-129.617	-5.3379	-0.8915	0.618337
368	W12X26	Beam	COMB22O	-112.012	-5.2905	0.0892	0.517957
376	W12X26	Beam	COMB22O	-112.184	-5.3006	0.8573	0.542418
384	W12X26	Beam	COMB22O	-112.751	-5.3273	0.7767	0.542543
392	W12X26	Beam	COMB26O	-102.911	-6.8627	0.4791	0.500503
395	W12X26	Beam	COMB26O	-102.867	-6.8561	0.4761	0.500177
399	W12X26	Beam	COMB26O	-118.543	-6.8559	-0.5088	0.568104
407	W12X26	Beam	COMB26O	-118.498	-6.8629	-0.5153	0.568163
409	W12X26	Beam	COMB26O	-94.974	-5.2138	0.2374	0.448233
413	W12X26	Beam	COMB26O	-94.928	-5.208	0.2217	0.447516
427	W12X26	Beam	COMB26O	-94.1	-5.1837	0.6831	0.458493
431	W12X26	Beam	COMB26O	-93.99	-5.1766	0.6551	0.457114
439	W12X26	Beam	COMB26O	-106.311	-5.1763	-0.7056	0.511351
447	W12X26	Beam	COMB26O	-106.202	-5.1839	-0.7363	0.51188
815	W12X26	Beam	COMB26O	-107.945	-8.1518	0.0059	0.509555
823	W12X26	Beam	COMB26O	-98.72	-7.9753	0.0056	0.473452
839	W12X26	Beam	COMB26O	-107.948	-8.1518	-0.0105	0.509706
847	W12X26	Beam	COMB26O	-98.718	-7.9753	-0.0111	0.473613
919	W12X26	Beam	COMB26O	-105.115	-11.4308	-0.0044	0.556562
927	W12X26	Beam	COMB26O	-105.114	-11.4318	0.0025	0.556506
929	W12X26	Beam	COMB26O	-111.65	-11.431	-0.000272	0.586218
933	W12X26	Beam	COMB26O	-111.649	-11.4315	0.0066	0.586417
936	W12X26	Beam	COMB26O	-96.766	-7.4296	0.0025	0.461896
944	W12X26	Beam	COMB26O	-96.736	-7.4297	-0.0087	0.461955
947	W12X26	Beam	COMB26O	-103.07	-7.4193	0.0052	0.488721
951	W12X26	Beam	COMB26O	-103.04	-7.4196	-0.006	0.488616

CURRICULUM VITAE

Name Surname: Samet KILIÇ

Place and Date of Birth: Trabzon/ 1988

E-Mail: kilicsamet123@gmail.com

EDUCATION:

B.Sc.: Istanbul Technical University

PROFESSIONAL EXPERIENCE

CGA Mühendislik (2013-2014) Design Engineer

Probi İnşaat (2014-2015) Design engineer